

DTIC ELECTE DEC19 1989

EVALUATION OF CHEMICALLY-SENSITIVE FIELD-EFFECT TRANSISTORS FOR DETECTION OF ORGANOPHOSPHORUS COMPOUNDS

Thesis

Jenny E. Shin, BSEE Captain, USAF

AFIT/GE/ENG/89D-47

DEPARTMENT OF THE AIR FORCE

AIR UNIVERSITY

# AIR FORCE INSTITUTE OF TECHNOLOGY

DESTABUTION STATEMENT A

Approved for public releases

Distribution Unlimited

Wright-Patterson Air Force Base, Ohio

89 12 18 097



EVALUATION OF
CHEMICALLY-SENSITIVE FIELD-EFFECT
TRANSISTORS FOR DETECTION OF
ORGANOPHOSPHORUS COMPOUNDS

Thesis

Jenny E. Shin, BSEE Captain, USAF

AFIT/GE/ENG/89D-47



Approved for public release; distribution unlimited.

# EVALUATION OF CHEMICALLY-SENSITIVE FIELD-EFFECT TRANSISTORS FOR DETECTION OF ORGANOPHOSPHORUS COMPOUNDS

#### THESIS

Presented to the Faculty of the School of Engineering
of the Air Force Institute of Technology
Air University
In Partial Fulfillment of the
Requirements for the Degree of
Master of Science in Electrical Engineering

Jenny E. Shin, BSEE Captain, USAF

5 December 1989

Approved for public release; distribution unlimited.

#### **Acknowledgements**

This thesis project has been the most challenging undertaking of my academic life. I could not have completed it without the assistance of many people, and I would like to thank everyone who have provided assistance during this research effort.

I am especially indebted to my thesis advisor, Maj Edward Kolesar, for his guidance and support. He provided me with invaluable technical assistance as well as timely encouragements. I am also indebted to Capt William Hodges and Dr. Matthew Kabrisky who reviewed my work and provided valuable comments.

I would also like to thank the laboratory technicians, Mr Don Smith and Mr William Trop, for their technical assistance and equipment maintenance. And finally, I would like to thank my fellow students, Capt John Wiseman, Capt James Lyke, Capt Douglas Ford, Capt John Wiseman, and Mr David Szczublewski, for their moral support. I am especially grateful to Capt Jenkins whose own concurrent thesis research provided significant groundwork for my thesis research.

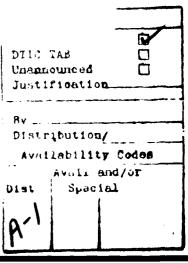


### Table of Contents

Acknowlegements	ii
List of Figures	V
List of Tables	xiv
Abstract	xv
I. Introduction	1-1
Background Problem Statement Scope Assumptions Approach Plan of Development	I-1 I-3 I-3 I-4 I-7 I-12
II. Background	II-1
Introduction Crganophosphorus Compounds Solid State Chemical Sensors Chemically-Sensitive Thin Films Theory of the CHEMFET's Operation in Frequency-Domain Summary	II-1 II-6 II-11 II-26
III. CHEMFET Design, Fabrication, and Operational Characteristics	111-1
Design	III-15
IV. Experimental Procedures	IV-1
Experimental Procedures	TV-1

	Data	a Re	cal Measurementsduction and Processing	IV-7 IV-11 IV-14
v.	Res	ults	and Discussions	V-1
	tì	he C	vity Performance of HEMFET Sensor Coated with CoPc	V-2
	t!	he C	vity Performance of HEMFET Sensor Coated with NiPc vity Performance of	V-21
	t!	he C	HEMFET Sensor Coated with PbPcvity Performance of	V-32
	t]	he C	HEMFET Sensor Coated with CuPcvity Performance of the CHEMFET Coated	V-43
	Sen	siti	2-Naphthol( $\beta$ )vity Performance of the CHEMFET Coated	V-54
	Sen	siti	Succinylchloridevity Performance of the CHEMFET Coated	V-59
	Sens	siti	L-Histidine Dihydrochloridevity Performance of the CHEMFET Coated	V-64
			Succinylcholine Chloride	V-68 V-74
VI.	Con	clus	ions and Recommendations	VI-1
			ionsndations	VI-1 VI-3
Appe	ndix	<b>A:</b>	Materials and Equipment	A-1
Appe	ndix	В:	CHEMFET Design Simulations and Fabrication Data	B-1
Appe	ndix	c:	Film Deposition Procedures	C-1
Appe	ndix	D:	Gas Generation and Delivery System	D-1
Appe	ndix	<b>E</b> :	Computer Programs	E-1
Appe	ndix	F:	Impedance Data	F-1
Bibl	iogra	aphy		Bib-1
Vita				Vit-1

# List of Figures

Figure	I.1.	An Interdigitated Gate Electrode CHEMFET	I-2
Figure	I.2.	2 X 5 CHEMFET Array Layout	I-8
Figure	II.1.	Toxic Organophosphorus Compound Chemical Structure	II-3
Figure	II.2.	Schematic of a Chemiresistor Structure	II-9
Figure	II.3.	Chemical Structure of Metal-Doped Phthalocyanine	II-14
Figure	II.4.	Chemical Structure of 2-Naphthol( $eta$ )	11-15
Figure	II.5.	Typical Input and Output Time-Domain Pulse Waveform of the CHEMFET	II <b>-</b> 22
Figure	III.1.	CHEMFET Multiplexer	III-2
Figure	III.2.	Decoder and Transmission Gates	III-3
Figure	III.3.	Differential Input Comparator	111-5
Figure	III.4.	Feedback Amplifier Stages	III-5
Figure	III.5.	CIF Plot of the First Amplifier Stage .	III-7
Figure	III.6.	Photomicrograph of the CHEMFET IC	111-8
Figure	III.7.	Example of a Shorted Interdigitated Gate Electrode	III-11
Figure	III.8.	DC Voltage Characteristics of the Five Amplifier Stages	III-12
Figure	III.9.	Gain of the Interdigitated Gate Electrode CHEMFET's Amplifier versus Frequency	III <b>-</b> 13
Figure	III.10.	Phase of the Interdigitated Gate Electrode CHEMFET's Amplifier versus Frequency	III-14
Figure		Floating Gates Connected to	TTT-17

Figure	IV.1.	CHEMFET 1: 1500Å Thick Phthalocyanine Films	IV-2
Figure	IV.2.	CHEMFET 2: 500Å Thick Phthalocyanine Films	IV-2
Figure	IV.3.	CHEMFET 3 and 4: Other Organic Thin Films	IV-3
Figure	IV.4.	Instrumentation Configuration	IV-6
Figure	IV.5.	Time-Domain Spectrum of the Excitation Pulse	IV-10
Figure	IV.6.	Frequency Spectrum of the Excitation Pulse	IV-10
Figure	IV.7.	Time-Domain Pulse Captured on the Digital Storage Oscilloscope	IV-12
Figure	IV.8.	Fourier Transform Spectra of the Excitation Pulse	IV-13
Figure	V.1.	Normalized Difference Fourier Transform Spectra of the CHEMFET Sensor Coated with a 1500Å Thick CoPc Film upon Exposure to DIMP at 25 °C	V-3
Figure	V.2.	Fourier Transform Spectra of the Excitation Pulse Offset at -40 mV	V-4
Figure	V.3.	Time-Domain Response of the CHEMFET Sensor Coated with a 1500Å Thick CoPc Film upon Exposure to a 0.5 ppm DIMP Challenge at 25 °C	V-6
Figure	V.4.	Time-Domain Response of the CHEMFET Sensor Coated with a 1500Å Thick CoPc Film upon Exposure to a 7.5 ppm DIMP Challenge at 25 °C	V-6
Figure	V.5.	Resistive Part of the Impedance of the 1500Å Thick CoPc Film upon Exposure to the DIMP at 25 °C	V-8
Figure	V.6.	Reactive Part of the Impedance of the 1500Å Thick CoPc Film upon Exposure to the DIMP at 25 °C	V-8

Figure V.7.	DC Resistance of the 1500Å Thick Metal- Doped Phthalocyanine Films upon Exposure to the 7.5 ppm DIMP	
Figure V.8.	Challenge at 25 °C	V <b>-</b> 9
	with the 1500Å Thick CoPc upon Exposure to DIMP at 120 °C	V-11
Figure V.9.	Normalized Difference Fourier Transform Spectra of the CHEMFET Sensor Coated with the 500Å and 1500Å Thick CoPc Film upon Exposure to 7.5 ppm DIMP at 120 °C	V-13
Figure V.10.	Normalized Difference Fourier Transform Spectra of the CHEMFET Sensor Coated with the 1500Å Thick CoPc Film upon Exposure to DMMP at 25 °C	V-14
Figure V.11.	Normalized Difference Fourier Transform Spectra of the CHEMFET Sensor Coated with the 1500Å Thick CoPc Film upon Exposure to DMMP at 120 °C	V-17
Figure V.12.	Normalized Difference Fourier Transform Spectra of the CHEMFET Sensor Coated with the 500Å and 1500Å Thick CoPc Films upon Exposure to the 3 ppm DIMP Challenge at 120 °C	V-18
Figure V.13.	Normalized Difference Fourier Transform Spectra of the CHEMFET Sensor Coated with the 1500A Thick NiPc Film upon Exposure to the DIMP Challenge at 25 °C	V-22
Figure V.14.	Normalized Difference Fourier Transform Spectra of the CHEMFET Sensor Coated with the 1500Å Thick NiPc Film upon Exposure to the DIMP Challenge at 120 °C	V-23
Figure V.15.	Normalized Difference Fourier Transform Spectra of the CHEMFET Sensor Coated with the 500Å and 1500Å Thick NiPc Films upon Exposure to the 7.5 ppm DIMP Challenge at 120 °C	V-24
Figure V.16.	Normalized Difference Fourier Transform Spectra of the CHEMFET Sensor Coated with the 1500Å Thick NiPc Film upon	
	Exposure to the DMMP Challenge at 25 °C	V-25

Figure V.17.	Normalized Difference Fourier Transform Spectra of the CHEMFET Sensor Coated with the 1500Å Thick NiPc Film upon Exposure to the DMMP Challenge at 120 °C	V-28
Figure V.18.	Normalized Difference Fourier Transform Spectra of the CHEMFET Sensor Coated with the 500Å and 1500Å Thick NiPc Films upon Exposure to the 3 ppm DMMP Challenge at 120 °C	V-29
Figure V.19.	Normalized Difference Fourier Transform Spectra of the CHEMFET Sensor Coated with the 1500Å Thick PbPc Film upon Exposure to the DIMP Challenge at 25 °C	V-32
Figure V.20.	Normalized Difference Fourier Transform Spectra of the CHEMFET Sensor Coated with the 1500Å Thick PbPc Film upon Exposure to DIMP at 120 °C	V-34
Figure V.21.	Normalized Difference Fourier Transform Spectra of the CHEMFET Sensor Coated with the 500Å and 1500Å Thick PbPc Films upon Exposure to the 7.5 ppm DMMP Challenge at 120 °C	V-36
Figure V.22.	Normalized Difference Fourier Transform Spectra of the CHEMFET Sensor Coated with the 1500Å Thick PbPc Film upon Exposure to the DMMP Challenge at 25 °C	V-37
Figure V.23.	Normalized Difference Fourier Transform Spectra of the CHEMFET Sensor Coated with the 1500Å Thick PbPc Film upon Exposure to the DMMP Challenge at 120 °C	V-39
Figure V.24.	Normalized Difference Fourier Transform Spectra of the CHEMFET Sensor Coated with the 500Å and 1500Å Thick PbPc Films upon Exposure to the 3 ppm DMMP Challenge at 120 °C	V-40
Figure V.25.	Normalized Difference Fourier Transform Spectra of the CHEMFET Sensor Coated with the 1500Å Thick CuPc Film upon Exposure to the DIMP Challenge at 25 °C	V-44
	pyhopare to the pink charrende at 50 c	v - 44

Figure V.T.	Normalized Difference Fourier Transform Spectra of the CHEMFET Sensor Coated with the 1500Å Thick CuPc Film upon Exposure to the DIMP Challenge at 120 °C	V-45
Figure V.27.	Normalized Difference Fourier Transform Spectra of the CHEMFET Sensor Coated with the 500Å and 1500Å Thick CuPc Films upon Exposure to the 7.5 ppm DMMP Challenge at 120 °C	V-47
Figure V.28.	Normalized Difference Fourier Transform Spectra of the CHEMFET Sensor Coated with the 1500Å Thick CuPc Film upon Exposure to the DMMP Challenge at 25 °C	V-48
Figure V.29.	Normalized Difference Fourier Transform Spectra of the CHEMFET Sensor Coated with the 1500Å Thick CuPc Film upon Exposure to DMMP Challenge at 120 °C.	V-50
Figure V.30.	Normalized Difference Fourier Transform Spectra of the CHEMFET Sensor Coated with the 500Å and 1500Å Thick CuPc Films upon Exposure to the 3 ppm DMMP Challenge at 120 °C	V-51
Figure V.31.	Normalized Difference Fourier Transform Spectra of the CHEMFET Sensor Coated with the 2-Naphthol( $\beta$ ) upon Exposure to the 7.5 ppm DIMP Challenge at 25 °C	V <b>-</b> 55
Figure V.32.	Time-Domain Response of the CHEMFET Sensor Coated with the 2-Naphthol(β) upon Exposure to the 7.5 ppm DIMP Challenge at 25 °C	V-56
Figure V.33.	Normalized Difference Fourier Transform Spectra of the CHEMFET Sensor Coated with the 2-Naphthol( $\beta$ ) upon Exposure to the 3 ppm DMMP Challenge at 25 °C	V-57
Figure V.34.	DC Resistance of the Organic Thin Films, Succinylcholine Chloride, 2-Naphthol(β), and Succinylcholine Chloride upon Exposure to the 3 ppm	
	DMMP Challenge at 25 °C	V-58

Figure	V.35.	Normalized Difference Fourier Transform Spectra of the CHEMFET Sensor Coated with the Succinylchloride Film upon Exposure to the 7.5 ppm DIMP Challenge at 25 °C	V-60
Figure	V.36.	Time-Domain Response of the CHEMFET Sensor Coated with the Succinylchloride Film upon Exposure to the 7.5 ppm DIMP Challenge at 25 °C	V-61
Figure	V.37.	Normalized Difference Fourier Transform Spectra of the CHEMFET Sensor Coated with the Succinylchloride Film upon Exposure to the 3 ppm DMMP Challenge at 25 °C	V-62
Figure	V.38.	Normalized Difference Fourier Transform Spectra of the CHEMFET Sensor Coated with the L-Histidine Dihydrochloride Film upon Exposure to the 7.5 ppm DIMP Challenge at 25 °C	V-65
Figure	V.39.	Time-Domain Response of the CHEMFET Sensor Coated with the L-Histidine Dihydrochloride Film upon Exposure to the 7.5 ppm DIMP Challenge at 25 °C	V-66
Figure	V.40.	Normalized Difference Fourier Transform Spectra of the CHEMFET Sensor Coated with the L-Histidine Dihydrochloride Film upon Exposure to the 3 ppm DMMP Challenge at 25 °C	V-67
Figure	V.41.	Normalized Difference Fourier Transform Spectra of the CHEMFET Sensor Coated with the Succinylcholine Chloride Film upon Exposure to the 7.5 ppm DIMP Challenge at 25 °C	V-69
Figure	V.42.	Time-Domain Response of the CHEMFET Sensor Coated with the Succinylcholine Chloride Film upon Exposure to the 7.5 ppm DIMP	••
		Challenge at 25 °C	V-70

Figure V.43.	Normalized Difference Fourier Transform Spectra of the CHEMFET Sensor Coated with the Succinylcholine Chloride Film upon Exposure to the 3 ppm DMMP Challenge at 25 °C	V-71
Figure V.44.	Time-Domain Response of the CHEMFET Sensor Coated with the Succinylcholine Chloride Film upon Exposure to Air at 25 °C	V-72
Figure V.45.	Time-Domain Response of the CHEMFET Sensor Coated with the Succinylcholine Chloride Film upon Exposure to the 3 ppm DMMP Challenge at 25 °C	V-73
Figure C.1.	Evaporation Mask Pattern	C-2
Figure C.2.	Structure of the RTV Sealant Dam on the BeCu Mask	C <b>-</b> 5
Figure C.3.	CHEMFET Mask Arrangement for Thermal Evaporation	C <b>-</b> 6
Figure C.4.	Thin Gold Film Sputtered onto a Phthalocyanine Film	C-8
Figure C.5.	Interdigitated Gate Electrode with RTV Sealant Dam	C-11
Figure D.1.	The Schematic Diagram of the Gas Generation and Delivery System	D-2
Figure D.2.	DIMP Permeation Tube, Model 23-7392, Part Number G-6942 Calibration Chart .	D-5
Figure D.3.	DIMP Permeation Tube, Mcdel 23-7392, Part Number G-5645 Calibration Chart .	D-6
Figure D.4.	DMMP Permeation Tube, Model 23-7082, Part Number G-5646 Calibration Chart .	D-7
Figure D.5.	Gilmont Instruments Flowmeter Model F-1200, Serial Number 25083, Size 2 Calibration Chart for the DIMP and DMMP Flowmeter	D-8
Figure D.6.	Gilmont Instruments Flowmeter Model F-1300, Serial Number C-8754, Size 3 Calibration Chart for the Purge	D 0
	Flowmeter	D-9

Figure	D.7.	Schematic Drawing of the Test Cell	D-11
Figure	D.8.	Schematic Drawing of the DIP Socket	D-13
Figure	F.1.	Resistive Part of the Impedance of 2-Naphthol(β) Film upon Exposure to the 7.5 ppm DIMP Cnallenge at 25 °C	F-2
Figure	F.2.	Reactive Part of the Impedance of 2-Naphthol( $\beta$ ) Film upon Exposure to the 7.5 ppm DIMP Challenge at 25 °C	F-2
Figure	F.3.	Resistive Part of the Impedance of 2-Naphthol(β) Film upon Exposure to the 3 ppm DMMP Challenge at 25 °C	F-3
Figure	F.4.	Reactive Part of the Impedance of 2-Naphthol(\beta) Film upon Exposure to the 3 ppm DMMP Challenge at 25 °C	F-3
Figure	F.5.	Resistive Part of the Impedance of Succinylchloride Film upon Exposure to the 7.5 ppm DIMP Challenge at 25 °C	F-4
Figure	F.6.	Reactive Part of the Impedance of Succinylchloride Film upon Exposure to the 7.5 ppm DIMP Challenge at 25 °C	F-4
Figure	F.7.	Resistive Part of the Impedance of Succinylchloride Film upon Exposure to the 3 ppm DMMP Challenge at 25 °C	F-5
Figure	F.8.	Reactive Part of the Impedance of Succinylchloride Film upon Exposure to the 3 ppm DMMP Challenge at 25 °C	F-5
Figure	F.9.	Resistive Part of the Impedance of L-Histidine Dihydrochloride Film upon Exposure to the 7.5 ppm DIMP	
		Challenge at 25 °C	F-6

Figure	F.10.	Reactive Part of the Impedance of L-Histidine Dihydrochloride Film upon Exposure to the 7.5 ppm DIMP Challenge at 25 °C	F-6
Figure	F.11.	Resistive Part of the Impedance of L-Histidine Dihydrochloride Film upon Exposure to the 3 ppm DMMP Challenge at 25 °C	F-7
Figure	F.12.	Reactive Part of the Impedance of L-Histidine Dihydrochloride Film upon Exposure to the 3 ppm DMMP Challenge at 25 °C	F-7
Figure	F.13.	Resistive Part of the Impedance of Succinylcholine Chloride Film upon Exposure to the 7.5 ppm DIMP Challenge at 25 °C	F-8
Figure	F.14.	Reactive Part of the Impedance of Succinylcholine Chloride Film upon Exposure to the 7.5 ppm DIMP Challenge at 25 °C	F-8
Figure	F.15.	Resistive Part of the Impedance of Succinylcholine Chloride Film upon Exposure to the 3 ppm DMMP Challenge at 25 °C	F-9
Figure	F.16.	Reactive Part of the Impedance of Succinylcholine Chloride Film upon Exposure to the 3 ppm DMMP Challenge at 25 °C	F <b>-</b> 9

# List of Tables

Table	I.1.	DIMP Test Matrix	I-5
Table	I.2.	DMMP Test Matrix	I-6
Table	II.1.	Basic Properties of Thin Film Materials	II-17
Table	III.1.	Interdigitated Gate Electrode Characteristics	III-2
Table	III.2.	CHEMFET Bond Pad Function Summary	III <b>-</b> 9
Table	IV.1.	Challenge Gas Generation Parameters	IV-5
Table	V.1.	Summary of the Normalized Difference Magnitudes of tje Fourier Transform Spectra for the CHEMFET Sensor Coated with 1500Å Thick CoPc Film	V <b>-</b> 19
Table	V.2.	Summary of the Normalized Difference Magnitudes of the Fourier Transform Spectra for the CHEMFET Sensor Coated with the 1500Å Thick NiPc Film	V-31
Table	V.3.	Summary of the Normalized Difference Magnitudes of the Fourier Transform Spectra for the CHEMFET Sensor Coated with the 1500Å Thick PbPc Film	V-42
Table	V.4.	Summary of the Normalized Difference Magnitudes of the Fourier Transform Spectra for the CHEMFET Sensor Coated with the 1500Å Thick CuPc Film	V-52
Table	A.1.	Instrumentation List	A-1
Table	A.2.	Materials List	A-4
Table	B.1.	Initial SPICE Simulation of the Amplifier	B-1
Table	B.2.	SPICE Simulation of the Amplifier with a 30pF Load	B-7
Table	B.3	SPICE Simulation of the Amplifier with a 200pF Load	B-8
Table	B.4.	MOSIS Parametric Test Results	B-10

#### **Abstract**

This study resulted in the design, fabrication, and evaluation of an interdigitated gate electrode Chemically-Sensitive Field-Effect Transistor (CHEMFET). The electrical performance of the CHEMFET sensors coated with the following thin films was evaluated in frequency domain for detecting the gas concentration changes of organophosphorus compounds (diisopropyl methylphosphonate (DIMP) and dimethyl methylphosphonate (DMMP)) in the air: cobalt phthalocyanine, nickel phthalocyanine, lead phthalocyanine, copper phthalocyanine, 2-naphthol( $\beta$ ), succinylchloride, succinylcholine chloride, and L-histidine dihydrochloride. The change in the chemical state of a film was manifested as a change in the CHEMFET sensors' output response, when the CHEMFET sensor was excited with a pulse. The results showed the CHEMFET sensor coated with cobalt phthalocyanine produced consistent responses upon exposure, with respect to three concentrations of DIMP and DMMP, at two measurement temperatures. The resulted also revealed that the CHEMFET sensors coated with 2-naphthol( $\beta$ ), succinylchloride, and succinylcholine chloride had promising gas exposure sensitivity.

#### **EVALUATION OF**

# CHEMICALLY-SENSITIVE FIELD-EFFECT TRANSISTORS FOR DETECTION OF ORGANOPHOSPHORUS COMPOUNDS

#### 1. Introduction

#### Background

The detection and measurement of environmentallysensitive chemical species has widespread application. Of
particular interest to the military is the detection and
identification of toxic organophosphorus compounds. One
method of detecting and identifying these particular
chemical species has recently been investigated at the Air
Force Institute of Technology (AFIT) (1). This technique
utilizes a microelectronic device known as the ChemicallySensitive Field-Effect Transistor (CHEMFET).

In the CHEMFET, as shown in Figure I.1, an interdigitated gate electrode structure has been devised which consists of a metallized driven electrode, and a floating electrode component which is connected to the gate oxide of a conventional Metal-Oxide-Semiconductor Field-Effect Transistor (MOSFET). A chemically-sensitive film is then deposited over these two physically and electrically isolated metallized electrode components. The chemical state of the deposited film determines its impedance, and

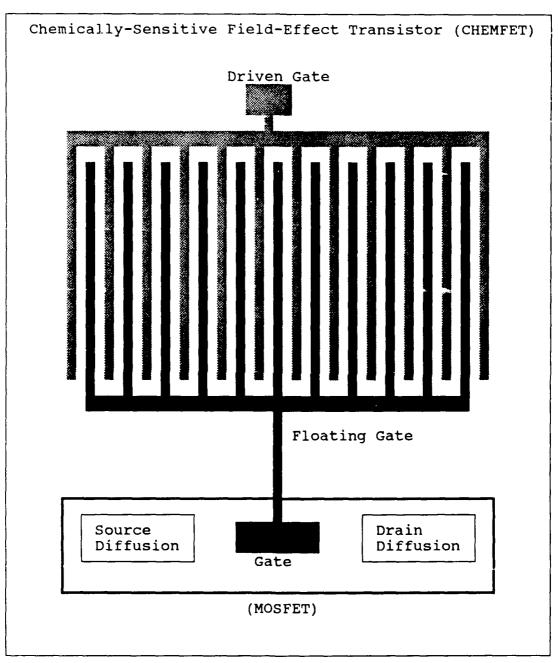


Figure I.1. Interdigitated Gate Electrode CHEMFET (1:1-3).

thus, the input impedance to the MOSFET's gate electrode. A pulsed excitation is used to excite the driven gate electrode, and an amplified response characteristic is reflected in the MOSFET's drain current signal. The Fourier transform of this time-domain signal contains spectral components which can be correlated with the state of the chemical reaction in the film.

The previous AFIT thesis research conducted by Captain Wiseman demonstrated the feasibility of using an interdigitated gate CHEMFET to detect trace quantities of nitrogen dioxide (NO<sub>2</sub>) and diisopropyl methylphosphonate (DIMP) (1:6-4, 2). However, a comprehensive evaluation of the CHEMFET's sensitivity and selectivity, as manifested in the device's spectral response to NO<sub>2</sub> and DIMP, is required.

#### Problem Statement

This thesis evaluates the spectral response of the CHEMFET to the chemical warfare nerve agent analog compounds, diisopropyl methylphosphonate (DIMP) and dimethyl methylphosphonate (DMMP). The sensor's performance with respect to sensitivity, specificity, and reversibility were the critical parameters of interest.

#### Scope

Initially, this thesis involved the design of a 2 X 5 array of CHEMFET sensing elements based on the

interdigitated gate electrode CHEMFET design developed in previous AFIT research (1:4-9). The primary modifications to the existing design were the addition of an electronic multiplexing circuit for interrogating discrete sensing elements in the array and MOSFET amplifier stages which provide a larger signal gain and 3-dB cut-off frequency.

This thesis also involved the evaluation of several chemically-sensitive thin films to determine the optimum film candidate for detecting DIMP and DMMP. The thin film candidates evaluated were copper phthalocyanine (CuPc), cobalt phthalocyanine (CoPc), lead phthalocyanine (PbPc), nickel phthalocyanine (NiPc), succinylchloride (SuCl), succinylchloride (SuCl), succinylchloride (SuCl), L-histidine dihydrochloride (LHDHCl), and 2-naphthol( $\beta$ ).

To evaluate the CHEMFET's response, these selected films were deposited over the interdigitated gate electrode, and the frequency responses associated with DIMP and DMMP gas-sensitivity were measured with respect to different film thicknesses, operating temperatures, and challenge gas concentrations. Table I.1 and I.2 summarize the test matrices.

#### Assumptions

As in the previous CHEMFET research, it was assumed that the CHEMFET is a linear, time-invariant system (1:1-5). In a linear system, the response of the system to a linear

Table I.1. DIMP Test Matrix

#### Relative Humidity Less Than 10%

エーラミ	۰ ر	תואג	Tr 1	20	° ~

			1500Å F	ilm Thickness	
DIMP	Conc.	CuPc	PbPc	CoPc(2x)*	NiPc(2x)
0.5	ppm	х	Х	Х	Х
3	ppm	x	Х	х	X
7.5	ppm	х	Х	x	X
! 					

T=120°C

500Å Film Thickness				
DIMP Conc.	CuPc(2x)	PbPc(2x)	CoPc(2x)	NiPc(2x)
0.5 ppm	Х	х	Х	Х
3 ppm	x	X	X	X
7.5 ppm	х	Х	X	x

T=25°C

DIMP Conc.	SuCl	SuChCl	LHDHCl(2x)	2-Naphthol(2x)
7.5 ppm	х	Х	Х	X

<sup>\*</sup> The (2x) notation is used to denote that 2 of these films were evaluated on the same microsensor.

Table I.2. DMMP Test Matrix

#### Relative Humidity Less Than 10%

	T=25	°C AND 1	T=120°C			
				1500Å Film	n Thickness	
	DMMP	Conc.	CuPc	PbPc	CoPc(2x)*	NiPc(2x)
	0.1	ppm	х	Х	Х	Х
	0.5	ppm	Х	X	Х	Х
	3	ppm	х	х	x	X
_ <b></b>	Т=	=120°C				
T						
				500Å Film	m Thickness	
	DMMP	Conc.	CuPc(2x)		Thickness CoPc(2x)	NiPc(2x)
	ļ	Conc.	CuPc(2x)		- <del></del>	NiPc(2x)
	0.1			PbPc(2x)	CoPc(2x)	
	0.1	ppm	X	PbPc(2x)	CoPc(2x)	X
	0.1	ppm	x x	PbPc(2x) X X	CoPc(2x) X X	x x
	0.1 0.5 3	ppm ppm	X X X	PbPc(2x) X X X	CoPc(2x) X X	x x x

<sup>\*</sup> The (2x) notation is used to denote that 2 of these films were evaluated on the same microsensor.

combination of two input signals is the sum of the responses produced by each signal applied separately. Typically, real systems are not completely linear for all ranges of input values. However, any continuous, differential function is linear over a sufficiently small range of input values. Thus, a non-linear real system, in general, can be treated as a linear system, provided the input signal is kept within a small range of values.

A system is time-invariant if the transfer function (output divided by the input) does not change with time. In other words, in time-invariant systems, the system structure does not change with time. In the CHEMFET, however, the impedance of the system changes due to a change in the chemical state of the thin film. Thus, the CHEMFET is not completely time-invariant. However, as in the case of the linearity property, the CHEMFET can be considered a time-invariant system, if the time period over which any measurement is performed is kept short relative to the rate of change occurring in the chemically-sensitive film.

#### Approach

#### CHEMFET Array Design.

As shown in Figure I.2, a 2X5 array of CHEMFET sensing elements were designed based on the previous interdigitated gate electrode CHEMFET configuration (1:4-9). The revised CHEMFET array included an integral multiplexing circuit, a

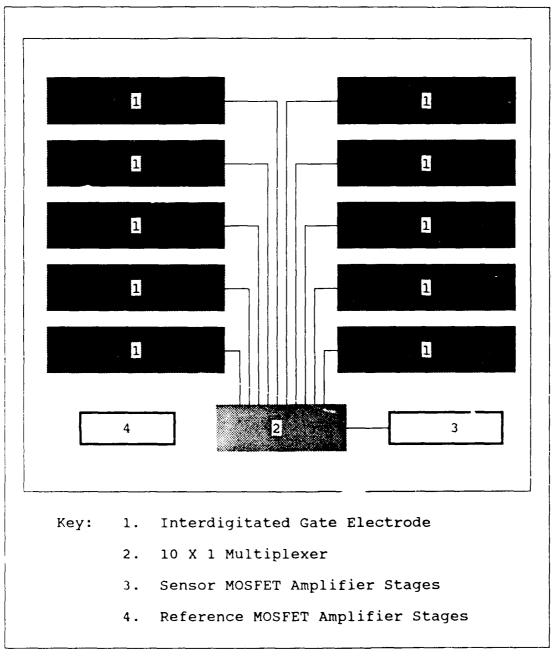


Figure I.2. 2 X 5 CHEMFET Array Layout.

sensor element MOSFET amplifier, and a reference MOSFET amplifier. The CHEMFET arrays were designed using a "modular" format to minimize the influence of fatal design or fabrication errors. The amplifier design was validated via the SPICE program.

The revised CHEMFET array design was fabricated by the Metal Oxide Semiconductor Implementation Service (MOSIS).

Upon receipt of the fabricated circuits, the amplifier and multiplexing circuits' performance were verified with a Semiconductor Parameter Analyzer (Hewlett-Packard Corp., Model HP 4145B, Palo Alto, CA) and a Gain/Phase Analyzer (Hewlett-Packard Corp., Model HP 4194A, Palo Alto, CA).

#### Gas-Sensitive Film Deposition.

The thin films were deposited on the interdigitated gate electrode structure using one of two methods: i) direct application with a syringe, or ii) thermal evaporation in a vacuum. The deposition method depended on whether the thin film material was soluble in a non-acidic solvent. The soluble thin film materials were first dissolved in a non-acidic solvent, and the corresponding liquid solution was then deposited over the gate electrode using a hypodermic needle and syringe. The solvents were removed from the solution covered electrode by evaporation.

For L-histidine dihydrochloride (LHCHCl) and succinylcholine chloride (SuChCl), 20% isopropyl alcohol was used as a solvent. The 2-naphthol( $\beta$ ) material was dissolved

in acetone. Succinylchloride (SuCl) was liquid at room temperature.

The metal-doped phthalocyanine thin films were deposited on the interdigitated electrode's surface using a thermal evaporation process in a vacuum. To confine the deposited films over the interdigitated gate electrode, a photolithographic mask process was used to create a metal stencil with windows for the interdigitated gate electrode structures.

#### Exposure to DIMP and DMMP.

The sensor's test and evaluation performance measurements were accomplished when the CHEMFET was exposed to DIMP or DMMP. To deliver these challenge gases, a gas generation and delivery system and a test cell for the device under test were utilized. The gas generation and delivery systems were modified from the previous AFIT research effort, and a new test cell was designed and fabricated. Appendix D discusses the details of the test cell and the gas generation and delivery systems used in this thesis.

Because water vapor might affect the film's gas sensitivity, the humidity of the challenge gases delivered to the test cell was controlled and monitored. The relative humidity of the challenge gas was regulated to be less than 10%. The CHEMFET's temperature was regulated at either 25°C

or 120  $^{\circ}$ C. The challenge gas concentration was varied in the range of 0.1-7.5 ppm (parts-per-million).

#### Electrical Measurements.

For each CHEMFET sensor performance measurement, the impedance of the film (real part and imaginary part) and the sensor's gain-phase response were measured at selected frequencies in the range spanning 100 HZ - 1 MHZ, using a impedance/gain-phase analyzer (Hewlett-Packard Corp., Model HP 4194A, Palo Alto, CA). Also, the film's DC resistance was measured using an electrometer (Keithley Instruments, Model 617, Cleveland, OH).

The frequency spectrum of both the excitation pulse and the response of the CHEMFET were measured using a spectrum analyzer (Hewlett-Packard Corp., Model HP 8556B, Palo Alto, CA). The driven gate of the CHEMFET was excited with a 5.24 V pulse, whose duration was 2.0  $\mu$ s and whose repetition frequency was 1 KHZ, using a pulse generator (Hewlett-Packard Corp., Model HP 8082A, Palo Alto, CA).

#### Data Collection.

The data collection and instrumentation configuration was automated via a Z-248 microcomputer and an IEEE-488 interface plug-in card. The data collected were: resistance data, impedance data, gain/phase data, and the frequency-domain (spectrum) data. The frequency-domain response was the focus of critical interest, and this data was processed to produce a normalized difference Fourier transform

spectra. This spectra was calculated by subtracting the Fourier transform spectra of the excitation pulse from the Fourier transform spectra of the CHEMFET sensor's response measured after each challenge gas exposure. The difference Fourier transform spectra was then normalized with respect to the "largest" spectrum magnitude contained in the excitation pulse. The normalized difference Fourier transform spectra were then compared for the two different challenge gases (DIMP and DMMP) and their respective concentrations.

#### Equipment and Materials.

The instrumentation and materials used in this thesis are listed in Appendix A.

#### Plan of Development

Chapter II presents the background information concerning the organophosphorus compounds, solid state sensors for detecting organophosphorus compounds, chemically-sensitive thin films, and the theory of the CHEMFET's operation in the frequency-domain. Chapter III presents the design, fabrication, and operating characteristics of the CHEMFET. Chapter IV describes the experimental procedures. The findings and results are presented in Chapter V, and the recommendations and conclusions are given in Chapter VI.

#### II. Background

#### Introduction

The detection and identification of toxic organophosphorus compounds has particular significance to the military. This is because certain organophosphorus compounds are used as nerve gases in chemical warfare. Relative to this military application, a number of solid state chemical sensors have been investigated during past decade. In order to understand the basic operation of these sensors, especially of the CHEMFET, the appropriate background information will be developed.

This chapter presents the current information concerning organophosphorus compounds, different types of solid state sensors investigated during the past decade for detecting organophosphorus compounds, the chemically-sensitive thin films investigated in this thesis, and finally, the theory of the CHEMFET's operation in frequency-domain.

#### Organophosphorus Compounds

#### Structure.

Organophosphorus compounds with specific formulations are very potent inhibitors of the cholinesterase enzyme. In the human body, the cholinesterase enzyme acts as a catalyst

in the hydrolysis of acetylcholine (3:2, 4:4):

This biochemical process is critical in a nerve impulse transmission.

Organophosphorus compounds of the type RR'P(Z)X, where R and R' are alkyl or alkoxy groups, Z is a doubly bonded oxygen or sulfur atom, and X is an easily displaceable group, react with the cholinesterase enzyme (4:4):

and thus, inhibit the enzyme from facilitating the catalytic hydrolysis process. By inhibiting the enzyme, the organophosphorus compound acts to block nerve impulse transmissions, which in turn, results in death by oxygen deprivation due to paralysis of the respiratory muscles (4:1).

The basic chemical structure of the toxic organophosphorus compounds which are reactive with the enzyme, is a molecule with the following characteristics depicted in Figure II.1. The central tetrahedrally coordinated

Figure II.1. Toxic Organophosphorus Compound Chemical Structures (4:2).

phosphorus atom, which has high cationic charge density and low polarizability, is bonded to an oxygen, sulfur, or nitrogen atom attached to an alkyl group. This phosphorus atom is also bonded to a small alkyl group, doubly-bonded to the adjacent oxygen atom, and weakly bonded to an easily displaceable X-group.

#### Reactive Chemicals:

In order to defend against the chemical warfare agents, both preventative measures and treatments have been investigated. The preventative measures led to the research of physiologically compatible reagents that would compete with the cholinesterase enzyme for the reaction with the toxic organophosphorus compounds. The treatments led to the research of compounds that would reactivate the phosphorylated cholinesterase enzyme.

The investigation for physiologically compat. le reagents that would react with the toxic organophosphorus compounds more strongly than the cholinesterase enzyme, revealed three candidate organic compounds: hydroxy amino acid esters, phenols, and hydroxylamine (4:6-8). For the hydroxy amino acid esters, the amine function (NH<sub>2</sub>) of the hydroxy amino acid ester can be phosphorylated (4:7):

Hydroxy amino Diisopropylacid ester chlorophosphate (DClP) For the hydroxylamine compound, the oxygen atom serves as the phosphorylated nucleophilic center rather than the nitrogen atom (4:7):

For the phenolic compounds (which is a benzene ring with one or more OH groups), the phenolate ion serves as the nucleophilic center (4:8):

$$\begin{array}{c} O \\ \parallel \\ F-P-C_2H_7 \\ \downarrow \\ OC_3H_7 \end{array} + \begin{array}{c} OH \\ \longrightarrow OH$$

Diisopropylfluorophosphate (DFP)

It was also found that histidine can act as a catalyst in the hydrolysis of DFP. In histidine, the tertiary amine structure was responsible for catalytic activity (2:9):

The investigation for the compounds that would reactivate the phosphorylated cholinesterase enzyme revealed three types of compounds: phenols, hydroxamic acids, and oximes (4:12).

The anions of these compounds cause nucleophilic displacement reactions with the phosphorus esters, and thus, they reactivate the phosphorylated cholinesterase enzyme.

#### Solid State Chemical Sensors

During the past decade, a number of solid state chemical sensors have been investigated for detecting organophosphorus compounds. These sensors are usually based on measuring some physical or electrical property of a thin film that undergoes a change when exposed to organophosphorus compounds. These sensors include the piezoelectric sorption detector, the chemiresistor, the Chemically-Sensitive Field-Effect Transistor (CHEMFET), and the notch filter detector (1:2-1). The next section discusses the basic operation of these sensors.

Piezoelectric Sorption Detector.

The piezoelectric effect is manifested by a crystal that mechanically deforms when an electric field is applied.

A piezoelectric crystal, which manifests the piezoelectric effect, will mechanically oscillate at a characteristic frequency known as the resonant frequency, when a timevarying electric field is applied. In a piezoelectric sorption detector, a piezoelectric crystal is coated with a material capable of selectively interacting with a chemical compound of interest, by either the absorption or adsorption process. Whenever the mass of the crystal's coating changes by the absorbed/adsorbed gas, the resonant frequency of the crystal correspondingly changes. Thus, by detecting the change in the crystal's resonant frequency, the concentration of the chemical compound can be measured (5:44). One significant problem associated with the piezoelectric sorption detector, however, is its inability to discriminate between a specific chemical compound and a very broad range of contaminants that can also be adsorbed on the crystal's coating.

A number of coatings have been investigated for detecting organophosphorus compounds using the piezoelectric detector. In 1972, Schiede and Guilbault evaluated a piezoelectric crystal detector that was coated with various inorganic salts: FeCl<sub>3</sub>, CuCl<sub>2</sub>, NiCl<sub>2</sub>, and CdCl<sub>2</sub> (6:1764-1768). The inorganic salt with the highest sensitivity (FeCl<sub>3</sub>) detected DIMP at concentration levels less than 10 ppm (parts-per-million) (6:1767). In 1981, Guilbault and his co-workers reported the evaluation of a piezoelectric

sorption detector for detecting organophosphorus compounds (5:43-47). The coatings evaluated were L-histidine hydrochloride, DL-histidine hydrochloride, succinylcholine chloride, succinylcholine iodide, 1-dodecyl-2-hydroximino-methylpyridinium iodide (2-PAD), and 1-n-dodecyl-3-hydroximinomethylpyridinium iodide (3-PAD). The piezoelectric scrption detector with a ternary coating mixture of 3-PAD, Triton X-100 and NaOH was able to detect DIMP concentrations in the parts-per-billion (ppb) range (5:52).

### Chemiresitor Detector.

The chemiresistor detector is based upon measuring the change in the conductivity of a membrane resulting from the device's exposure to a chemical environment (7:1170). As shown in Figure II.2, a chemically-sensitive material is deposited on an interdigitated electrode. During operation, the conductivity of the material is monitored while the coated interdigitated electrode is exposed to a chemical challenge gas. Thus, the chemiresistor measures only one aspect of the film's response, the direct current conductivity.

In 1985, Barger and co-workers evaluated chemiresistors with a number of organic derivatives of phthalocyanine (PC) and metal-substituted phthalocyanine films (MPC) for sensitivity to DMMP (8:410-413). The phthalocyanine films evaluated were lead, zinc, copper, platinum, nickel, palladium, cobalt, and hydrogen (H<sub>2</sub>) phthalocyanine. Among

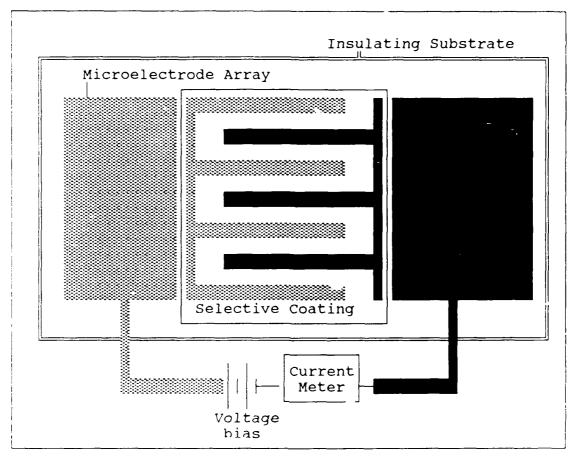


Figure II.2. Schematic of a Chemiresistor Structure (7:1170).

these, the nickel-Pc showed the greatest sensitivity to a 2 ppm (10  $\mu$ g/L) concentration of DMMP with a corresponding 128% change in its conductivity (8:412).

### CHEMFET Detector.

The CHEMFET detector is based on the sensitivity of a field-effect transistor's channel resistance to changes in the chemical composition of its gate electrode (9:107-174). An interdigitated electrode coated with a chemically-sensitive thin film, similar to the chemiresistor, is used

to replace the conventional gate electrode of Metal-Oxide-Semiconductor Field-Effect Transistor (MOSFET). Thus, in essence, the CHEMFET can be analyzed as the integration of a miniaturized chemical sensor and a MOSFET amplifier.

In 1981, an assessment of the potential application of a CHEMFET for detecting organophosphorus compounds concluded that the CHEMFET structure based on measuring changes in the membrane's work function is the optimum device configuration (10:666-671). The assessment further suggested that an organic compound with semiconductor properties may be best suited for the gate electrode's thin film coating material.

In 1988, a CHEMFET consisting of an interdigitated electrode coated with copper phthalocyanine was fabricated and investigated by Wiseman (1, 2). The CHEMFET was found to be sensitive to DIMP spanning a concentration range of 0.1 - 4 ppm (1:5-39, 2). Wiseman also reported that when a voltage pulse excitation was applied to the interdigitated electrode, the characteristic response of the CHEMFET changed as a function of the adsorbed chemical species and the material used for the thin film.

### Notch Filter Detector.

The notch filter detector for organophosphorus compounds, developed by Kolesar, is a frequency-dependent electrical network which has a null in its transfer function (11, 12). When exposed to a chemical compound of interest, the conductivity of a thin chemically-sensitive and highly

resistive film changes, resulting in a shift in the null frequency, as well as the depth of the null (notch). Thus, the fundamental principle of the notch filter detector is the measurement of the change of a chemically-sensitive membrane's conductivity upon exposure to an environment containing a chemical species of interest.

A notch filter consists of a highly conductive electrode, a dielectric layer, and a resistive electrode. In the notch filter detector for organophosphorus compounds, Kolesar used a discontinuous copper and cuprous oxide film for the resistive electrode. The detector was able to measure concentrations of DIMP at less than 10 ppm (11:404, 12).

### Chemically-Sensitive Thin Films

A number of different thin film candidates were screened with the CHEMFET in this thesis. These thin films were of two types: organic semiconductors and organic compounds. The organic semiconductor thin films were metaldoped phthalocyanine and 2-naphthol( $\beta$ ). The other organic compounds were L-histidine dihydrochloride, succinylcholine chloride, and succinylchloride. This section presents background information concerning the thin films used in this thesis research.

### Organic Semiconductors.

The 1°51 assessment of a CHEMFET for detecting organophosphorus compounds recommended the utilization of organic compounds with semiconductor properties as being the best candidates for the work function dependent CHEMFET (10:666-671). These organic semiconductors have conventional semiconductor properties, such as a decrease in resistance with increasing temperature. However, unlike conventional inorganic semiconductors, the conduction mechanisms in organic semiconductors are not yet fully understood.

As potential thin film candidates to be used with the CHEMFET for detecting organophosphorus compounds, several semiconducting polymers have been evaluated since 1980. For example, in 1982, poly(1,2,4,5-tetraaminobenzene copper(II) chloride) [Cu(TAB)], poly(1,2,4,5-tetraaminobenzene nickel(II) chloride) [Ni(TAB)], poly(vinylbenzylchloride) + tetramethylenediamine copper(II) chloride, and polyvinyl-pyrolidone + 2,2'-bipyridine copper(II) chloride were evaluated (13:3). This evaluation revealed that Cu(TAB) and Ni(TAB) were not suitable, while poly(vinylbenzylchloride) + tetramethylenediamine copper(II) chloride and polyvinyl-pyrolidone + 2,2'-bipyridine copper(II) chloride showed some promise.

In 1988, the copper-doped phthalocyanine thin film was first used with the interdigitated gate electrode CHEMFIT

for detecting DIMP by Wiseman (1, 2). Historically, the metal-doped phthalocyanine thin film was used for detecting NO<sub>2</sub>, because the phthalocyanines were known to be very sensitive to electron donor gases. However, as Wiseman's thesis reports, the metal-doped phthalocyanine thin films can also be used for detecting organophosphorus compounds as well. Figure II.3 shows the chemical structure of a metal-doped phthalocyanine.

Another organic semiconductor used in this thesis was 2-naphthol( $\beta$ ), shown in Figure II.4. A study in 1975 reported that, in comparison with phthalocyanine (metalfree), 2-naphthol( $\beta$ ) may be more suitable for detecting organophosphorus compounds (15:11). In this study, a metalfree phthalocyanine and 2-naphthol( $\beta$ ) were used as coatings for a chemiresistor. It was reported that, while phthalocyanine has a high sensitivity (manifested by change in conductivity) to  $NO_2$ , 2-naphthol( $\beta$ ) showed a similar high sensitivity to phosphorus containing compounds ((CH3O),POF and (EtO),PO), in the concentration range of 0.5 ppm to 57 ppm (15:10). This potential sensitivity to organophosphorus compounds is further supported by 2-naphthol( $\beta$ )'s structural similarity with the phenols (see Page II-5), which are also known to be reactive toward organophosphorus compounds (4:8).

### Other thin films.

The other thin films studied in this thesis research were L-histidine dihydrochloride, succinylcholine

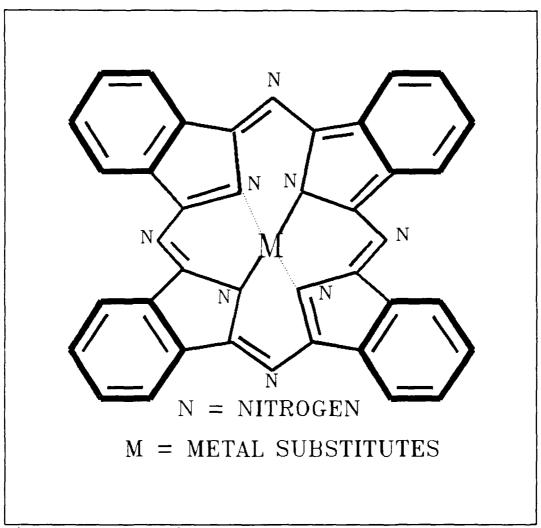


Figure II.3. Chemical Structure of a Metal-Doped Phthalocyanine (14:374).

chloride, and succinylchloride. L-histidine dihydrochloride  $(C_6H_9N_3O_2\cdot 2HCl)$  and succinylcholine chloride  $([CH_3)_3)$   $NCH_2CH_2OCOCH_2$   $Cl_2\cdot 2H_2O)$  were used earlier as coatings for a piezoelectric sorption detector configured for detecting organophosphorus compounds (5). As discussed earlier (see Page II-5), histidine is a catalyst for the hydrolysis of a certain organophosphorus compound (DFP), and thus, L-

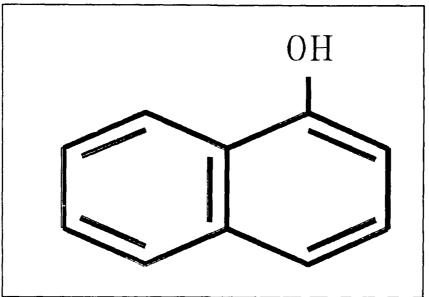


Figure II.4. Chemical Structure of 2-Naphthol( $\beta$ ) (14:924).

histidine dihydrochloride may prove to be a suitable thin film to be used with the interdigitated gate electrode CHEMFET for detecting organophosphorus compounds.

Succinylcholine chloride was also considered to be a potential candidate for detecting organophosphorus compounds. This assumption was based upon the fact the "choline" structure of succinylcholine chloride is the same "choline" structure found in acetylcholine.

As discussed earlier (see Page II-7), a number of chlorine containing inorganic salts were used as coatings for a piezoelectric crystal detector for detecting DIMP (6). As a chlorine containing organic compound, succinylchloride (ClCOCH<sub>2</sub>CH<sub>2</sub>COCl) was also considered to be a potential

candidate thin film for use with the interdigitated gate electrode CHEMFET.

## Basic Properties.

Table II.1 shows the basic properties of the undoped phthalocyanine and the other organic thin film materials evaluated in this thesis.

### Theory of the CHEMFET in the Frequency-Domain

In the interdigitated gate electrode CHEMFET, a chemically-sensitive thin film is deposited over the gate structure, which is connected to a MOSFET amplifier. The theory of the impedance measurements of materials using an interdigitated gate electrode CHEMFET design has been explained by Wiseman (1:3-1, 2). As discussed by Wiseman, a change in the chemical state of the thin film produces a change in the electrical impedance of the film, and thus, electrical impedance measurements can be used to probe the chemical state of a thin film coating (1:3-20, 2).

One method for measuring the electrical impedance of the thin film which was introduced by Wiseman, is to apply Fourier transform techniques to measure the associated harmonic changes in the CHEMFET sensor's response signal (1:3-11). Since the chemical state of the deposited film determines its impedance, it also determines the input impedance to the MOSFET's gate electrode. When a pulsed excitation is used to excite the driven gate electrode, an amplified response is reflected at the output of the

Table II.1 Basic Properties of Thin Film Materials (14).

Solvents	Acetone	Acetone	Water Acetone	Water	1
Melting Point (°C)		121-122	240-245	159-164	15-18
Molecular Mass	514.25	144.18	228.08	387.36	154.98
Chemical Formula	C32H18N8	C <sub>10</sub> H <sub>8</sub> O	C <sub>6</sub> H <sub>9</sub> N <sub>3</sub> O <sub>2</sub> 2HCl	$C_{14}H_{30}C1_{2}N_{2}O_{4}$ 2H <sub>2</sub> O	C,H,Cl <sub>2</sub> O <sub>2</sub>
	Phthlocyanine	2-Naphthol $(eta)$	L-histidine dihydrochloride	Succinylcholine Chloride	Succinychloride

amplifier. The corresponding Fourier transform of this time-domain response signal contains spectral components which can be correlated with the state of the chemical reaction in the film (1:3-21). As background information, this section discusses the theory behind the Fourier transform and how the Fourier transform of a time-domain signals can be used to determine a change in the chemical state (impedance) of a thin film. Next, the desired frequency-dependent characteristics associated with the excitation pulse and the MOSFET amplifier are discussed.

### Fourier Series.

Mathematically, any vector of finite length can be expressed as a sum of its components along n-mutually orthogonal vectors, provided that these vectors form a complete set of mutually perpendicular coordinates (16:17). The representation of a function f(t) by an infinite set of mutually orthogonal functions is called a generalized Fourier series representation, and one such representation is the exponential Fourier series representation (16:26):

$$f(t) = \sum_{n=-\infty}^{\infty} F_n e \qquad (t_1 < t < t_2) \qquad (2.1)$$

where

$$F_n = \frac{1}{(t_2 - t_1)} \int_{t_1}^{t_2} f(t) e^{-jn\omega_0 t} dt$$
 (2.2)

For a periodic function whose period is T, f(t) = f(t+T), the Fourier series representation is given by (16:35):

$$f(t) = \sum_{n}^{\infty} F_n e$$
 (2.3)

where the line spectrum,  $F_n$ , is (16:46):

$$F_{n} = \frac{1}{T} \int_{-T/2}^{T/2} f(t) e^{-jn\omega_{o}t} dt$$
 (2.4)

and 
$$\omega_0 = \frac{2\pi}{T}$$
 . (2.5)

## Fourier Transform.

The Fourier transform of a function f(t) is defined as (16:80-81):

$$F\{f(t)\} = F(\omega) = \int_{-\infty}^{\infty} f(t) e dt$$
 (2.6)

which is essentially

$$F(\omega) = T \times F_n$$
 as  $T \to \infty$ .

Consequently, the Fourier transform (spectral density) of a periodic function, f(t) = f(f+T), is given by (16:90):

$$F(f(t)) = F(\omega) = 2\pi \sum_{n=-\infty}^{\infty} F_n \delta(\omega - n\omega_0)$$
 (2.7)

where  $F_n$  is the line spectrum from Equation (2.4). In other words, the Fourier transform of a periodic signal consists of a set of impulse functions located at the harmonic frequencies of the signal. The weight of each impulse is  $2\pi$  times the value of its corresponding expenential Fourier series coefficient (16:90).

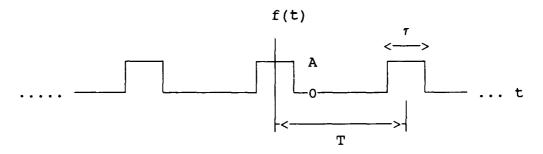
Generally, the shape of the periodic signal determines  $F_n$ , which describes the envelope of the spectral density, while the period of the signal determines the harmonic frequencies. For instance, a rectangular function,  $f(t) = \text{rect}(t/\tau), \text{ where}$ 

$$rect(t/\tau) = \begin{cases} 1 & |t| \le \tau/2 \\ 0 & |t| > \tau/2 \end{cases}$$
 (2.8)

has as its Fourier transform, the sinc function (16:88):

$$F(\omega) = \tau \frac{\sin(\omega\tau/2)}{(\omega\tau/2)}$$
 (2.9).

Correspondingly, a periodic function, f(t) = f(t+T), like the example below:



has the Fourier transform of Equation (2.7), with

$$F_{n} = \frac{A\tau}{T} \frac{\sin(n\omega_{o}\tau/2)}{(n\omega_{o}\tau/2)} = \frac{A\tau}{T} \frac{\sin(n\pi\tau/T)}{(n\pi\tau/T)}$$
(2.10)

where  $\omega_0 = 2\pi/T$ 

which has a sinc function envelope. Thus, the shape, or envelope, of the spectrum is dependent upon the pulse shape (for instance, rectangular pulse, triangular pulse, etc).

There is an inverse relationship between the pulse duty cycle,  $\tau/T$ , in the time-domain and the associated frequency "spread" in the frequency-domain (16:48). As expressed in Equation (2.10), for a shorter duty cycle,  $\tau/T$ , in the time-domain (for example, approaching that of an impulse signal whose Fourier transform is a constant), the corresponding line spectrum,  $F_n$ , remains constant for a larger number of n.

### CHEMFET Response in the Frequency-Domain.

The chemically-sensitive thin films used in the interdigitated gate electrode CHEMFET typically have very high impedances. When a rectangular pulse is applied to the driven gate of the interdigitated gate electrode, a distorted pulse similar to that shown in Figure II.5 is measured at the output of the CHEMFET. The shape of the distorted pulse, which is dependent on the impedance of the film, will change if the film's chemical state changes; for example, when the film is exposed to a certain chemical challenge gas. Since the change in the shape of the pulse

can be detected by measuring the change in the envelope of the corresponding Fourier frequency spectrum, the change in film's impedance (chemical state) can be detected by measuring the change in the envelope of the frequency spectrum of the Fourier transformed pulse.

## Characteristics of the Excitation Pulse.

The shape of the time-domain excitation pulse is important because the shape of the original pulse will influence the shape of the corresponding frequency-domain's envelope associated with the CHEMFET's response. Since the objective is to detect the change in the thin film's impedance spanning a broad range of frequency, it is

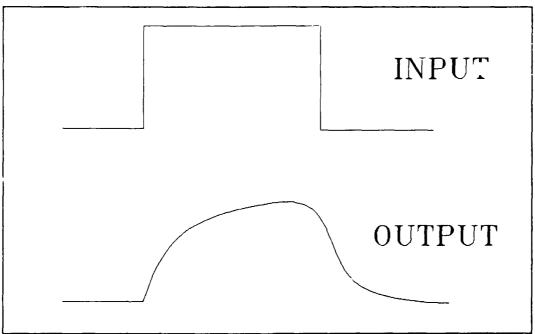


Figure II.5. Typical Input and Output Time-Domain Pulse Waveform of the CHEMFET.

essential that the excitation pulse contains sufficient spectral energy at each harmonic frequency within the bandwidth of interest. Otherwise, a change in spectral magnitude, at a frequency where the excitation pulse did not have sufficient spectral energy would not be revealed.

Thus, an ideal excitation pulse to use with the CHEMFET would be an impulse signal, which has a constant spectral density at each frequency. Since the impulse signal cannot be realized in the real world, the best candidate is a pulse with a very short pulse duration; this approximation will have relatively constant spectral energy spanning a broad frequency range.

However, another consideration has to be given before choosing the amplitude and width of the excitation pulse. The average power of a signal, P, which influences the magnitude of the components in the corresponding spectrum, is a function of the pulse amplitude, duration, and period (17:15):

$$P = \frac{1}{T} \int_{-T/2}^{T/2} f^{2}(t) dt = \sum_{n=-\infty}^{\infty} |F_{n}|^{2}$$
 (2.11)

$$= \frac{1}{T} \int_{-\tau/2}^{\tau/2} A^2 dt , \quad f(t) = \begin{cases} A & |t| \le \tau/2 \\ 0 & |t| > \tau/2 \end{cases} . \quad (2.12)$$

Thus, in order to maximize the average power, a pulse with large amplitude (A), long duration (7), and short period (T) should be chosen. But a long pulse duration and short period will degrade the frequency "spread" of the spectrum. Thus, in order to maximize the magnitude of the spectral components, an optimum pulse with high average power should be chosen, without sacrificing the frequency "spread" of the spectrum within the frequency range of interest.

### Characteristics of the MOSFET Amplifier.

One requirement for the MOSFET amplifier in the CHEMFET is high gain. This requirement exists because the chemically-sensitive thin films used in the CHEMFET typically have very high impedances (for example, greater than  $10^9$  ohms at DC). Thus, when an excitation pulse is applied to the driven gate of the interdigitated gate electrode, the pulse response at the floating gate typically has a maximum pulse amplitude which is two or more orders of magnitude less than the original pulse. However, since the floating gate is attached to the gate of the MOSFET, the pulse is amplified at the drain of the MOSFET. this amplification (gain) should be large. Otherwise, the amplified CHEMFET's response will not have sufficient signal energy to permit reliable electrical measurements. Thus, the MOSFET amplifier in the CHEMFET must provide sufficient gain to allow measurements.

Additionally, in frequency domain, the MOSFET amplifier must also have a constant gain and a large 3-dB cut-off frequency. These two characteristics will allow all the frequencies in the range of interest to be amplified with the same gain.

For these MOSFET amplifier design considerations, the de ice geometry must be optimized to provide a large constant gain and high operating frequency. The MOS transistor gain factor,  $\beta$ , which is dependent on both the process parameters and the transistor geometry, is given by (18:40):

$$\beta = \frac{\mu_{n}\epsilon}{t_{ox}} \left\{ \frac{W}{L} \right\}$$
 (2.13)

where  $\mu_{\rm n}$  is the effective surface mobility of the electrons in the channel,  $\epsilon$  is the permittivity of the gate oxide,  $t_{\rm ox}$  is the thickness of the gate oxide, W is the width of the channel, and L is the length of the channel. The maximum operating frequency of a MOSFET is given by (19:207):

$$f_t = \frac{\mu_n V_D}{2\pi L^2}$$
 (2.14)

where  $V_0$  is the drain voltage. Thus, for a large constant gain and high operating frequency, the geometry of MOSFET must be designed with a large (W/L) ratio and a small L.

### Summary

In this Chapter, background information concerning organophosphorus compounds, their associated chemical reactions, and candidate chemically-sensitive thin films for detecting these toxic compounds were presented. Also surveyed were different types of solid state sensors which could be utilized for detecting the organophosphorus compounds, of which the interdigitated gate electrode CHEMFET was one. Finally, the theoretical background of the CHEMFET's operation in frequency-domain was presented.

# III. CHEMFET Design,

# Fabrication, and Operational Characteristics

This chapter describes the design, fabrication results, and operational characteristics of the interdigitated gate electrode CHEMFET.

### Design

The interdigitated gate electrode CHEMFET design was implemented using the MOSIS (Metal Oxide Semiconductor Implementation Service) 2 µm CMOS (Complementary Metal Oxide Semiconductor) double-level metal technology, using Magic, the VLSI (Very Large Scale Integration) CAD (Computer Aided Design) software program. As shown previously in Figure I.1, the overall CHEMFET design included ten interdigitated gate electrode structures, a 10 X 1 multiplexer connecting the 10 floating gates to the test amplifier, and a reference amplifier. The design also included a pn-junction diode and sixty-four bond pads.

### Interdigitated Gate Electrode.

The interdigitated gate electrode, whose design was based upon the interdigitated electrode design used in the previous AFIT research, was implemented using second-level metal, with the dimensions shown in Table III.1.

Table III.1. Interdigitated Gate Electrode Characteristics.

Number of Fingers on Driven Gate	30	
Number of Fingers on Floating Gate	29	
Finger Width $(\mu m)$	8	
Finger Separation $(\mu m)$		
Overall Array Length (µm) 3800		
Overall Array Width (µm) 93		

## Multiplexer.

The 10 X 1 multiplexer was designed with a 4-input decoder and 10 transmission gates. Figure III.1 shows the overall structure. The four inputs to the decoder (S0, S1, S2, and S3) were inverted once to drive the complementary values, and then inverted twice to drive the uncomplementary

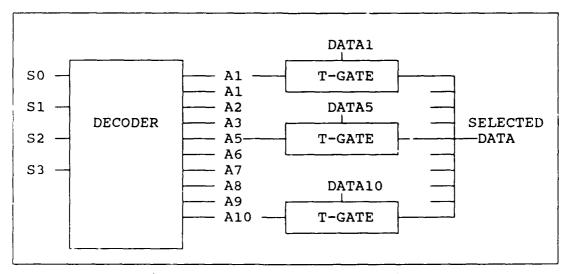


Figure III.1. CHEMFET Multiplexer.

values. For example, Figure III.2 shows the detailed design of the fifth (0100) select line, A5, and the associated transmission gates.

The decoder has its pull-up p-transistors always on, which maintains a signal high-level at the select line nodes. When SO,  $\overline{S1}$ , S2, and S3 are all at a signal low, the n-transistors are all off, and the select line, A5, remained high. However, if any of SO,  $\overline{S1}$ , S2, or S3 were at a signal high, then at least one n-transistor was on, and the select line became a signal low. The p-transistors and n-transistors were designed (sized) such that the resistance across the n-transistor was much lower than the resistance across the p-transistor, and consequently, the largest voltage value is dropped across the p-transistor when both the p- and n-transistors are on. The transmission gates

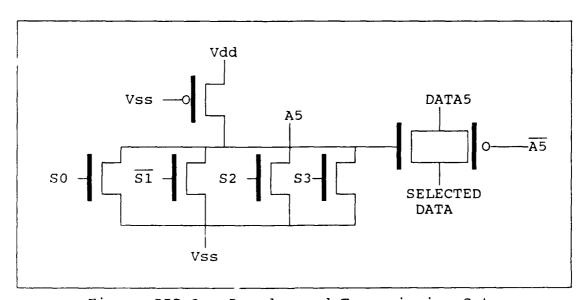


Figure III.2. Decoder and Transmission Gates.

passed the data only when the selected line, A5, was at a signal high.

The channel resistance associated with a MOS transistor,  $R_{\rm c}$ , is given by (18:121):

$$R_c = k (L/W) (3.1)$$

where L is the channel length, W is the channel width, and k is a material constant which is inversely proportional to the carrier mobility,  $\mu$ .

## Amplifier.

The MOSFET amplifier was initially designed for a signal gain of 1000 and a 3-dB cut-off frequency of 10 MHZ. To realize this 3-dB cut-off frequency, the amplifier was designed with feedback, which increased its bandwidth at the expense of signal gain. For the basic amplifier, a differential input comparator design shown in Figure III.3 was used (20:330). To increase the signal gain and the operating frequency, a large channel width and small channel length were used for the transistors in the basic amplifier. The actual transistor geometry was optimized through SPICE simulations.

To achieve the desired 3-dB cut-off frequency, this basic amplifier was combined with a feedback network, shown in Figure III.4. The voltage gain with feedback,  $A_{\rm f}$ , is given by (21:541):

$$A_{f} = \frac{\text{Vout}}{\text{Vin}} = \frac{A}{1 + \beta A}$$
 (3.2)

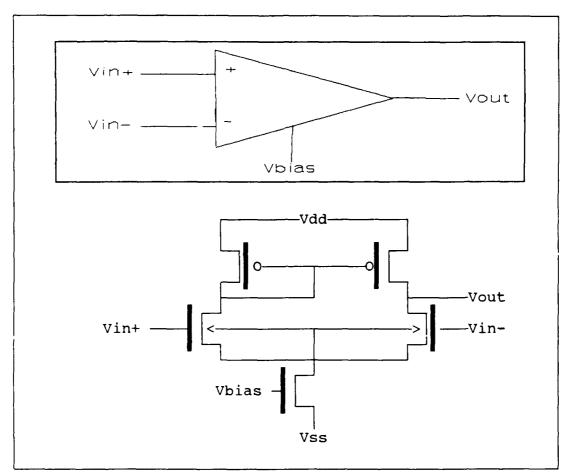


Figure III.3. Differential Input Comparator (20:330).

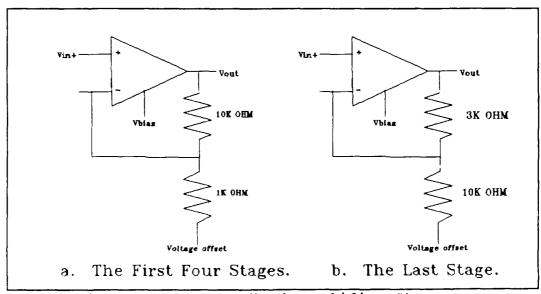


Figure III.4. Feedback Amplifier Stages.

where A is the voltage gain of the basic amplifier, and  $\beta$  is the proportionality factor. The  $\beta$  used in Figure III.4a is (1/11) and in Figure III.4b it is (10/13). The resistor values and  $\beta$  values were optimized through SPICE simulations. Because of the feedback, the overall gain of the amplifier in Figure III.4a decreased to approximately 2.5. To achieve a reasonable signal gain of 40, four stages of the feedback amplifier design shown in Figure III.4a were used. To further increase the 3-dB cut-off frequency, a fifth amplifier stage, shown in Figure III.4b was added. Thus, the CHEMFET amplifier was designed with five amplifier stages to achieve a signal gain of 32 dB and a 3-dB cut-off frequency of 10 MHZ. The results of the SPICE simulation used to verify the design is shown in Table B-1 in Appendix B.

Figure III.5 shows the CIF (Caltech Intermediate Form) plot of the first feedback amplifier stage. For the resistors, n-diffusions were used.

#### Related Component Designs.

Additional components in the interdigitated gate electrode CHEMFET IC included the arrangements of the 64 bonding pads. Each bond pad was designed to be 400  $\mu m$  by 400  $\mu m$ . The total interdigitated gate electrode CHEMFET die area was 7.9 mm by 9.2 mm.

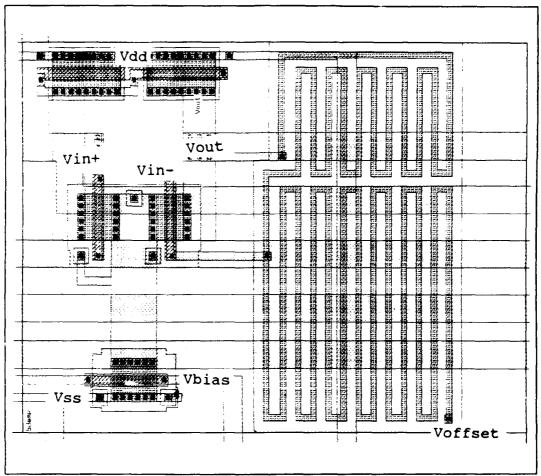


Figure III.5. CIF plot of the First Amplifier Stage.

### Fabrication

The CHEMFET design was submitted to MOSIS for fabrication. Twelve unpackaged die and twelve packaged die were received approximately eight weeks after they were submitted to MOSIS. Table B-4 in Appendix B contains the MOSIS Process Characterization Data Sheet associated with the interdigitated gate electrode CHEMFET's fabrication. The data sheet includes the performance of the MOSIS test transistors and a comparison with the predicted performance

from an associated SPICE model analysis. The data sheet also includes information concerning the critical fabrication process parameters, such as gate oxide thickness.

Figure III.6 depicts a photomicrograph of the fabricated CHEMFET die. As shown, the ten interdigitated

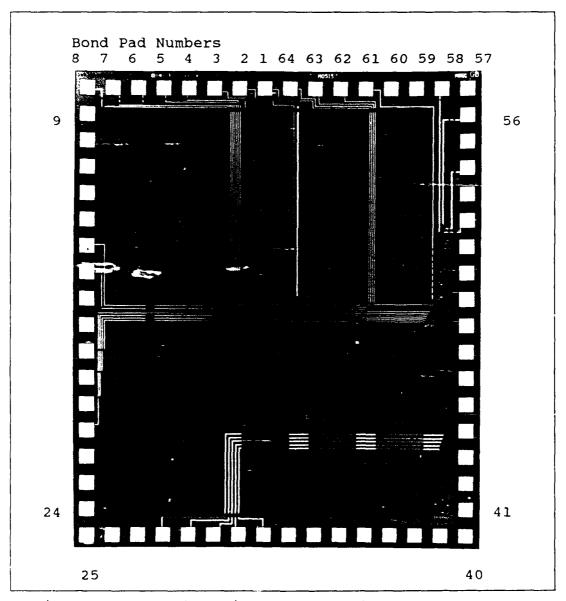


Figure III.6. Photomicrograph of the CHEMFET IC.

gate electrode structures were arranged in two rows of five elements each. The 10 X 1 multiplexer and the test amplifier stages are located along the right-hand edge of the die. The die was packaged in a standard 64-pin dual-in-line (DIP) package. Table III.2 summarizes the function of each bond pad, as numbered in Figure III.6.

Table III.2. CHEMFET Bond Pad Function Summary.

Pad	Number	r	Signal Name and Function
	1	A7,	Select Line 7 from Decoder
	2	A6,	Select Line 6 from Decoder
	3	DG,	Driven Gate for F6 to F10
	4	A5,	Select Line 5 from Decoder
	5	,	Select Line 4 from Decoder
	6		Select Line 3 from Decoder
	7		Select Line 2 from Decoder
	8	•	Select Line 1 from Decoder
	à	Not	Uscd
	10		Used
	11		Used
	12		, Floating Gate 10
	13		Floating Gate 9
	14		Floating Gate 8
	15		Floating Gate 7
	16		Floating Gate 6
	17		Floating Gate 5
	18		Floating Gate 4
	19		Floating Gate 3
	20		Floating Gate 2
	21	F1,	Floating Gate 1
	22		Used
	23		Used
	24	_	Used
	25		Used
	26		Used
	27		Driven gate for F1 to F5
	28		Reference Amplifier First Stage Output
	29		Reference Amplifier Second Stage Output
	30		Reference Amplifier Third Stage Output
	31		Reference Amplifier For th Stage Output
	32	The	Reference Amplifier Fitch Stage Output

```
33
      The Reference Amplifier First Stage Offset Voltage
34
      The Reference Amplifier Second Stage Offset
        Voltage
35
      The Reference Amplifier Third Stage Offset Voltage
36
      The Reference Amplifier Fourth Stage Offset
        Voltage
37
      The Reference Amplifier Fifth Stage Offset Voltage
38
      Input to the Reference Amplifier
      Vn, Diode Voltage at n-diffusion
39
40
      Vp, Diode Voltage at p-diffusion
      Vss, The Negative Voltage Supply to Reference
41
        Amplifier
      Vbias, The Bias Voltage of Reference Amplifier
42
43
      Vdd, The Positive Voltage Supply to Ref. Amp.
      S3, The first bit in the 4-input decoder
44
45
      S2, The second bit in the 4-input decoder
46
      S1, The third bit in the 4-input decoder
      SO, The fourth bit in the 4-input decoder
47
      Vss, The Negative Voltage Supply to CHEMFET
48
49
      Vdd, The Positive Voltage Supply to CHEMFET
50
      Vbias, The Bias Voltage of Test Amplifier
51
      The Test Amplifier First Stage Offset Voltage
52
      The Test Amplifier First Stage Output
53
      The Test Amplifier Second Stage Offset Voltage
54
      The Test Amplifier Second Stage Output
55
      The Test Amplifier Third Stage Offset Voltage
      The Test Amplifier Third Stage Output
56
57
      The Test Amplifier Fourth Stage Offset Voltage
58
      The Test Amplifier Fourth Stage Output
59
      The Reference Amplifier Fifth Stage Offset Voltage
60
      Out, The Test Amplifier Fifth Stage Output
61
      MUX Output/Input to the Test Amplifier
      Alo, Select Line 10 from Decoder
62
63
      A9, Select Line 9 from Decoder
      A8, Select Line 8 from Decoder
64
```

## Operational Characteristics

Preliminary Electrical Performance.

The preliminary electrical performance of the multiplexer and amplifier stages was initially investigated. The results revealed proper functioning of all the circuits,

which indicated that no fatal errors were committed in the design process. However, the amplifiers were very susceptible to permanent failures when an abrupt change in the power supply voltage was made. Also, some die revealed there was severe current leakage occurring in the multiplexer. Since there were other die which worked perfectly, it was determined that these leakage currents were the result of individual fabrication variations. Further inspection of the die revealed a few shorted interdigitated electrodes. Figure III.7 depicts a typical shorted interdigitated gate electrode. As shown, the short



Figure III.7. Example of a Shorted Interdigitated Gate Electrode.

was due to a surface scratch. This defect was likely caused by improper handling, since the electrode area was not protected with passivation glass.

## Amplifier Stages.

Figure III.8 shows the DC voltage characteristics measured at the five amplifier stages of the CHEMFET, using the Hewlett-Packard, Model HP 4145B, Semiconductor Parameter Analyzer. The amplifier stages had their Vbias set at 0 V, and all Voffsets were set at 0.074 V, which centered each amplifier's operational point in the vicinity of 0 V. As

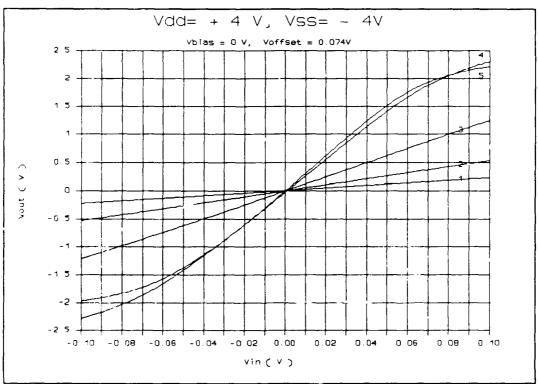


Figure III.8. DC Voltage Characteristics of the Five Amplifier Stages.

shown, the output at the fourth stage had slightly higher gain than at the fifth stage. The fifth stage, however, increased the 3-dB cut-off frequency.

The gain and phase of the CHEMFET, measured with the Hewlett-Packard, Model HP 4194A, Gain/Phase Analyzer, are shown in Figures III.9 and III.10. Using a supply voltage of  $\pm 4$  V, the CHEMFET (from one of the floating gates, through the multiplexer, to the output of the amplifier) had a relatively flat gain of 29.3 dB, which was similar to the

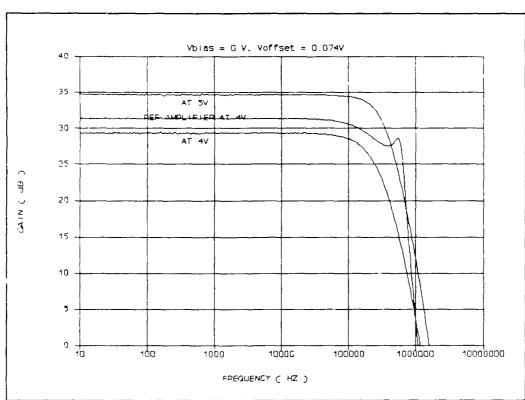


Figure III.9. Gain of the Interdigitated Gate Electrode CHEMFET's Amplifier versus Frequency.

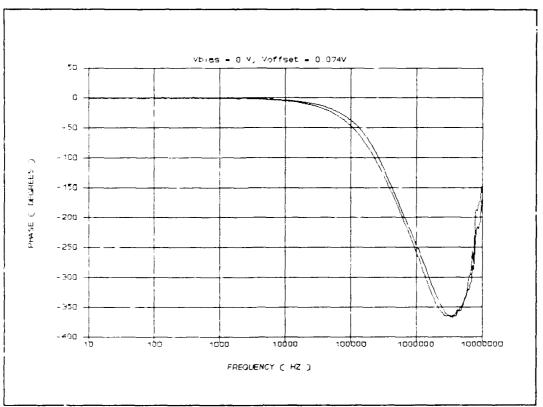


Figure III.10. Phase of the Interdigitated Gate Electrode CHEMFET's Amplifier versus Frequency.

gain predicted from the SPICE simulation. The 3-dB cut-off frequency was approximately 200 KHZ. Without the multiplexer, the reference amplifier had a gain of 31.3 dB, and it had a 3-dB cut-off frequency of approximately 600 KHZ.

With a larger ±5 V supply voltage, the CHEMFET's gain increased to 34 dB, while the 3-dB cut-off frequency increased to 280 KHZ. The phase did not change significantly with the change in the supply voltage.

One unusual operational characteristic of the amplifier occurred when the input to the amplifier was open-circuited; the output floated to 2.75 V. The consequence of this charateristic, revealed in the experiment, was that when there was not sufficient leakage current through the chemically-sensitive thin film to the floating gate at 0 V, the amplifier's output rose to 2.75 V.

There was concern for the total voltage difference supplied to the CMOS transistors, which were normally designed to operate within 0-5 V. Thus, a  $\pm 4$  V supply instead of  $\pm 5$  V, was used for Vdd and Vss which resulted in a total potential difference of 8 V across the transistors.

## Multiplexer.

As shown in the gain plot (Figure III.9), the transmission gates of the multiplexer introduced attenuation with respect to the gain and frequency. The DC resistance across selected transmission gates of the multiplexer were measured with an electrometer (Keithley Instruments, Model 617, Cleveland, OH) to be 600 ohms when the transmission gates were "on". When the transmission gates were "off", the DC resistance across the transmission gates was on the order of  $2 \times 10^3$  ohms.

### Discrepancies and Design Errors

## Discrepancies.

The only significant discrepancy between the interdigitated gate electrode CHEMFET design and the actual operational characteristics was, of course, the 3-dB cut-off frequency. The design SPICE simulation, included in Table B-1 in Appendix B predicted a 3-dB cut-off frequency of 10 MHZ at a ±5 V supply. When a load capacitance of 30pF was added, the SPICE simulation (Table B-2, Appendix B) predicted a 3-dB cut-off frequency of 1.4 MHZ. The actual 3-dB cut-off frequency measured with ±5 V supply was 280 KHZ. The input resistance and capacitance of the gain/phase analyzer, with which the gain measurement was made, was specified to be 28 ±3 pF and 1M ohm, respectively.

Another SPICE simulation (Table B-3) was conducted with a load capacitance of 200 pF, and it predicted a 3-dB cutoff frequency of 280 KHZ, indicating that the discrepancy between the design and the actual 3-dB cut-off frequency is likely due to the total load capacitance which consists of the test fixture, microprobes, coaxial cables, connectors, and the instrument itself.

#### Design Errors.

A significant conceptual error in the interdigitated gate electrode CHEMFET's design was committed during the design stage of this thesis. This error occurred due to the

effect of the high impedance of the chemically-sensitive thin films was not properly considered.

As shown in Figure III.11, the floating gate component of the interdigitated gate electrode of the CHEMFET was connected directly to the transmission gates in the multiplexer. When the transmission gates were "off", because that particular select line was not selected, the resistance across the transmission gate was 10° ohms. In digital applications, this order of resistance would normally isolate a signal at the floating gate from Node 1, provided the resistance across the floating gate was several orders of magnitude less than 10° ohms. However, in this analog application, the resistance across the film was typically 10° ohms, which is approximately the same order

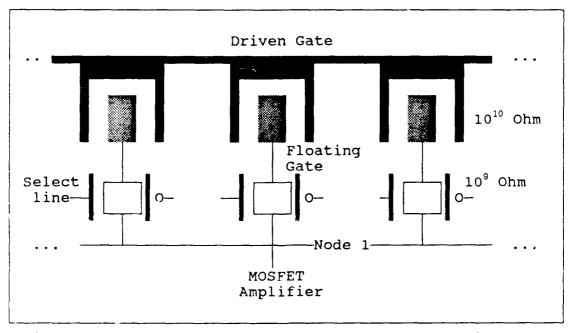


Figure III.11. Floating Gates Connected to Multiplexer.

of magnitude as the "isolation" resistance. Thus, the level of isolation between the different floating gates does not really exist because they were all tied together at Node 1. If the driven electrode components on each interdigitated gate electrode were truly isolated from each other, this design would have performed as intended, because the excitation pulse could have been applied separately to each electrode. A superior design would position two stages of the total MOSFET amplifier between the floating gates and the transmission gates in the multiplexer. The remaining three stages could be utilized to realize a common amplifier for the CHEMFET detector.

# Operation.

Fortunately, the overall CHEMFET design was in a "modular" format. Thus, it was possible to sever all the transmission lines from the floating gates to the multiplexer which physically isolated each floating gate from each other. These transmission lines were laid out in metal 2, and they were not difficult to cut with an ultrasonic cutter and the Micromanipulator Probe Station (Micromanipulator Co., Model 6200, Carson City, NV). As a consequence of this procedure, each floating gate was connected to the reference amplifier through external wiring which completely bypassed the multiplexer.

#### Summary

The design, fabrication, and operational characteristics of the interdigitated gate electrode CHEMFET were presented. The MOSFET amplifier stage had the desired large constant gain. However, the 3-dB cut-off frequency was much less than expected, due to the load capacitance posed by the measurement scheme.

Also, a significant design error was committed regarding the high impedance nature of the chemically-sensitive thin films. The multiplexer should not have been placed between the floating gates and the MOSFET amplifier. Instead, the signal at the floating gate should have been amplified before being multiplexed.

# IV. Experimental Procedures

This chapter describes the experimental procedures implemented to measure the electrical performance of the CHEMFET sensor in response to chemical changes induced in the thin film coatings on the interdigitated gate electrode structure. The first section discusses the experimental procedures, which includes the circuit arrangement and instrumentation configuration. Subsequent sections present the electrical measurements and the data reduction techniques.

#### Experimental Procedures

Film Deposition.

The initial experimental activity always started with a preliminary electrical test of the packaged die. Once assured that the interdigitated gate electrode structures were not shorted, the chemically-sensitive thin films were deposited following the film deposition procedure discussed in Appendix C.

The four CHEMFET die were coated with the chemicallysensitive thin films as shown in Figures IV.1 through IV.3.

The two CHEMFET die coated with the phthalocyanine films had
the average film thicknesses, as shown, which were
determined following the film thickness measurement
procedure discussed in Appendix C.

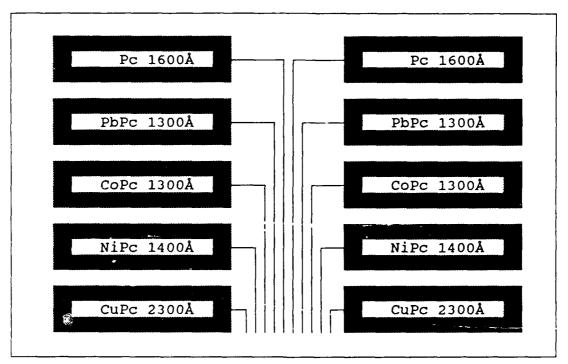


Figure IV.1. CHEMFET 1: 1500Å Thick Phthalocyanine Films.

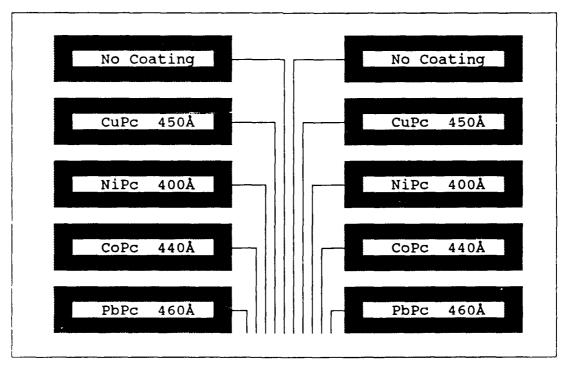


Figure IV.2. CHEMFET 2: 500Å Thick Phthalocyanine Films.

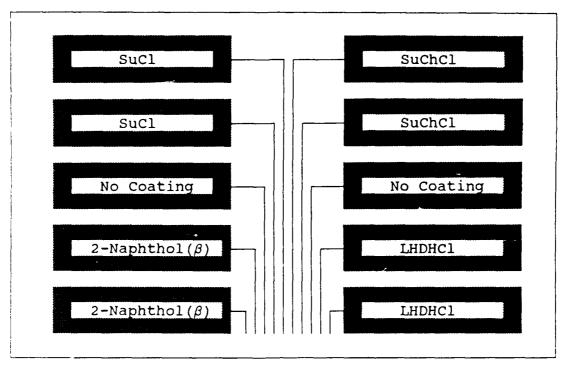


Figure IV.3. CHEMFET 3 and 4: Other Organic Thin Films.

Each film candidate deposited or the CHEMFET sensor was placed in the test cell, and the gas generation and delivery system was then used to deliver a selected flow of air at a relative humidity less than 10%. A detailed description of the test cell and operation of the gas generation and delivery system are contained in Appendix D.

Once the air flow was stable, power was supplied to the test cell, which heated the CHEMFET sensor to a specific temperature. Next, the electrical measurements were accomplished for a zero challenge gas concentration to provide the baseline measurements. After the zero challenge gas concentration measurements, the gas generation and delivery system was adjusted to deliver a specific challenge

gas (DIMP or DMMP) at a selected concentration. After a period of time (approximately 30 minutes to 1 hour) when the entire gas delivery system and the test cell were expected to be at an equilibrium gas concentration, the electrical measurements were repeated. The air flowrates and permeation rates used to generate each challenge gas concentration are listed in Table IV.1.

# Circuit Configuration.

As mentioned in Chapter III, because the transmission gates of the multiplexer would not provide sufficient isolation between the floating gates, the floating electrode components were physically severed from the multiplexer, and thus, from the MOSFET amplifier stages on the CHEMFET chip. Consequently, as shown in Figure IV.4, a reference MOSFET amplifier from another CHEMFET chip was arranged outside of the test cell, and the floating electrode components were connected to this reference amplifier using coax cables. The reference amplifier was operated with following bias voltages: Vdd was +4 V, Vss was -4 V, Vbias was 0 V, and the Voffsets were 0.074 V.

## Instrumentation Configuration.

Figure IV.4 illustrates the instrumentation configuration.

Table IV.1. Challenge Gas Generation Parameters.

	Gas	: Concentration	u
DIMP	0.5 ppm	mdd E	7.5 ppm
Air Flowrate	200 ml/min	200 ml/min	138 ml/min
Permeation Tube Temperature	46.5 °C	26 °C	os ، 0s
Permeation Tube Identification	G-5645	G-6942	G-6942
Permeation Rate	735 ng/min	4411 ng/min	7600 ng/min
DMMP	0.1ppm	0.5ppm	3ppm
Air Flowrate	1000 ml/min	200 ml/min	72 ml/min
Permeation Tube Temperature	10 °C	10 °C	2، 0s
Permeation Tube Identification	G-5646	G-5646	G-5646
Permeation Rate	508 ng/min	508 ng/min	1100 ng/min

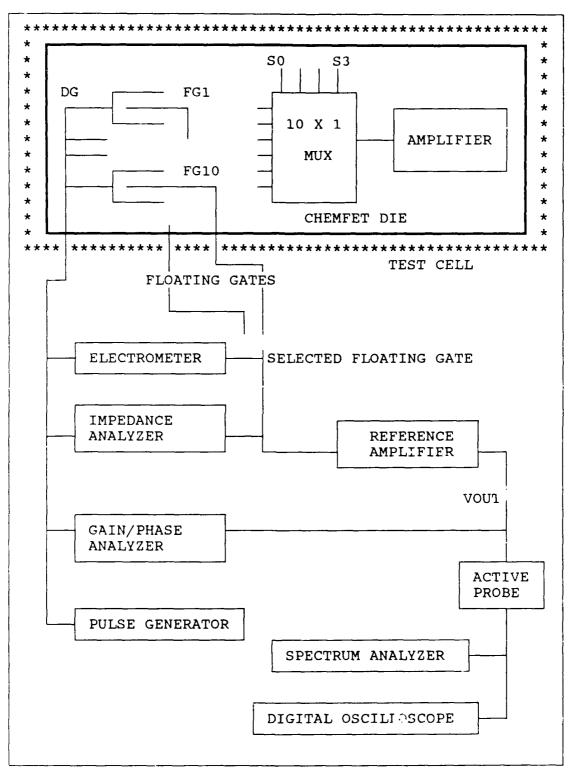


Figure IV.4. Instrumentation Configuration.

### Electrical Measurements

# DC Resistance Measurement.

As shown in Figure IV.4, the DC resistance of each thin film was initially measured across the driven and floating gates. The DC resistance of each thin film was measured sequentially with an electrometer (Keithley Instruments, Model 617, Cleveland, OH). The electrometer was used in its V/I (ohms) measurement mode with a constant voltage of 3 7. Control of the electrometer and the corresponding data acquisition process was accomplished using a BASIC program and a Z-248 Microcomputer equipped with an IEEE-488 interface card. The BASIC program (DC.bas) is listed in Appendix E.

#### Impedance Measurement.

After the initial DC measurements, the impedance of the thin films were measured across the driven and floating gate contacts using an Impedance/Gain-Phase Analyzer (Hewlett-Packard Corp., Model HP 4194A, Palo Alto, CA). For the impedance measurements, the Impedance/Gain-Phase Analyzer was used in its impedance measurement mode with the DC bias set at 0.5 V and the oscillation level at 1 V. Prior to the actual measurement conditions, offset calibration measurements were accomplished for the short circuit condition, and these values were stored. The real and imaginary (R and X) components of the impedance measurements were collected over frequency range that spanned 100 HZ to

1 MHZ using a logarithmic scanning sweep (a total of 401 frequency points). The BASIC program used in the data a:quisition process (Imp.bas) is listed in Appendix E.

# Gain and Phase Measurements.

Once the baseline thin film electrical measurements were accomplished, the gain and phase of each thin film along with the reference amplifier were measured. Each floating gate was connected to the reference amplifier manually. The gain and phase of the CHEMFET sensor was measured across the driven gate and Vout (the output voltage of the reference amplifier) using the Impedance/Gain-Phase Analyzer (Hewlett-Packard Corp., Model HP 4194A, Palo Alto, CA).

The Impedance/Gain-Phase Analyzer was used in the gainphase measurement mode with an oscillation level set at

0.1 V. Whenever required, the oscillation level was
increased to a higher voltage (typically 0.5 V) in order to
establish a noise-free measurement without simultaneously
overloading the analyzer. There was no applied DC bias for
the gain and phase measurements. Prior to the actual
measurements, the offset measurements were accomplished for
the short circuit calibration, and they were stored in the
instrument's memory for the offset compensation calculations.
The gain (in dB) was measured relative to the reference
channel in the analyzer. The measurement was accomplished
from 10 HZ to 1 MHZ using a logarithmic sweep, and a total of
401 frequency data points were collected. The BASIC program

used in the data acquisition process (GP.bas) is listed in Appendix E.

# Frequency Spectrum And Waveform Measurements.

After the initial gain and phase measurements, the frequency spectrum and time-domain waveform response of each CHEMFET sensor to a voltage pulse excitation was measured sequentially with a spectrum analyzer (Hewlett-Packard Corp., Model HP 8556B, Palo Alto, CA) and a digital storage oscilloscope (Hewlett-Packard Corp., Model HP 54100A, Palo Alto, CA).

The driven gate was excited with a 5.24 V pulse whose period (T) was 1 ms period and whose duration ( $\tau$ ) was 2  $\mu$ s. The pulses were generated from a pulse generator (Hewlett-Packard Corp., Model HP 8082A, Palo Alto, CA). The excitation pulse was initially not offsetted. However, because there was not sufficient leakage current through the thin film to the amplifier when the pulse was at 0 V, the input to the amplifier started to float. Consequently, the excitation pulse was offset at -40 mV to prevent the amplifier's input from floating. For subsequent experiments, the excitation pulse was further offset at -400 mV.

The exact characteristics of the generated pulse were adjusted by visual inspection using a digital storage oscilloscope (Hewlett-Puckard Corp., Model HP 54100A, Palo Alto, CA). Figures IV.5 and IV.6 depict the pulse characteristics in the time- and frequency-domains.

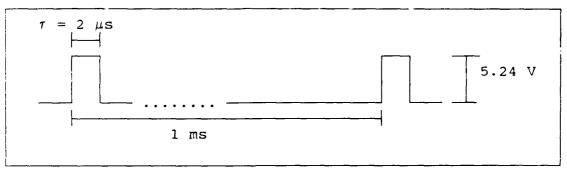


Figure IV.5. Time-Domain Spectrum of the Excitation Pulse.

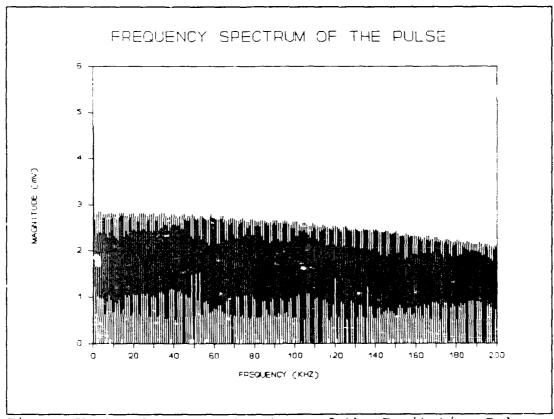


Figure IV.6. Frequency Spectrum of the Excitation Pulse.

The frequency spectrum of the response at Vout was measured from 0 to 200 KHZ, at each 200 HZ interval using the spectrum analyzer. To prevent overloading the CHEMFET amplifier circuits (since the input impedance of the spectrum analyzer was 50 ohms), an active probe (Micromanipulator Co., Model FET-1, Carson City, NV) was used to match the input impedance. The active probe introduced approximately 5 dB of attenuation.

In addition to measuring the frequency spectrum of the output waveform, i\*a time-domain response was captured on the digital storage oscilloscope. Figure IV.7 shows the captured time-domain waveform of the excitation pulse. The BASIC data acquisition program (FFT.bas) is listed in Appendix E.

# Data Reduction and Processing

The Fourier transform spectra of the CHEMFET's timedomain excitation response was generated from the frequency
spectrum data by filtering the magnitude data at the
corresponding harmonic frequencies (the multiples of 1 KHZ).
The magnitudes at the harmonic frequencies were found by
identifying the local maximum in the vicinity of the harmonic
frequencies. Figure IV.8 depicts the Fourier transform
spect of the excitation pulse.

The Fourier transform spectra data were further processed to produce a difference Fourier transform spectra between the challenge gas exposed CHEMFET response and the

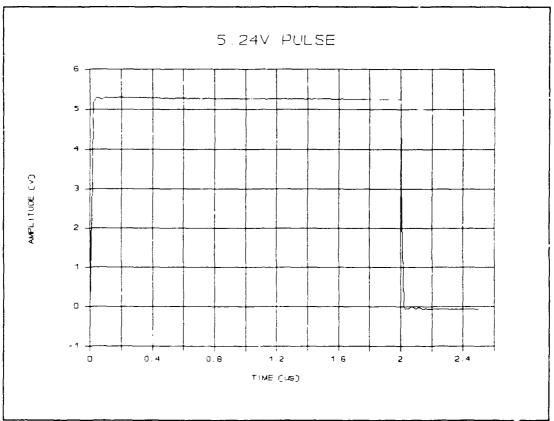


Figure IV.7. Time-Domain Pulse Captured on the Digital Storage Oscilloscope.

excitation pulse. Since the frequency spectrum was measured in dBm (referenced with respect to 1 milli-Watt), the spectrum data in the dBm units were changed to mV units, using the following transformation equation:

Power (Watts) = 
$$\frac{V^2 \text{ (Voltage}^2)}{R \text{ (ohms)}}$$

where the input resistance of the spectrum analyzer, R, was 50 ohms. The Fourier transform spectra of the excitation pulse was then subtracted from the Fourier transform spectra of the exposed CHEMFET response.

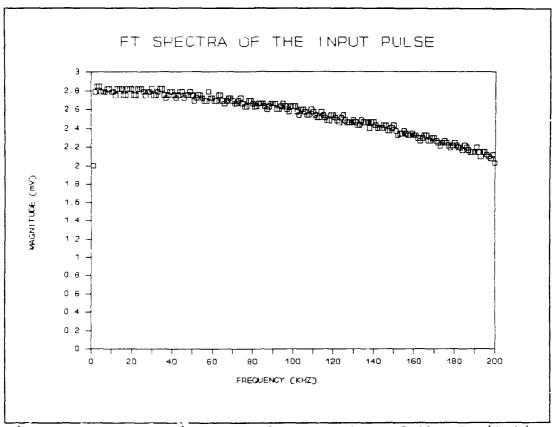


Figure IV.8. Fourier Transform Spectra of the Excitation Pulse.

The difference Fourier transform spectra were further processed to produce normalized difference Fourier transform spectra. The difference Fourier transform spectra was normalized with respect to the "largest" harmonic magnitude contained within the excitation pulse spectrum. This normalization process generated a spectrum whose shape was identical but the magnitudes of each harmonic had a dimensionless value typically between -1 and 1. The data points in the normalized difference spectra were arithmetically averaged (5 data points) to produce the "smooth looking" normalized difference spectra.

The data processing was accomplished using BASIC computer programs. The BASIC computer program which processed the frequency spectral data into the Fourier transform spectra, and the program which calculated the normalized difference Fourier transform spectra, are listed in Appendix E.

# Summary

The experimental procedures used to evaluate the electrical properties of the CHEMFET in response to chemical changes in the various thin film coatings of the interdigitated gate structure were discussed in this chapter. The experimental instrumentation configuration, electrical measurements, and data processing techniques were described.

# V. Results and Discussion

This chapter contains the results and analysis of the electrical measurements performed with the CHEMFET sensors coated with various thin films that were exposed to the DIMP and DMMP challenge gases. The results are presented from a perspective concerning the sensitivity-performance of the thin films. Two categories of films are considered: metaldoped phthalocyanine films and the other organic thin films. The thin films evaluated were cobalt phthalocyanine (CoPc), copper phthalocyanine (CuPc), lead phthalocyanine (PbPc), nickel phthalocyanine (NiPc), 2-naphthol( $\beta$ ), L-histidine dihydrochloride (LHDHCl), succinylcholine chloride (SuChCl), and succinylchloride (SuCl).

The gas exposure sensitivity-performance of the CHEMFET sensors toward the organophosphorus challenge compounds (DIMP and DMMP) for the various thin film coatings was evaluated primarily from the normalized difference Fourier transform spectra of the CHEMFET's response to a voltage excitation pulse. The microsensor's gain and phase data were collected but not used in the data reduction and analysis. The reason for this position include i) the initial data reduction and analysis revealed that the gain and phase data contained too much noise to be valuable and ii) the film impedance data and Fourier transform spectra data were mutually supportive.

For each of the phthalocyanine films discussed, two different film thicknesses (1500Å and 500Å) were deposited onto the interdigitated gate electrode structure of the CHEMFET. Most of the electrical measurements were made utilizing the 1500Å phthalocyanine film at two different temperatures (25 °C and 120 °C) and three different challenge gas concentrations (0.5 ppm, 3 ppm, and 7.5 ppm for DIMP, and 0.1 ppm, 0.5 ppm, and 3 ppm for DMMP). Only one temperature (120 °C) and one challenge gas concentration (7.5 ppm for DIMP and 3 ppm for DMMP) measurement was accomplished for the 500Å phthalocyanine films.

For the other organic thin films, 2-naphthol( $\beta$ ), LHDHCl, SuCl, and SuChCl, only one temperature (25 °C) and one challenge gas concentration (7.5ppm for DIMP and 3ppm for DMMP) measurement was accomplished.

The results for each film are discussed in separate sections. With respect to each film, the results are presented first for the DIMP and then for the DMMP challenge gas.

# Sensitivity Performance of the CHEMFET Sensor Coated with CoPc

DIMP Challenge Gas Exposure at 25 °C.

Figure V.1 dep:cts the normalized difference Fourier transform spectra data for the CHEMFET sensor coated with the 1500Å thick cobalt phthalocyanine film at 25 °C with respect

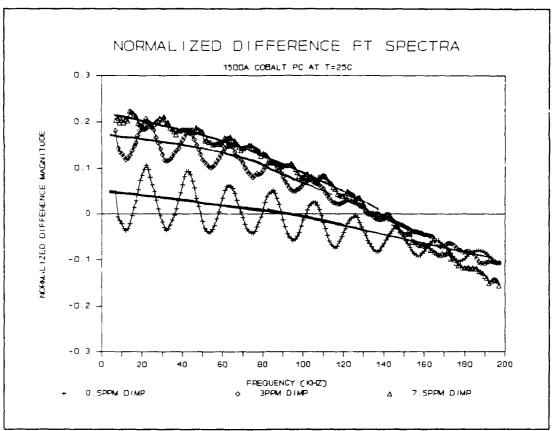


Figure V.1. Normalized Difference Fourier Transform Spectra of the CHEMFET Sensor Coated with a 1500Å Thick CoPc Film upon Exposure to DIMP at 25 °C.

to three different DIMP gas concentrations. These normalized difference spectra were computed by first subtracting the spectra of the excitation pulse from the spectra of the CHEMFET's pulse response due to a challenge gas exposure. The difference spectra was then normalized with respect to the "largest" harmonic magnitude contained in the excitation pulse spectrum. Figure V.2 depicts the Fourier transform spectra of the excitation pulse with an offset of -40 mV.

The excitation pulse was offset at -40 mV to provide enough

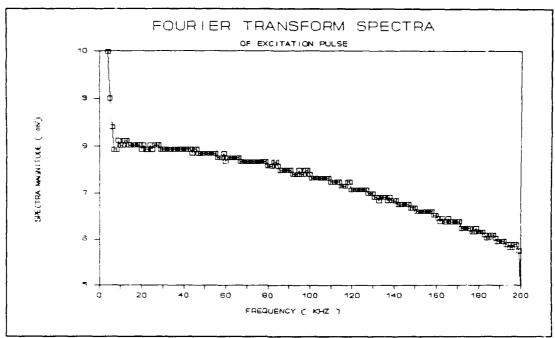


Figure V.2. Fourier Transform Spectra of the Excitation Pulse Offset at -40 mV.

leakage current through the thin films to the amplifier (see Page III-15 and IV-9). Because of the offset, the spectra contained much energy at the lower harmonic frequencies (5 KHZ and below). The spectra data at these frequencies were not used in the data reduction. The "largest" harmonic magnitude contained in this excitation pulse spectrum was 8.4 mV.

As mentioned in Chapter III, the difference in the pulse response is reflected in the general shape of the spectrum's envelope. Thus, not only the magnitude of the difference but, also the shape of the difference spectrum is important.

The response of the interdigitated gate electrode CHEMFET sensor coated with CoPc to a pulse excitation

depended upon the DIMP challenge gas concentration, as shown in Figure V.1. The greatest change in the CHEMFET's response with respect to the excitation pulse occurred upon exposure to the greatest DIMP concentration (7.5 ppm). Also, an interesting characteristic in the CHEMFET's response was observed in the normalized difference Fourier transform spectra. This unusual feature was the occurrence of an oscillation frequency of approximately 20 KHZ. This oscillation frequency was more prominent at the lower challenge gas concentrations, where the change in the response was smaller.

Even with the oscillation, the shape of the overall (the lines through the midpoints of the oscillation peaks, as shown in Figure V.1) spectrum envelope for the two greater concentration cases (3 ppm and 7.5 ppm) were similar. They were both curved. In comparison, the shape of the envalope for 0.5 ppm concentration case was linear.

A normalized difference magnitude of 0.2 was observed for the 7.5 ppm DIMP exposure at those frequencies less than 20 KHZ. For the 3 ppm DIMP exposure, a normalized difference magnitude of 0.16 was extrapolated as the average value at frequencies less than 20 KHZ. For the 0.5 ppm DIMP exposure, an average magnitude of 0.05 was similarly extrapolated. The greater normalized difference magnitude associated with the larger gas concentrations indicates that the conductivity of

the cobalt film has increased upon exposure to the challenge gas.

The time-domain responses of the CHEMFET sensor coated with the 1500Å thick CoPc film to the excitation pulse for the 0.5 ppm and 7.5 ppm DIMP challenges are depicted in Figure V.3. and Figure V.4. The time-domain responses also show the differences between the CHEMFET's response upon exposure to the two different concentrations of DIMP gas. However, the differences in the responses are not as readily visible as are the differences in the Fourier transform spectra.

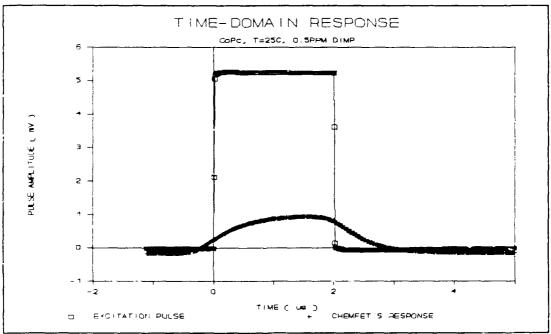


Figure V.3. Time-Domain Response of the CHEMFET Jensor Coated with a 1500Å Thick CoPc Film upon Exposure to a 0.5 ppm DIMP Challenge at 25 °C.

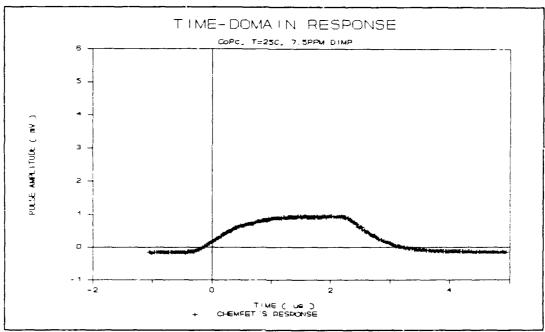


Figure V.4. Time-Domain Response of the CHEMFET Sensor Coated with a 1500Å Thick CoPc Film upon Exposure to a 7.5 ppm DIMP Challenge at 25 °C.

The impedance of the interdigitated gate electrode coated with the 1500Å thick cobalt phthalocyanine film upon exposure to the DIMP challenge gas is depicted in Figures V.5 and V.6. As shown, below 1 KHZ frequency, the magnitude of the reactance was on order of 10<sup>6</sup> ohms, while the resistance was on order of 10<sup>4</sup> ohms. Thus, an incremental change in the reactance would have the most significant influence on a change in the overall impedance's magnitude.

The reactance of the (interdigitated gate electrode coated with CoPc) film upon exposure to the three DIMP gas concentrations were approximately the same. However, in comparison with the reactance of the film prior to the

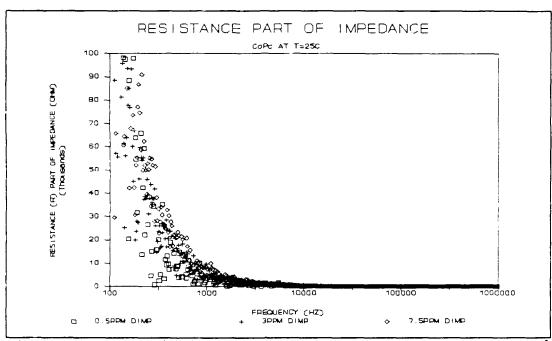


Figure V.5. Resistive Part of the Impedance of the 1500Å Thick CoPc Film upon Exposure to the DIMP at 25 °C.

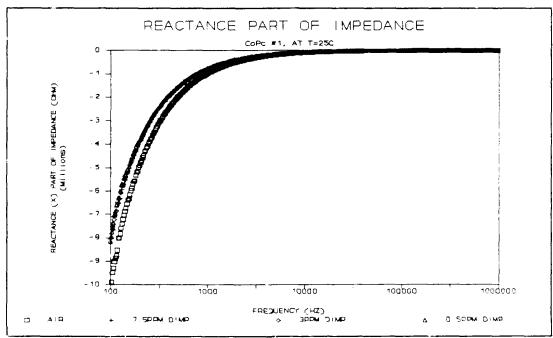


Figure V.6. Reactive Part of the Impedance of the 1500Å Thick CoPc Film upon Exposure to the DIMP at 25 °C.

challenge gas exposures at the three concentrations (shown as the air in Figure V.6), the reactance of the cobalt phthalocyanine film decreased in magnitude upon exposure to DIMP challenge gas.

The DC resistance data of the cobalt phthalocyanine film showed no visible change. As shown in Figure V.7, the DC resistance drift with respect to time was greater than any noticeable change due to the 7.5 ppm DIMP challenge gas exposure for all of the metal-doped phthalocyanine films at 25 °C. However, this lack of change in DC resistance may be due to a prior exposure to the DIMP gas, since the responses of the films were not totally reversible upon purge with air.

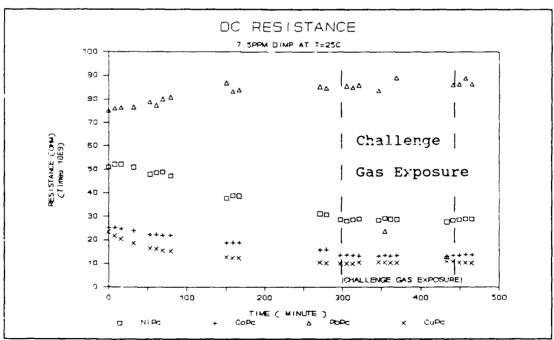


Figure V.7. DC Resistance of the 1500Å Thick Metal-Doped Phthalocyanine Films upon Exposure to the 7.5 ppm DIMP Challenge at 25 °C.

Of the data evaluated (the Fourier transform spectra data of the CHEMFET sensor, the time-domain response data of the CHEMFET sensor, the impedance data of the interdigitated gate electrode, and DC resistance data of the interdigitated gateelectrode), the Fourier transform spectra data reflected the changes caused by the exposure to the different concentrations of challenge gas most clearly. Thus, for subsequent sections, the data analysis is accomplished with respect to the normalized difference Fourier transform spectra data.

# DIMP Challenge Gas Exposure at 120 °C.

Figure V.8 depicts the normalized difference Fourier transform spectra data for the CHEMFET sensor coated with the 1500Å thick cobalt phthalocyanine film at 120 °C with respect to three different DIMP gas concentrations. Similar to the responses at 25 °C, the responses of the interdigitated gate electrode CHEMFET coated with the CoPc film to a pulse excitation at 120 °C also depended upon the DIMP challenge gas concentration. At the lower frequencies (below 100 KHZ), the greatest change in the CHEMFET's response with respect to the excitation pulse occurred upon exposure to the greatest DIMP concentration (7.5 ppm).

The oscillation frequency of approximately 20 KHZ was also observed. This oscillation frequency was prominent at all three challenge gas concentrations. The shapes of the overall spectrum envelope (defined as the line through the

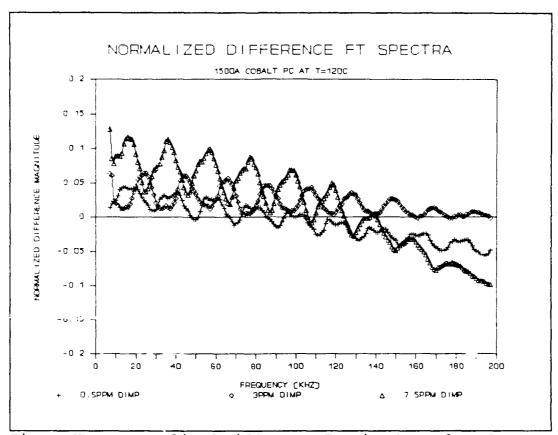


Figure V.8. Normalized Difference Fourier Transform Spectra of the CHEMFET Sensor Coated with the 1500Å Thick CoPc upon Exposure to DIMP at 120 °C.

midpoints of the oscillation peaks) were similar for the two DIMP gas concentrations (0.5 ppm and 3 ppm). At those frequencies greater than 140 KHZ, the slope of the spectrum envelope for these two gas concentrations were both linear.

The shape of the overall spectrum envelope (defined as the line through the midpoints of the oscillation peaks) for the greatest gas concentration (7.5 ppm DIMP) was curved downward with increasing frequency, compared with the shapes for two other gas concentrations. Additionally, the shape of

the spectrum envelope for the 7.5 ppm DIMP gas concentration at 120 °C was similar to the shapes of the spectrum envelopes observed for the DIMP gas challenge concentrations of 3 ppm and 7.5 ppm at 25 °C (Figure V.1). All three spectrum envelopes had a zero normalized difference magnitude approximately at 140 KHZ.

At 120 °C, a normalized difference magnitude of 0.1 was extrapolated as the average value for the 7.5 ppm DIMP exposure at those frequencies less than 20 KHZ. For the 3 ppm DIMP exposure, a normalized difference magnitude of 0.04 was extrapolated as the average value at those frequencies less than 20 KHZ. For the 0.5 ppm DIMP exposure, an average magnitude of 0.03 was extrapolated. The greater normalized difference magnitudes associated with the greater challenge gas concentrations observed at 25 °C, were also observed at 120 °C.

Figure V.9 depicts the normalized difference Fourier transform spectra data for the CHEMFET sensors coated with the 500Å and 1500Å thick cobalt phthalocyanine films at 120 °C. The normalized difference Fourier transform spectra revealed that the response of the CHEMFET sere coated with the 500Å thick CoPc did not change upon the first exposure to the DIMP challenge gas (7.5 ppm) with respect to the response of the unexposed CHEMFET sensor (0 ppm DIMP). At 120 °C the CHEMFET sensor coated with 1500Å thick CoPc showed significant sensitivity to the 7.5 ppm DIMP challenge gas (as

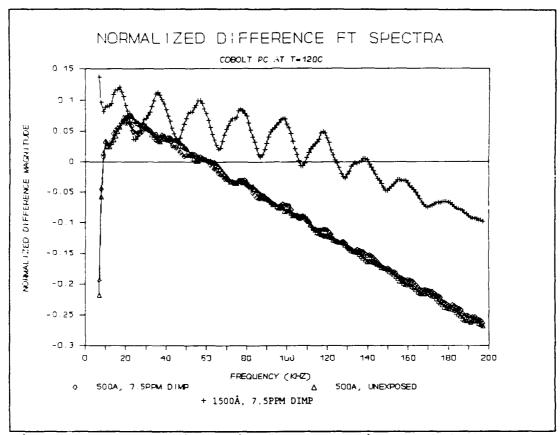


Figure V.9. Normalized Difference Fourier Transform Spectra of the CHEMFET Sensors Coated with the 500Å and 1500Å Thick CoPc Films upon Exposure to the 7.5 ppm DIMP Challenge at 120 °C.

shown previously in Figure V.8 as the response change with the concentration) compared to the CHEMFET sensor coated with the 500Å thick CoPc film.

## DMMP Challenge Gas Exposure at 25 °C.

Figure V.10 depicts the normalized difference Fourier transform spectra data for the CHEMFET sensor coated with the 1500Å thick cobalt phthalocyanine film at 25 °C with respect to three different DMMP challenge gas concentrations. The

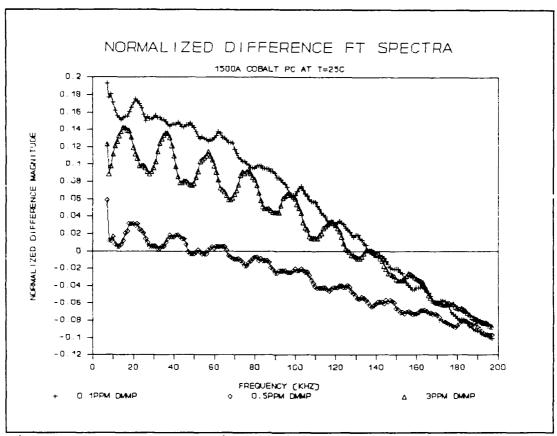


Figure V.10. Normalized Difference Fourier Transform Spectra of the CHEMFET Sensor Coated with the 1500Å Thick CoPc Film upon Exposure to DMMP at 25 °C.

response of the interdigitated gate electrode CHEMFET sensor coated with the 1500Å thick CoPc film to a pulse excitation were not consistent with the magnitudes of the challenge gas concentrations. This inconsistency was due to an inadequate purge of the CHEMFET sensor between the measurements. For the DMMP challenge gas measurements at 25 °C, the 0.5 ppm measurement was taken first, followed by the 3 ppm measurement, and then the 0.1 ppm measurement. The normalized difference Fourier transform spectra data revealed

that the change in the CHEMFET sensor's response increased with the chronological order utilized to implement the challenge gas measurement. Normalized difference magnitudes of 0.02, 0.12, and 0.16 were extrapolated as the average value at those frequencies less than 20 KHZ for the 0.5 ppm, 3 ppm, and 0.1 ppm DMMP challenge gas concentrations, respectively.

The CHEMFET sensor's responses upon exposure to the 0.5 ppm and 3 ppm DMMP gas concentrations revealed that, in comparison with the responses observed with the DIMP challenge gas at 25 °C (Figure V.1), the CHEMFET sensor had a similar frequency response upon exposure to both the 3 ppm DIMP and DMMP challenge gases. Both responses had approximately the same normalized difference Fourier transform spectra magnitude (0.16 for DIMP and 0.12 for DMMP), and the prominent 20 KHZ oscillation was present. The CHEMFET sensor's response in the frequency-domain also revealed approximately the same normalized difference magnitude upon exposure to both the 0.5 ppm DIMP and DMMP gases (0.05 for DIMP and 0.02 for DMMP). The characteristic 20 KHZ oscillation was, however, less prominent in the CHEMFET sensor's response upon exposure to the 0.5 ppm DMMP challenge gas. Overall, in the Fourier transform spectra, the CHEMFET sensor's responses to the DIMP and DMMP challenge gases were similar in magnitude at 25 °C.

# DMMP Challenge Gas Exposure at 120 °C.

Figure V.11 depicts the normalized difference Fourier transform spectra data for the CHEMFET sensor coated with the 1500Å thick cobalt phthalocyanine film at 120 °C with respect to three different DMMP challenge gas concentrations. At 120 °C, the response of the interdigitated gate electrode CHEMFET coated with the 1500Å thick CoPc film to a pulse excitation depended upon the DMMP challenge gas concentration. At the lower frequencies (below 140 KHZ) the greatest change in the CHEMFET's response occurred upon exposure to the greatest DMMP concentration (3 ppm). The oscillation frequency of approximately 20 KHZ was also observed. This oscillation frequency was prominent at all three challenge gas concentrations.

At 120 °C, a normalized difference magnitude of 0.6 was extrapolated as the average value for the 3 ppm DMMP exposure at those frequencies less than 20 KHZ. For the 0.5 ppm DIMP exposure, a normalized difference magnitude of 0.25 was extrapolated as the average at those frequencies less than 20 KHZ. For the 0.1 ppm DMMP exposure, an average magnitude of 0.1 was extrapolated. The greater normalized difference magnitudes associated with the greater gas concentrations, partly observed at 25 °C, were also observed at 120 °C. For the DMMP gas exposure measurements at 120 °C, the 0.1 ppm measurement was taken first, followed by the 0.5 ppm measurement, and then the 3 ppm measurement.

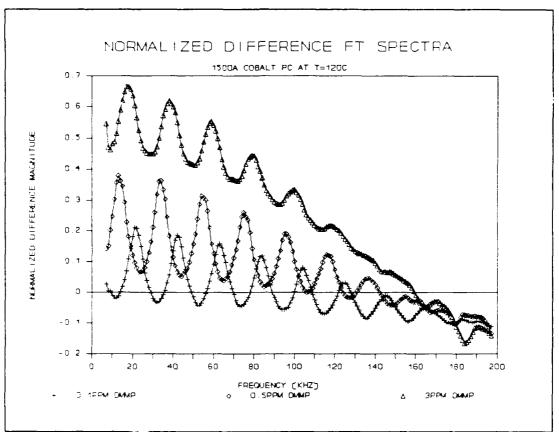


Figure V.11. Normalized Difference Fourier Transform Spectra of the CHEMFET Sensor Coated with the 1500Å Thick CoPc Film upon Exposure to DMMP at 120 °C.

In comparison with the responses observed with the DIMP challenge gas at 120 °C (Figure V.8), the CHEMFET sensor manifested a greater change in the frequency response upon exposure to the DMMP challenge gas than upon exposure to DIMP at 120 °C.

Figure V.12 depicts the normalized difference Fourier transform spectra data for the CHEMFET sensors coated with the 500Å and 1500Å thick cobalt phthalocyanine films at 120 °C. The normalized difference Fourier transform spectra

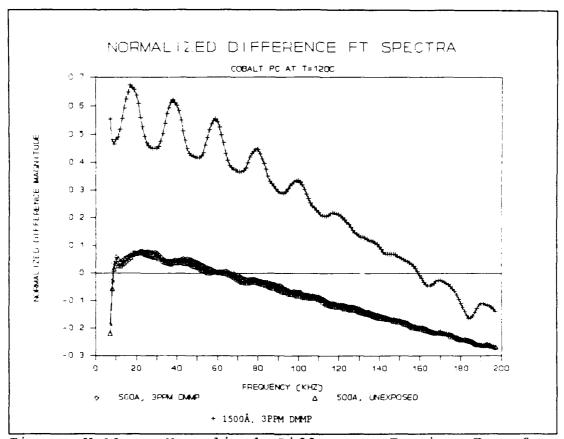


Figure V.12. Normalized Difference Fourier Transform Spectra of the CHEMFET Sensors Coated with the 500Å and 1500Å Thick CoPc Films upon Exposure to the 3 ppm DMMP Challenge at 120 °C.

revealed that the response of the CHEMFET sensor coated with the 500Å thick CoPc film did not change upon exposure to the 3 ppm DMMP challenge gas concentration with respect to the response of the unexposed CHEMFET sensor. At 120 °C, the CHEMFET sensor coated with the 1500Å thick CoPc film showed more sensitivity to the 3 ppm DMMP challenge gas compared to the CHEMFET sensor coated with the 500Å thick CoPc film. A similar observation was made previously with the DIMP challenge gas at 120 °C.

#### Summary.

Of the data evaluated (the Fourier transform spectra data of the CHEMFET sensor, the time-domain response data of the CHEMFET sensor, the impedance data of the interdigitated gate electrode, and DC resistance data of the interdigitated gate electrode), the Fourier transform spectra data most clearly reflected the changes caused by the exposure to different concentrations of challenge gases. The Fourier transform spectra data revealed that the response of the interdigitated gate electrode CHEMFET sensor coated with the 1500Å thick CoPc film to an excitation pulse depended upon the concentrations of the challenge gases (DIMP and DMMP). Table V.1 summarizes the normalized difference magnitudes of Fourier transform spectra data observed at each challenge gas concentration and temperature.

The interdigitated gate electrode CHEMFET sensor coated with the 1500Å thick CoPc film was more sensitive to the changes in the DMMP challenge gas concentrations compared to the changes in the DIMP concentrations at 120 °C. At 25 °C, the CHEMFET sensor was slightly more sensitive to the changes in the DIMP concentrations. The greatest sensitivity of the CHEMFET sensor was observed at 120 °C upon exposure to the 3 ppm DMMP. The frequency spectrum data measured at both the 7.5 ppm DIMP concentration and 3 ppm DMMP exposure at 120 °C revealed that the CHEMFET sensor coated with the 1500Å thick CoPc film was more sensitive to the changes in the challenge

Table V.1. Summary of the Normalized Difference Magnitudes of the Fourier Transform Spectra for the CHEMFET Sensor Coated the with 1500Å Thick CoPc Film.

		3 N - 4	<u>*</u>		
	Challenge Gas Concentration (ppm)				
	0.1	0.5	3	7.5	
DMMP at 25 °C		0.02	0.12		
DMMP at 120 °C	0.1	0.25	0.6		
DIMP at 25 °C		0.05	0.16	0.2	
DIMP at 120 °C		0.03	0.04	0.1	

gas concentrations compared to the CHEMFET sensor coated with the 500Å thick CoPc film.

## Sensitivity Performance of the CHEMFET Sensor Coated with NiPc

DIMP Challenge Gas Exposure at 25 °C.

Figure V.13 depicts the normalized difference Fourier transform spectra data for the CHEMFET sensor coated with the 1500Å thick nickel phthalocyanine film at 25 °C with respect to three different DIMP gas concentrations. The response of the interdigitated gate electrode CHEMFET sensor coated with the NiPc film to a pulse excitation depended upon the DIMP challenge gas concentration. At the lower frequencies (below 100 KHZ) the greatest change in the CHEMFET's response with respect to the excitation pulse occurred upon exposure to the greatest DIMP concentration (7.5 ppm). Also shown in Figure V.13 is the response of the CHEMFET sensor exposed to the purge air prior to the DIMP concentration measurements.

The oscillation frequency of approximately 20 KHZ, which was observed with the CHEMFET sensor coated with the CoPc film, was also observed. The oscillation frequency was more prominent at the lower challenge gas concentrations.

A normalized difference magnitude of 0.2 was extrapolated as the average value for the 7.5 ppm DIMP exposure at those frequencies less than 20 KHZ. For the 3 ppm DIMP exposure, a normalized difference magnitude of 0.18 was extrapolated as the average value at those frequencies less than 20 KHZ. For the 0.5 ppm DIMP exposure, an average magnitude of 0.12 was extrapolated. The greater normalized

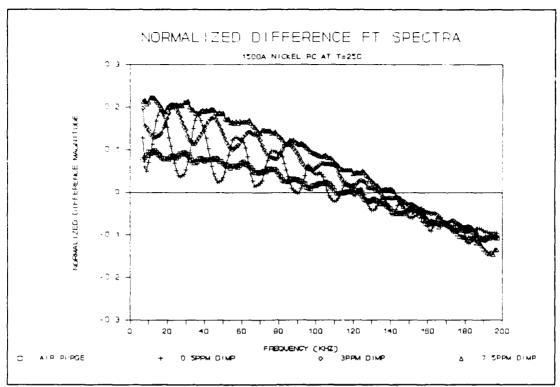


Figure V.13. Normalized Difference Fourier Transform Spectra of the CHEMFET Sensor Coated with the 1500Å Thick NiPc Film upon Exposure to the DIMP Challenge at 25 °C.

difference magnitudes associated with the greater gas concentrations, which was also observed with the cobalt phthalocyanine films was also observed with nickel phthalocyanine at 25 °C.

### DIMP Challenge Gas Exposure at 120 °C.

Figure V.14 depicts the normalized difference Fourier transform spectra data for the CHEMFET sensor coated with the 1500Å thick nickel phthalocyanine film at 120 °C with respect to different DIMP gas concentrations. The data for the 3 ppm DIMP exposure was not included, because it was not consistent with the remainder of the data. Instead, the CHEMFET

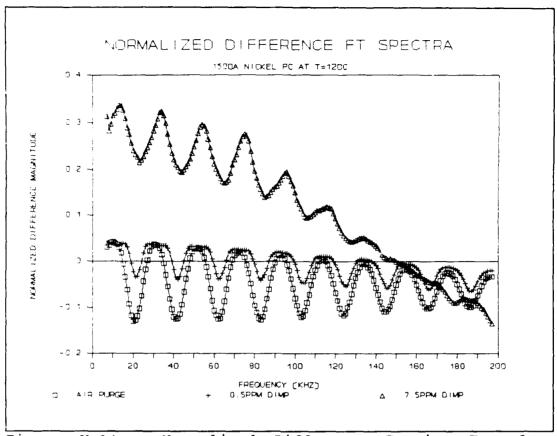


Figure V.14. Normalized Difference Fourier Transform Spectra of the CHEMFET Sensor Coated with the 1500Å Thick NiPc Film upon Exposure to the DIMP Challenge at 120 °C.

sensor's response to the air purge prior to the 0.5 ppm DIMP exposure was included to show the differences in the responses. Similar to the responses at 25 °C, the responses of the interdigitated gate electrode CHEMFET coated with the 1500Å NiPc film to a pulse excitation at 120 °C also depended upon the DIMP challenge gas concentration. At the lower frequencies (below 140 KHZ), the greatest change in the CHEMFET's response with respect to the excitation pulse occurred upon exposure to the greatest DIMP concentration (7.5 ppm).

The oscillation frequency of approximately 20 KHZ was, again observed. This oscillation frequency was prominent at all three challenge gas concentrations. The shape of the overall spectrum envelope for the 7.5 ppm DIMP gas concentration was similar to the one observed at 25 °C.

These spectral envelopes had a zero normalized difference magnitude at approximately 140 KHZ.

At 120 °C, a normalized difference magnitude of 0.3 was extrapolated as the average value for the 7.5 ppm DIMP exposure at those frequencies less than 20 KHZ. For the 0.5 ppm DIMP exposure, a normalized difference magnitude of zero was extrapolated as the average value at those frequencies less than 20 KHZ. For the purge air exposure, an average magnitude of -0.5 was extrapolated. Thus, the greater normalized difference magnitudes associated with the greater gas concentrations, observed at 25 °C, were also observed at 120 °C.

Figure V.15 depicts the normalized difference Fourier transform spectra data for the CHEMFET sensors coated with the 500Å and 1500Å thick nickel phthalocyanine films at 120 °C. The response of a second CHEMFET sensor coated with the 1500Å thick NiPc film, which manifested a lesser sensitivity, was used in the comparison. The normalized difference Fourier transform spectra revealed that the response of the CHEMFET sensor coated with the 500Å thick NiPc film did not change as much upon exposure to the 7.5 ppm DIMP challenge

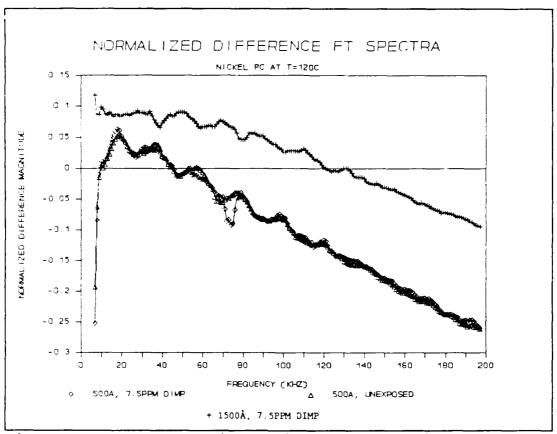


Figure V.15. Normalized Difference Fourier Transform Spectra of the CHEMFET Sensors Coated with the 500Å and 1500Å Thick NiPc Films upon Exposure to the 7.5 ppm DIMP Challenge at 120 °C.

gas with respect to the response of the unexposed CHEMFET sensor. At 120 °C, the CHEMFET sensor coated with the 1500Å thick NiPc film showed more sensitivity to 7.5 ppm DIMP challenge gas compared to the CHEMFET sensor coated with the 500Å thick NiPc film.

### DMMP Challenge Gas at 25 °C.

Figure V.16 depicts the normalized difference Fourier transform spectra data for the CHEMFET sensor coated with the 1500Å thick nickel phthalocyanine film at 25 °C with respect

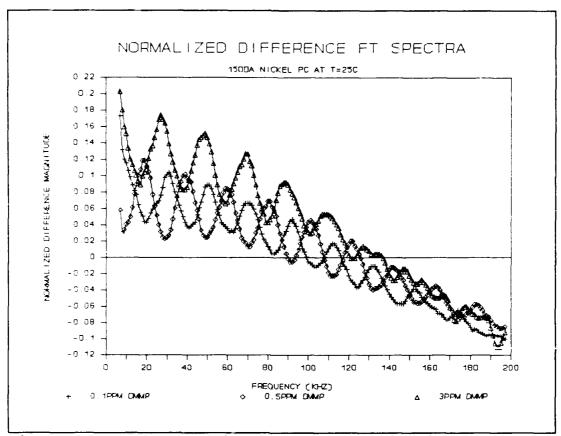


Figure V.16. Normalized Difference Fourier Transform Spectra of the CHEMFET Sensor Coated with the 1500Å Thick NiPc Film upon Exposure to the DMMP Challenge at 25 °C.

to three different DMMP gas concentrations. The response of the interdigitated gate electrode CHEMFET sensor coated with NiPc film to a pulse excitation were consistent with respect to the 0.5 ppm and 3 ppm challenge gas concentrations. The responses for the 0.1 ppm and 0.5 ppm DMMP concentrations were similar in magnitude. As mentioned earlier in the cobalt phthalocyanine section (Page V-14), the responses observed with the 0.1 ppm DMMP Challenge at 25 °C was due to an inadequate purge of the CHEMFET sensor between the measurements.

The normalized difference magnitude of 0.08, 0.08, and 0.14 were extrapolated as the average values at those frequencies less than 20 KHZ for 0.1 ppm, 0.5 ppm, and 3 ppm DMMP challenge gas concentrations, respectively.

The CHEMFET sensor's responses upon exposure to 0.5 ppm and 3 ppm DMMP gas concentrations revealed that, in comparison with the responses observed with the DIMP challenge gas at 25 °C (Figure V.13), the CHEMFET sensor had a similar frequency response upon exposure to the DIMP and DMMP challenge gases. The responses had approximately the same normalized difference magnitude (from 0.08 to 0.18), and the prominent 20 KHZ oscillation. Overall, in the Fourier transform spectra, the CHEMFET sensor's responses to the DIMP and DMMP challenge gases were similar in shape at 25 °C, with the zero normalized difference magnitude at approximately 140 KHZ, and the normalized difference magnitudes for DIMP were slightly greater than those for DMMP.

#### DMMP Challenge Gas at Exposure 120 °C.

Figure V.17 depicts the normalized difference Fourier transform spectra data for the CHEMFET sensor coated with the 1500Å thick nickel phthalocyanine film at 120 °C with respect to three different DMMP gas concentrations. At 120 °C, the response of the interdigitated gate electrode CHEMFET coated with NiPc film to a pulse excitation was not consistent with the challenge gas concentrations. The normalized difference magnitudes of 0.35, 0.2, and 0.6 were extrapolated as the average values at those frequencies less than 20 KHZ for 0.1

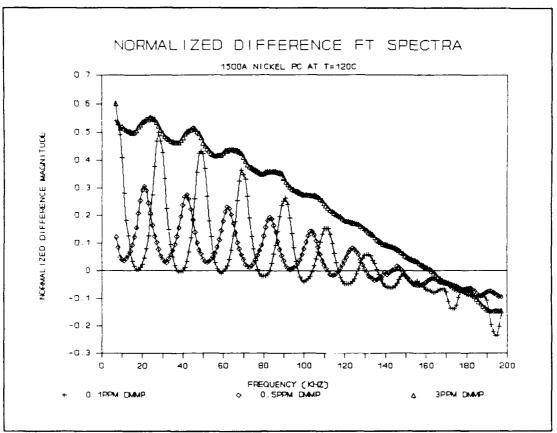


Figure V.17. Normalized Difference Fourier Transform Spectra of the CHEMFET Sensor Coated with the 1500Å Thick NiPc Film upon Exposure to the DMMP Challenge at 120 °C.

ppm, 0.5 ppm, and 3 ppm DMMP gas concentrations. The inconsistency of the responses is attributed to the 0.1 ppm and 0.5 ppm DMMP gas exposures. A greater change in the response with respect to the excitation pulse was observed at 0.1 ppm (0.35 vs 0.2). This inconsistency was not explainable.

The oscillation frequency of approximately 20 KHZ was also observed. This oscillation frequency was most prominent at the lower challenge gas concentrations.

Compared with the responses observed with the DIMP challenge gas at 120 °C (Figure V.14), the CHEMFET sensor manifested a greater change in the frequency response upon exposure to the DMMP challenge gas at 120 °C (0.6 for 3 ppm DMMP and 0.3 for 7.5 ppm DIMP).

Figure V.18 depicts the normalized difference Fourier transform spectra data for the CHEMFET sensors coated with 500Å and 1500Å thick nickel phthalocyanine films at 120 °C. The normalized difference Fourier transform spectra revealed

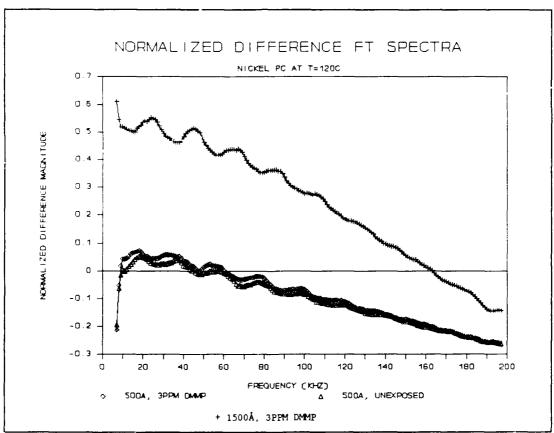


Figure V.18. Normalized Difference Fourier Transform Spectra of the CHEMFET Sensors Coated with the 500Å and 1500Å Thick NiPc Films upon Exposure to the 3 ppm DMMP Challenge at 120 °C.

that the response of the CHEMFET sensor coated with the 500Å NiPc film did not change significantly upon exposure to the 3 ppm DMMP challenge gas relative to the response of the unexposed CHEMFET sensor. At 120 °C, the CHEMFET sensor coated with the 1500Å thick NiPc film showed more sensitivity to the 3 ppm DMMP challenge gas compared to the CHEMFET sensor coated with the 500Å thick NiPc film. A similar observation was made previously with the DIMP challenge gas at 120 °C.

#### Summary.

The Fourier transform spectra data did not reveal that the response of the interdigitated gate electrode CHEMFET sensor coated with the 1500Å thick NiPc film to an excitation pulse was consistent with the concentrations of the challenge gases (DIMP and DMMP). Table V.2 summarizes the normalized difference magnitudes of the Fourier transform spectra observed at each challenge gas concentration and temperature.

The interdigitated gate electrode CHEMFET sensor coated with the 1500Å thick NiPc film was more sensitive to the changes in the DMMP concentrations compared to the changes in the DIMP concentrations at 120 °C. At 25 °C, the CHEMFET sensor was slightly more sensitive to the changes in the DIMP concentrations. The greatest sensitivity of the CHEMFET sensor was observed at 120 °C upon exposure to the 3 ppm DMMP challenge.

Table V.2. Summary of the Normalized Difference Magnitudes of the Fourier Transform Spectra for the CHEMFET Sensor Coated with the 1500Å Thick NiPc film.

	Challenge Gas Concentration (ppm)				
	0.1	0.5	3	7.5	
DMMP at 25 °C	0.08	0.08	0.14		
DMMP at 120 °C	0.35	0.2	0.6		
DIMP at 25 °C		0.12	0.18	0.2	
DIMP at 120 °C		0		0.3	

The data measured at both the 7.5 ppm DIMP and the 3 ppm DMMP challenge exposure at 120 °C revealed that the CHEMFET sensor coated with the 1500Å thick NiPc film was more sensitive to the changes in the challenge gas concentrations compared to the CHEMFET sensor coated with the 500Å thick NiPc film.

## Sensitivity Performance of the CHEMFET Sensor Coated with PbPc

DIMP Challenge Gas Exposure at 25 °C.

Figure V.19 depicts the normalized difference Fourier transform spectra data for the CHEMFET sensor coated with the 1500Å thick lead phthalocyanine film at 25 °C with respect to three different DIMP gas concentrations. The response of the interdigitated gate electrode CHEMFET sensor coated with PbPc

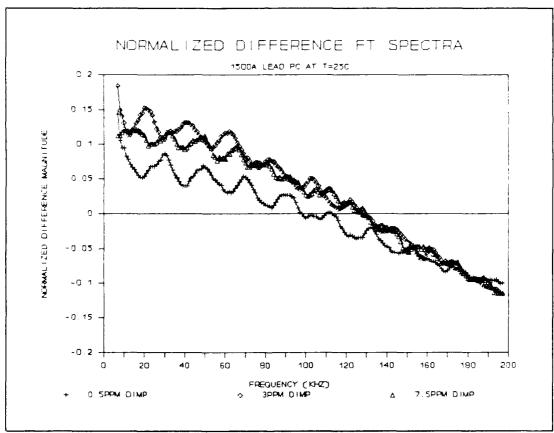


Figure V.19. Normalized Difference Fourier Transform Spectra of the CHEMFET Sensor Coated with the 1500Å Thick PbPc Film upon Exposure to the DIMP Challenge at 25 °C.

film to a pulse excitation was not consistent with the DIMP challenge gas concentrations. At the lower frequencies (below 100 KHZ), the greatest change in the CHEMFET's response with respect to the excitation pulse occurred upon exposure to the 3 ppm DIMP concentration.

The oscillation frequency of approximately 20 KHZ, which was observed with the CHEMFET sensor coated with CoPc and NiPc, was also observed. The oscillation frequency was more prominent at the lower challenge gas concentrations.

A normalized difference magnitude of 0.12 was extrapolated as the average value for the 7.5 ppm DIMP exposure at those frequencies less than 20 KHZ. For the 3 ppm DIMP exposure, the normalized difference magnitude of 0.13 was extrapolated as the average value at those frequencies less than 20 KHZ. For the 0.5 ppm DIMP exposure, an average magnitude of 0.08 was extrapolated. The average normalized difference magnitude for the 3 ppm DIMP challenge was slightly greater than the magnitude observed for the 7.5 ppm DIMP exposure. In Figure V.19, the difference between these two responses was more visible because of the greater oscillation level at the 3 ppm DIMP case. The inconsistency was not explainable.

### DIMP Challenge Gas Exposure at 120 °C.

Figure V.20 depicts the normalized difference Fourier transform spectra data for the CHEMFET sensor coated with the 1500Å thick lead phthalocyanine film at 120 °C with respect to different DIMP gas concentrations. Unlike the responses

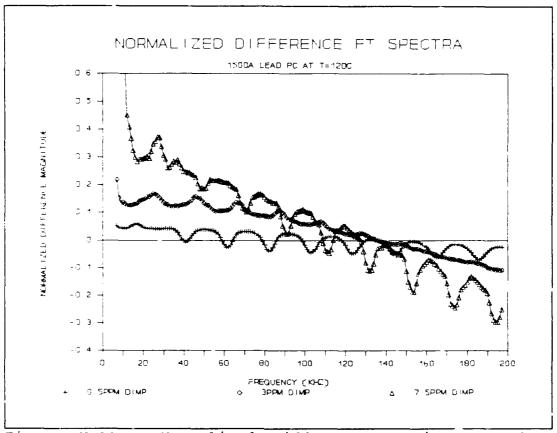


Figure V.20. Normalized Difference Fourier Transform Spectra of the CHEMFET Sensor Coated with 1500Å Thick PbPc upon Exposure to DIMP at 120 °C.

observed at 25 °C, the response of the interdigitated gate electrode CHEMFET sensor coated with NiPc to a pulse excitation at 120 °C were consistent with the DIMP challenge gas concentrations. At the lower frequencies (below 100 KHZ) the greatest change in the CHEMFET's response with respect to the excitation pulse occurred upon exposure to the greatest DIMP concentration (7.5 ppm).

The oscillation frequency of approximately 20 KHZ was again observed. This oscillation frequency was not as

prominent at the 3 ppm DIMP gas concentration. The shape of the overall spectral envelope for all three gas concentrations was linear. The slope of the envelope changed with respect to the gas concentrations.

At 120 °C, a normalized difference magnitude of 0.3 was extrapolated as the average value for the 7.5 ppm DIMP exposure at those frequencies less than 20 KHZ. For the 3 ppm DIMP exposure, a normalized difference magnitude of 0.15 was extrapolated as the average value at those frequencies less than 20 KHZ. For the 0.5 ppm DIMP exposure, an average magnitude of 0.05 was extrapolated. Thus, the greater normalized difference magnitudes associated with the greater gas concentrations, were observed at 120 °C.

Figure V.21 depicts the normalized difference Fourier transform spectra for the CHEMFET sensors coated with the 500Å and 1500Å thick lead phthalocyanine films at 120 °C. The normalized difference Fourier transform spectra revealed that the response of the CHEMFET sensor coated with the 500Å thick PbPc film did change considerably upon exposure to the 7.5 ppm DIMP challenge gas with respect to the response of the unexposed CHEMFET sensor, when compared with the CoPc and NiPc films (Figure V.9 and Figure V.15). However, at 120 °C, the CHEMFET sensor coated with the 1500Å thick PbPc film still showed more sensitivity to the 7.5 ppm DIMP challenge gas compared to the CHEMFET sensor coated with the 500Å thick NiPc film.

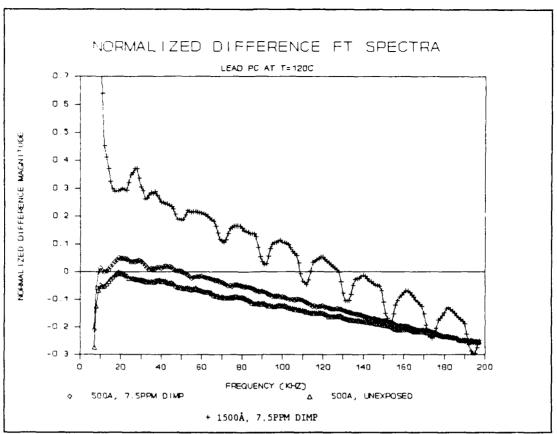


Figure V.21. Normalized Difference Fourier Transform Spectra of the CHEMFET Sensors Coated with the 500Å and 1500Å Thick PbPc Films upon Exposure to the 7.5 ppm DIMP Challenge at 120 °C.

### DMMP Challenge Gas Exposure at 25 °C.

Figure V.22 depicts the normalized difference Fourier transform spectra data for the CHEMFET sensor coated with the 1500Å thick lead phthalocyanine film at 25 °C with respect to three different DMMP gas concentrations. The response of the interdigitated gate electrode CHEMFET sensor coated with the PbPc film to a pulse excitation were consistent with the 0.5 ppm and 3 ppm challenge gas concentrations. The magnitude of the response for the 0.1 ppm challenge also was consistent

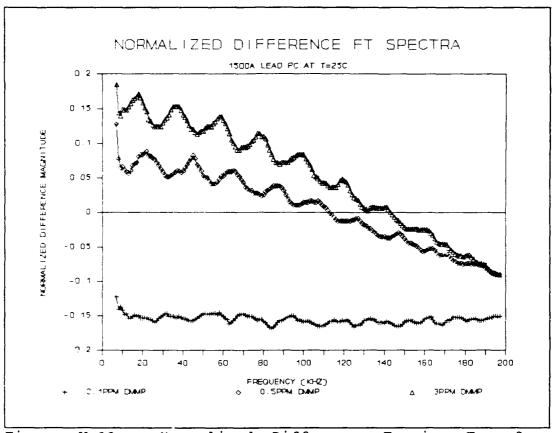


Figure V.22. Normalized Difference Fourier Transform Spectra of the CHEMFET Sensor Coated with the 1500Å Thick PbPc Film upon Exposure to the DMMP Challenge at 25 °C.

with the gas concentration. However, as mentioned earlier in the cobalt phthalocyanine section (Page V-14), the response observed for the 0.1 ppm DMMP challenge at 25 °C was associated with an inadequate purge of the CHEMFET sensor between the gas challenges and was not used in further data analysis.

The normalized difference magnitudes of -0.15, 0.08, and 0.15 were extrapolated as the average value at those frequencies less than 20 KHZ for 0.1 ppm, 0.5 ppm, and 3 ppm DMMP gas concentrations, respectively.

The CHEMFET sensor's responses upon exposure to 0.5 ppm and 3 ppm DMMP challenge gas concentrations revealed when compared with the responses observed with the DIMP challenge gas at 25 °C (Figure V.19), the CHEMFET sensor had a similar frequency response upon exposure to the DIMP and DMMP challenge gases. The responses had approximately the same normalized difference magnitude (from 0.08 to 0.19), and the prominent 20 KHZ oscillation. Overall, in the Fourier transform spectra, the CHEMFET sensor's responses to the DIMP and DMMP challenge gases were similar in shape at 25 °C, with the normalized difference magnitudes for DIMP slightly greater than those associated with DMMP.

## DMMP Challenge Gas Exposure at 120 °C.

Figure V.23 depicts the normalized difference Fourier transform spectra data for the CHEMFET sensor coated with the 1500Å thick lead phthalocyanine film at 120 °C with respect to three different DMMP gas concentrations. At 120 °C, the response of the interdigitated gate electrode CHEMFET coated with the PbPc film to a pulse excitation was consistent with the challenge gas concentrations. Normalized difference magnitudes of 0.04, 0.06, and 0.45 were extrapolated as the average value at those frequencies less than 20 KHZ for the 0.1 ppm, 0.5 ppm, and 3 ppm DMMP challenge gas concentrations. The oscillation frequency of approximately 20 KHZ was also observed.

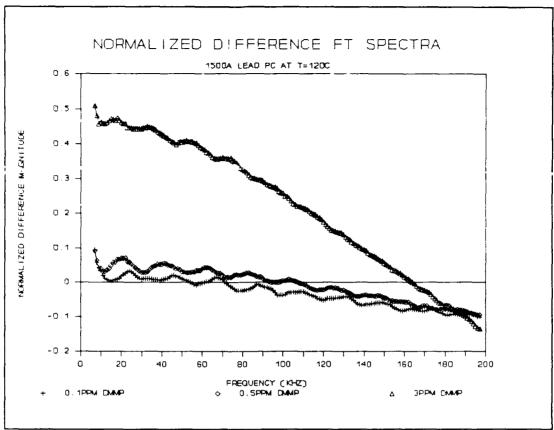


Figure V.23. Normalized Difference Fourier Transform Spectra of the CHEMFET Sensor Coated with the 1500Å Thick PbPc Film upon Exposure to the DMMP Challenge at 120 °C.

This oscillation was less prominent in the responses at 120 °C upon exposure to the DMMP challenge gas compared to the responses observed at 25 °C, or in the responses observed upon exposure to the DIMP challenge gas (Figures V.19, V.20, and V.22).

Compared with the responses observed with the DIMP challenge gas at 120 °C (Figure V.20), the CHEMFET sensor had a greater change in the frequency response upon exposure to the DMMP challenge gas at 120 °C (0.45 for 3 ppm DMMP and 0.3 for 7.5 ppm DIMP).

Figure V.24 depicts the normalized difference Fourier transform spectra data for the CHEMFET sensors coated with the 500Å and 1500Å thick lead phthalocyanine films at 120 °C. The normalized difference Fourier transform spectra revealed that the response of the CHEMFET sensor coated with the 500Å thick PbPc film did change considerably upon exposure to the 3 ppm DMMP gas with respect to the response of the unexposed CHEMFET sensor. The same observation was made previously with the 7.5 ppm DIMP challenge gas (Figure V.21). However,

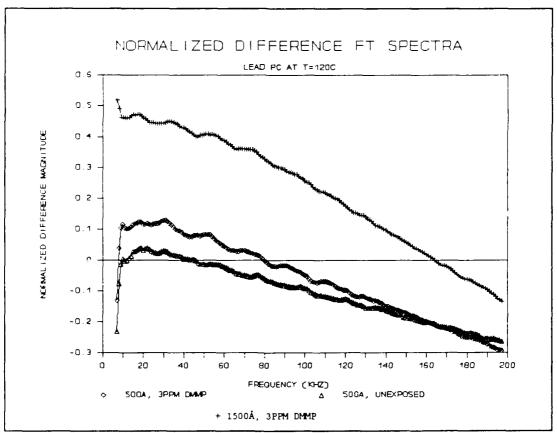


Figure V.24. Normalized Difference Fourier Transform Spectra of the CHEMFET Sensors Coated with the 500Å and 1500Å Thick PbPc Films upon Exposure to the 3 ppm DMMP Challenge at 120 °C.

similar to the response observed with the 7.5 ppm DIMP gas at 120 °C, the CHEMFET sensor coated with 1500Å thick PbPc film showed more sensitivity to 3 ppm DMMP challenge gas than the CHEMFET sensor coated with the 500Å thick PbPc film.

#### Summary.

The Fourier transform spectra data revealed that the response of the interdigitated gate electrode CHEMFET sensor coated with the 1500Å thick PbPc film to an excitation pulse was generally consistent with the concentrations of the challenge gases (DIMP and DMMP), with an exception observed upon exposure to 3 ppm of DIMP at 25 °C. Table V.3 summarizes the normalized difference magnitudes data associated with the Fourier transform spectra observed at each challenge gas concentration and temperature.

The interdigitated gate electrode CHEMFET sensor coated with the 1500Å thick PbPc film was more sensitive to the changes in the DMMP concentration compared to the changes in the DIMP concentration at both 25 °C and 120 °C. The greatest sensitivity of the CHEMFET sensor was observed at 120 °C upon exposure to the 3 ppm DMMP.

The data taken at both the 7.5 ppm DIMP challenge and the 3 ppm DMMP exposure at 120 °C revealed that the CHEMFET sensor coated with the 1500Å thick PbPc film was more sensitive to the change in the challenge gas concentration than the CHEMFET sensor coated with the 500Å thick PbPc film. It was also observed that the CHEMFET sensor coated with the

500Å thick PbPc film was more sensitive to the challenge gases compared to the CHEMFET sensors coated with the other phthalocyanine films that were 500Å thick.

Table V.3. Summary of the Normalized Difference Magnitudes of the Fourier Transform Spectra for the CHEMFET Sensor Coated with the 1500Å Thick PbPc Film.

Challenge Gas Concentration (ppm)						
	0.1	0.5	3	7.5		
DMMP at 25 °C		0.08	0.15			
DMMP at 120 °C	0.04	0.06	0.45			
DIMP at 25 °C		0.08	0.13	0.12		
DIMP at 120 °C		0.05	0.15	0.3		

# Sensitivity Performance of the CHEMFET Sensor Coated with CuPc

DIMP Challenge Gas Exposure at 25 °C.

Figure V.25 depicts the normalized difference Fourier transform spectra data for the CHEMFET sensor coated with the 1500Å thick copper phthalocyanine film at 25 °C with respect to three different DIMP gas concentrations. The response of the interdigitated gate electrode CHEMFET sensor coated with CuPc to a pulse excitation depended upon the DIMP challenge gas concentration. At the lower frequencies (less than 160 KHZ), the greatest change in the CHEMFET's response with respect to the excitation pulse occurred upon exposure to the greatest DIMP concentration (7.5 ppm).

The oscillation frequency of approximately 20 KHZ, which was observed with the CHEMFET sensor coated with CoPc, was also observed. The oscillation frequency was more prominent at the lower challenge gas concentrations.

A normalized difference magnitude of 0.2 was extrapolated as the average value for the 7.5 ppm DIMP exposure at those frequencies less than 20 KHZ. For the 3 ppm DIMP exposure, a normalized difference magnitude of 0.11 was extrapolated as the average value at those frequencies less than 20 KHZ. For the 0.5 ppm DIMP exposure, an average magnitude of 0.02 was extrapolated. The greater normalized difference magnitudes associated with the greater gas concentrations, which was also observed with the cobalt and

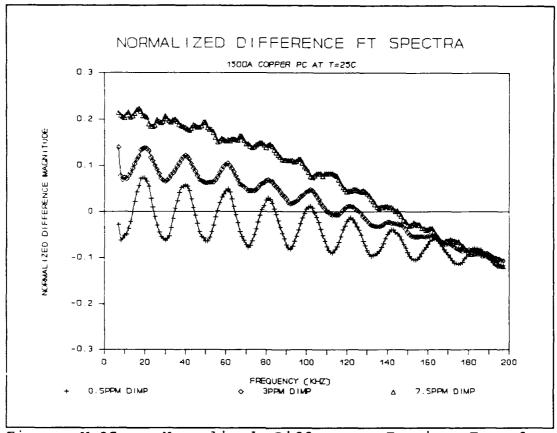


Figure V.25. Normalized Difference Fourier Transform Spectra of the CHEMFET Sensor Coated with the 1500Å Thick CuPc upon Exposure to the DIMP Challenge at 25 °C.

lead phthalocyanine films, was also observed with the copper phthalocyanine at 25 °C.

### DIMP Challenge Gas Exposure at 120 °C.

Figure V.26 depicts the normalized difference Fourier transform spectra data for the CHEMFET sensor coated with the 1500Å thick copper phthalocyanine film at 120 °C with respect to two different DIMP gas concentrations. The data for the 0.5 ppm DIMP exposure was not included because it was not consistent with the rest of the data. Similar to the responses at 25 °C, the response of the interdigitated gate

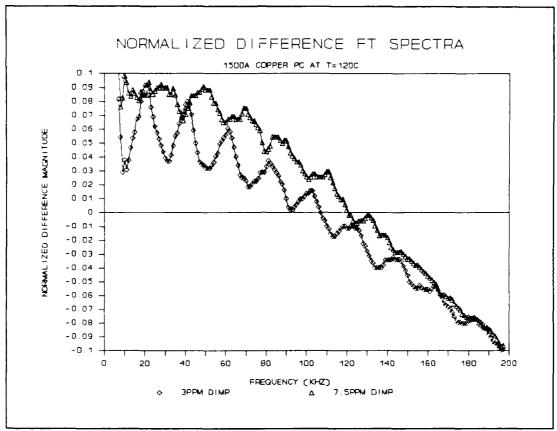


Figure V.26. Normalized Difference Fourier Transform Spectra of the CHEMFET Sensor Coated with the 1500Å Thick CuPc upon Exposure to the DIMP Challenge at 120 °C.

electrode CHEMFET coated with CuPc to a pulse excitation at 120 °C also depended upon the DIMP challenge gas concentration. At all frequencies below 200 KHZ, a greater change in the CHEMFET's response with respect to the excitation pulse occurred upon exposure to the greater DIMP concentration (7.5 ppm).

The oscillation frequency of approximately 20 KHZ was again observed. This oscillation frequency was prominent at the both challenge gas concentrations. The shape of the

overall spectrum envelope for the 7.5 DIMP gas concentration was similar to the one observed at 25 °C. These spectrum envelopes had a zero normalized difference magnitude at approximately 140 KHZ.

At 120 °C, the normalized difference magnitude of 0.09 was extrapolated as the average value for the 7.5 ppm DIMP exposure at those frequencies less than 20 KHZ. For the 3 ppm DIMP exposure, a normalized difference magnitude of 0.07 was extrapolated as the average value at those frequencies less than 20 KHZ.

Figure V.27 depicts the normalized difference Fourier transform spectra data for the CHEMFET sensors coated with the 500Å and 1500Å thick copper phthalocyanine films at 120 °C. The normalized difference Fourier transform spectra revealed that the response of the CHEMFET sensor coated with the 500Å thick CuPc film did not change upon exposure to the 7.5 ppm DIMP gas with respect to the response of the unexposed CHEMFET sensor. At 120 °C the CHEMFET sensor coated with the 1500Å thick CuPc film manifested more sensitivity to the 7.5 ppm DIMP challenge gas compared to the CHEMFET sensor coated with the 500Å thick CuPc film.

### DMMP Challenge Gas Exposure at 25 °C.

Figure V.28 depicts the normalized difference Fourier transform spectra data for the CHEMFET sensor coated with the 1500Å thick copper phthalocyanine film at 25 °C with respect to three different DMMP gas concentrations. The response of the interdigitated gate electrode CHEMFET sensor

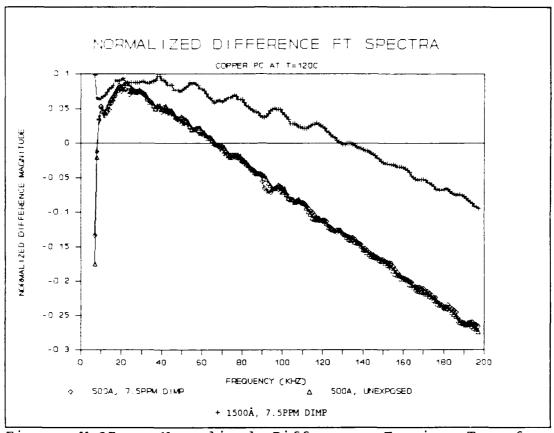


Figure V.27. Normalized Difference Fourier Transform Spectra of the CHEMFET Sensors Coated with the 500Å and 1500Å Thick CuPc Films upon Exposure to the 7.5 ppm DIMP Challenge at 120 °C.

coated with the CuPc film to a pulse excitation was consistent with respect to the 0.5 ppm and 3 ppm challenge gas concentrations. As mentioned earlier in the cobalt phthalocyanine section (Page V-14), the response observed with the 0.1 ppm DMMP challenge at 25 °C was due to inadequate purge of the CHEMFET sensor between the measurements. The response of each CHEMFET sensor coated with the 1500Å thick CoPc, NiPc, and CuPc films upon exposure to the 0.1 ppm DMMP challenge at 25 °C (Figure V.10, Figure

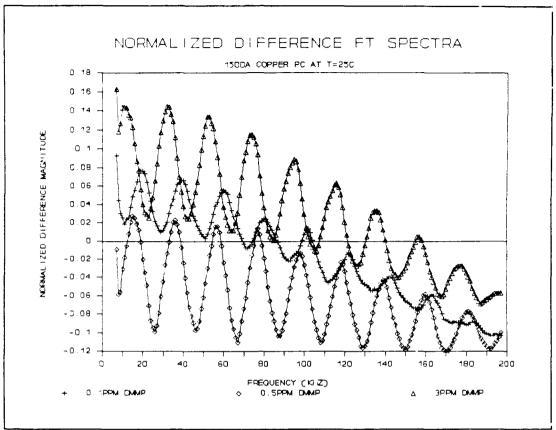


Figure V.28. Normalized Difference Fourier Transform Spectra of the CHEMFET Sensor Coated with the 1500Å Thick CuPc Film upon Exposure to the DMMP Challenge at 25 °C.

V.16, and Figure V.28), consistently manifested a greater change than expected, indicating that these sensors were affected by the inadequate purge.

Normalized difference magnitudes of 0.05, -0.02, and 0.09 were extrapolated as the average values at those frequencies less than 20 KHZ for the 0.1 ppm, 0.5 ppm, and 3 ppm DMMP gas concentrations, respectively. The CHEMFET sensor's response upon exposure to the 3 ppm DMMP gas concentration revealed that, when compared with the response

observed with the DIMP challenge gas at 25 °C (Figure V.25), the CHEMFET sensor had a similar frequency response upon exposure to the DIMP and DMMP challenge gases. The responses had approximately the same normalized difference magnitude (0.11 for DIMP and 0.09 for DMMP) and the prominent 20 KHZ oscillation. Overall, in the Fourier transform spectra, the CHEMFET sensor's responses to the 3 ppm DIMP and 3 ppm DMMP challenge gases were similar in their envelope shapes at 25 C, with the zero normalized difference magnitude occuring at approximately 125 KHZ, and the normalized difference magnitudes for DIMP were slightly greater than for DMMP.

### DMMP Challenge Gas Exposure at 120 °C.

Figure V.29 depicts the normalized difference Fourier transform spectra data for the CHEMFET sensor coated with the 1500Å thick copper phthalocyanine film at 120 °C with respect to the three different DMMP challenge gas concentrations. At 120 °C, the response of the interdigitated gate electrode CHEMFET coated with CuPc to a pulse excitation was not consistent with the challenge gas concentrations. The normalized difference magnitudes of 0.24, 0.18, and 0.5 were extrapolated as the average values at those frequencies less than 20 KHZ for the 0.1 ppm, 0.5 ppm, and 3 ppm DMMP challenge gas concentrations. The inconsistency associated with the responses due to the 0.1 ppm and 0.5 ppm DMMP gas exposures was also observed. A greater change in the response with respect to the excitation pulse was observed at

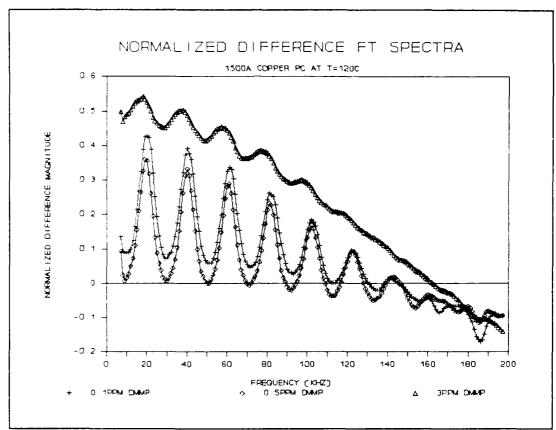


Figure V.29. Normalized Difference Fourier Transform Spectra of the CHEMFET Sensor Coated with the 1500Å Thick CuPc Film upon Exposure to DMMP Challenge at 120 °C.

0.1 ppm (0.24 vs 0.18). This inconsistency was not explainable.

The oscillation frequency of approximately 20 KHZ was also observed. This oscillation frequency was prominent at the lower challenge gas concentrations.

In comparison with the responses seen with the DIMP challenge gas at 120 °C (Figure V.26), the CHEMFET sensor manifested a greater change in the frequency response upon exposure to the DMMP challenge gas compared to the exposure

to DIMP at 120 °C (0.5 for 3 ppm DMMP and 0.09 for 7.5 ppm DIMP).

Figure V.30 depicts the normalized difference Fourier transform spectral data for the CHEMFET sensors coated with the 500Å and 1500Å thick copper phthalocvanine films at 120 °C. The normalized difference Fourier transform spectra revealed that the response of the CHEMFET sensor coated with the 500Å thick CuPc did not change as much upon exposure to the 3 ppm DMMP gas challenge compared to the response of the

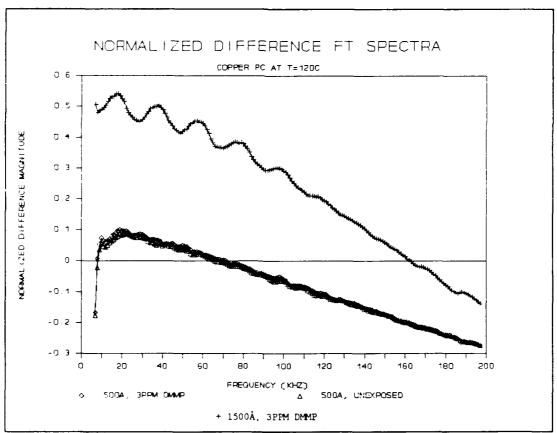


Figure V.30. Normalized Difference Fourier Transform Spectra of the CHEMFET Sensors Coated with the 500Å and 1500Å Thick CuPc Films upon Exposure to the 3 ppm DMMP Challenge at 120 °C.

unexposed CHEMFET sensor. At 120 °C, the CHEMFET sensor coated with the 1500Å thick CuPc film manifested more sensitivity to the 3 ppm DMMP challenge gas compared to the CHEMFET sensor coated with the 500Å thick CuPc film. A similar observation was made previously with the DIMP challenge gas at 120 °C.

## Summary.

The Fourier transform spectra data revealed that the response of the interdigitated gate electrode CHEMFET sensor coated with the 1500Å thick CuPc film to an excitation pulse was generally consistent with the concentrations of the challenge gases (DIMP and DMMP), with an exception observed upon exposure to the 0.1 ppm DMMP challenge at 120 °C. Table V.4 summarizes the normalized difference magnitude of the

Table V.4. Summary of the Normalized Difference Magnitudes of the Fourier Transform Spectra for the CHEMFET Sensor Coated with the 1500Å Thick CuPc Film.

			Challenge Gas Concentration (ppm)				
			0.1	0.5	3	7.5	
•	<del></del>				<del></del>	··· <u>·</u> ·	
	DMMP at	25 °C	0.05	-0.02	0.09		
	DMMP at	120 °C	0.24	0.18	0.5		
	DIMP at	25 °C		0.02	0.11	0.2	
	DIMP at	120 °C			0.07	0.09	

Fourier transform spectra observed at each challenge gas concentration and temperature.

The interdigitated gate electrode CHEMFET sensor coated with the 1500Å thick CuPc film was more sensitive to the changes in the DIMP concentration compared to the changes in the DMMP concentration at 25 °C. At 120 °C, the CHEMFET sensor was more sensitive to the changes in the DMMP concentrations. The greatest sensitivity of the CHEMFET sensor was observed at 120 °C upon exposure to the 3 ppm DMMP challenge.

The data measured at both the 7.5 ppm DIMP and 3 ppm DMMP exposure at 120 °C revealed that the CHEMFET sensor coated with the 1500Å thick CuPc film was more sensitive to the change in the challenge gas concentration compared to the CHEMFET sensor coated with the 500Å thick CuPc film.

# Sensitivity Performance of the CHEMFET Sensor Coated with 2-Naphthol( $\beta$ )

DIMP Challenge Gas Exposure at 25 °C.

Figure V.31 depicts the normalized difference Fourier transform spectra data of the CHEMFET sensor coated with 2-naphthol( $\beta$ ) at 25 °C upon exposure to the 7.5 ppm DIMP challenge gas concentration, and the response observed prior to the exposure (unexposed).

The response of the interdigitated gate electrode CHEMFET sensor coated with 2-naphthol( $\beta$ ) to a pulse excitation changed upon exposure to the challenge gas when compared to the unexposed response. A normalized difference magnitude of -0.03 was observed for the 7.5 ppm DIMP exposure at those frequencies less than 20 KHZ. For the unexposed trial, a normalized difference value of 0.5 was observed. The 20 KHZ oscillation frequency, which was observed with the CHEMFET sensor coated with metal-doped phthalocyanine films, was not present with the CHEMFET sensor coated with 2-naphthol( $\beta$ ) film. The decrease in the spectrum magnitude observed upon exposure to the challenge gas indicates that the impedance of the 2-naphthol( $\beta$ ) film has increased after exposure to the challenge gas.

The time-domain responses of the CHEMFET sensor coated with 2-naphthol( $\beta$ ) to an excitation pulse are depicted in Figure V.32. The time-domain responses also revealed a

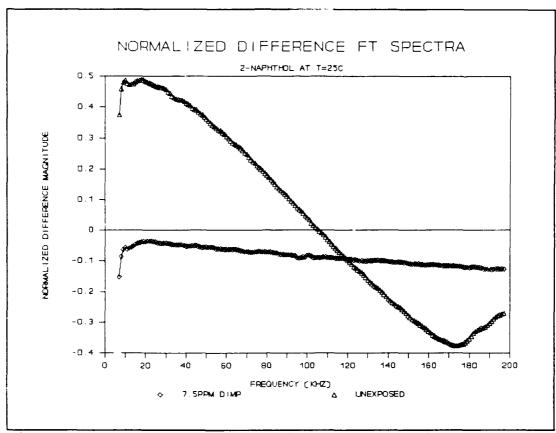


Figure V.31. Normalized Difference Fourier Transform Spectra of the CHEMFET Sensor Coated with the 2-Naphthol( $\beta$ ) upon Exposure to the 7.5 ppm DIMP Challenge at 25 °C.

drastic change between the exposed and the unexposed responses. The duration of the response pulse changed from 3.5  $\mu$ s without the challenge gas exposure to 1.5  $\mu$ s with the exposure). The impedance data of the film, depicted in Figures F.1 and F.2 (Appendix F) also revealed that a significant impedance change has occurred. The impedance of the film increased after exposed to a 7.5 ppm DIMP challenge. Both the resistive part and reactive part of the impedance increased from nearly 100K ohms to approximately 1M ohms at

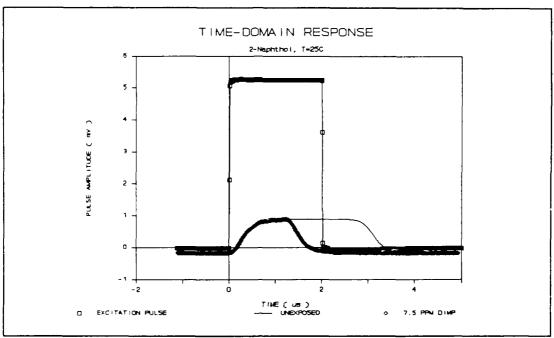


Figure V.32. Time-Domain Response of the CHEMFET Sensor Coated with the 2-Naphthol( $\beta$ ) upon Exposure to the 7.5 ppm DIMP Challenge at 25 °C.

those frequencies less than 1000 HZ. The DC resistance data did not reveal any noticeable change and thus are not shown here.

### DMMP Challenge Gas at 25 °C.

Figure V.33 depicts the normalized difference Fourier transform spectra data of the CHEMFET sensor coated with 2-naphthol( $\beta$ ) at 25 °C upon exposure to the 3 ppm DMMP gas concentration, and the response observed prior to the exposure.

The response of the interdigitated gate electrode CHEMFET sensor coated with 2-naphthol( $\beta$ ) to a pulse excitation changed upon exposure to the 3 ppm DMMP challenge gas compared to the response of the unexposed sensor. Again,

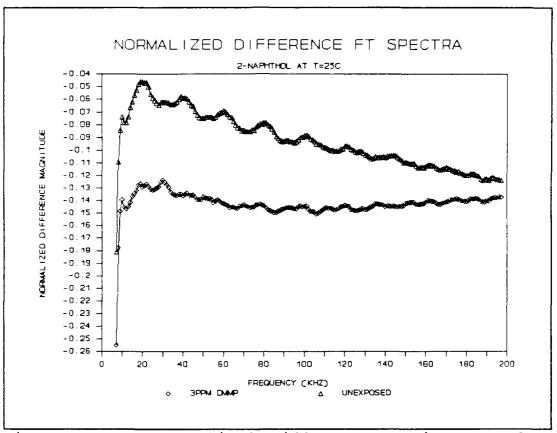


Figure V.33. Normalized Difference Fourier Transform Spectra of the CHEMFET Sensor Coated with the 2-Naphthol( $\beta$ ) upon Exposure to the 3 ppm DMMP Challenge at 25 °C.

a decrease in the spectral magnitude was observed. The normalized difference magnitude of -0.13 was observed for the 3 ppm DMMP exposure at those frequencies less than 20 KHZ. For the unexposed trial, a normalized difference of -0.03 was observed. The 20 KHZ oscillation frequency, which was observed with the responses in the CHEMFET sensor coated with the metal-doped phthalocyanine films, was present in the response of the CHEMFET sensor coated with the 2-naphthol( $\beta$ ) film upon exposure to air (unexposed). The decrease in the

spectrum magnitude observed upon exposure to the challenge gas indicates, again, that the impedance of the 2-naphthol( $\beta$ ) film has increased after exposure to the challenge gas. The impedance measurements (Figures F.3 and F.4 in Appendix F) show the corresponding changes. The resistive part of the impedance has decreased (at 1 KHZ, from 90K ohms to 40K ohms).

Figure V.34 depicts the DC resistance measured during the 3 ppm DMMP exposure. The DC resistance of the interdigitated gate electrode coated with the 2-naphthol( $\beta$ ) film has increased from 200M ohms to 900M ohms during the 3 ppm DMMP gas exposure.

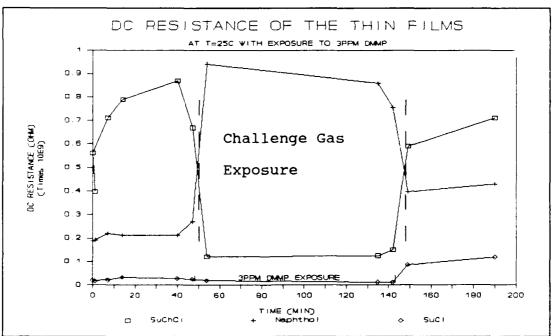


Figure V.34. DC Resistance of the Organic Thin Films, Succinylcholine Chloride, 2-Naphthol( $\beta$ ), and Succinylchloride upon Exposure to the 3 ppm DMMP Challenge at 25°C.

## Summary.

The interdigitated gate electrode CHEMFET sensor coated with 2-naphthol( $\beta$ ) showed a change in response upon exposure to the challenge gases (7.5 ppm DIMP and 3 ppm DMMP) at 25 °C. The impedance of the film increased during the exposure. The changes observed were more significant compared to those changes observed previously with the CHEMFET sensors coated with the metal-doped phthalocyanine films.

# Sensitivity Performance of the CHEMFET Sensor Coated with Succinvlchloride

DIMP Challenge Gas Exposure at 25 °C.

Figure V.35 depicts the normalized difference Fourier transform spectra data of the CHEMFET sensor coated with succinylchloride at 25 °C upon exposure to the 7.5 ppm DIMP challenge gas concentration, and the response observed prior to the exposure (unexposed).

The response of the interdigitated gate electrode

CHEMFET sensor coated with succinylchloride to a pulse

excitation changed upon exposure to the challenge gas

compared to the unexposed response. The normalized

difference magnitude of 0.4 was observed for the 7.5 ppm DIMP

exposure at those frequencies less than 20 KHZ. For the

unexposed trial, a normalized difference of 0.6 was observed.

The 20 KHZ oscillation frequency, which was observed with the

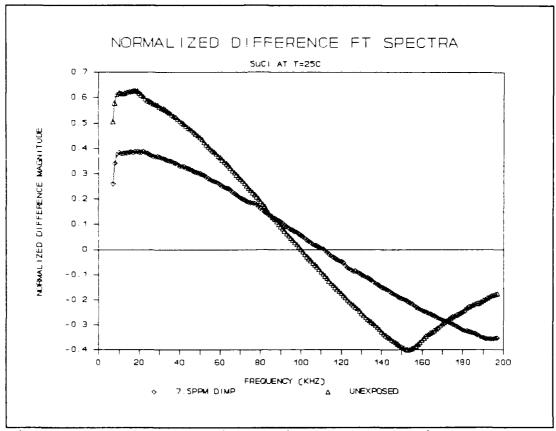


Figure V.35. Normalized Difference Fourier Transform Spectra of the CHEMFET Sensor Coated with the Succinylchloride Film upon Exposure to the 7.5 ppm DIMP Challenge at 25 °C.

CHEMFET sensor coated with metal-doped phthalocyanine films, was not present with the CHEMFET sensor coated with succinylchloride film. The time-domain responses of the CHEMFET sensor are depicted in Figure V.36.

The time-domain responses also show a drastic change between the exposed and the unexposed responses. The impedance data of the interdigitated gate electrode coated with the succinylchloride, depicted in Figures F.5 and F.6 (Appendix F), also reveals that an impedance change has

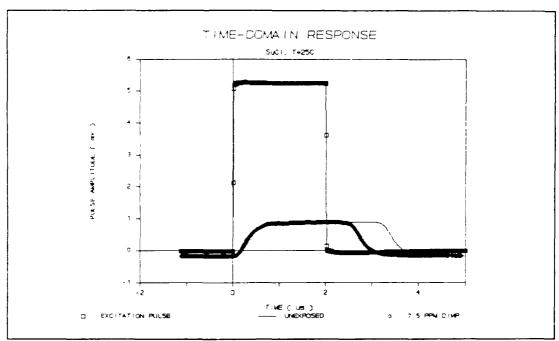


Figure V.36. Time-Domain Response of the CHEMFET Sensor Coated with the Succinylchloride Film upon Exposure to the 7.5 ppm DIMP Challenge at 25 °C.

occurred. The resistive part of the impedance of the film decreased by 20K ohms after exposure to the 7.5 ppm DIMP challenge.

## DMMP Challenge Gas Exposure at 25 °C.

Figure V.37 depicts the normalized difference Fourier transform spectra data of the CHEMFET sensor coated with succinylchloride at 25 °C upon exposure to the 3 ppm DMMP gas concentration and the response observed prior to the exposure.

The response of the interdigitated gate electrode

CHEMFET sensor coated with succinylchloride to a pulse

excitation changed upon exposure to the 3 ppm DMMP challenge

gas compared to the response of the unexposed sensor. Again,

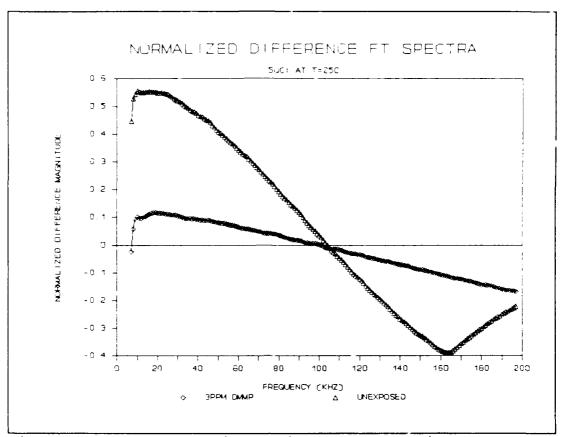


Figure V.37. Normalized Difference Fourier Transform Spectra of the CHEMFET Sensor Coated with the Succinylchloride Film upon Exposure to the 3 ppm DMMP challenge at 25 °C.

a decrease in the spectral magnitude was observed. A normalized difference magnitude of 0.1 was observed for the 3 ppm DMMP exposure at those frequencies less than 20 KHZ. For the unexposed trial, a normalized difference of 0.55 was observed. The 20 KHZ oscillation frequency, which was observed with the responses in the CHEMFET sensor coated with the metal-doped phthalocyanine films, was not present in the response of the CHEMFET sensor coated with the succinylchloride film upon exposure to air (unexposed).

The impedance measurements (Figures F.7 and F.8 in Appendix F) reveal that the impedance change upon exposure to the 3 ppm DMMP gas challenge. The resistive part of the impedance has decreased at frequencies greater than 1 KHZ, while the reactivepart decreased at frequencies less than 1KHZ.

The DC resistance (Figure V.34) of the interdigitated gate electrode coated with succinylchloride decreased slightly during the 3 ppm DMMP challenge gas exposure.

## Summary.

The interdigitated gate electrode CHEMFET sensor coated with succinylchloride showed a change in response upon exposure to the challenge gases (7.5 ppm DIMP and 3 ppm DMMP) at 25 °C. The impedance of the film decreased during the exposure. The magnitudes of changes observed were less than those observed previously with the CHEMFET sensors coated with 2-naphthol( $\beta$ ).

# Sensitivity Performance of the CHEMFET Sensor Coated with L-Histidine Dihydrochloride

DIMP Challenge Gas Exposure at 25 °C.

Figure V.38 depicts the normalized difference Fourier transform spectra data of the CHEMFET sensor coated with L-histidine dihydrochloride at 25 °C upon exposure to the 7.5 ppm DIMP challenge gas concentration and the response observed prior to the exposure (unexposed).

The response of the interdigitated gate electrode

CHEMFET sensor coated with L-histidine dihydrochloride to a

pulse excitation changed upon exposure to the challenge gas

compared to the unexposed response. A normalized difference

magnitude of -0.12 was observed for the 7.5 ppm DIMP exposure

at those frequencies less than 20 KHZ. For the unexposed

trial, an average normalized difference of 0.1 was observed.

The 20 KHZ oscillation frequency, which was observed with the

CHEMFET sensor coated with metal-doped phthalocyanine films,

was observed with the CHEMFET sensor coated with L-histidine

dihydrochloride film upon exposure to air. The decrease in

the spectral magnitude observed upon exposure to the

challenge gas indicates that the impedance of the L-histidine

dihydrochloride film has increased after exposure to the

challenge gas.

The time-domain responses of the CHEMFET sensor coated with L-histidine dihydrochloride to an excitation pulse are

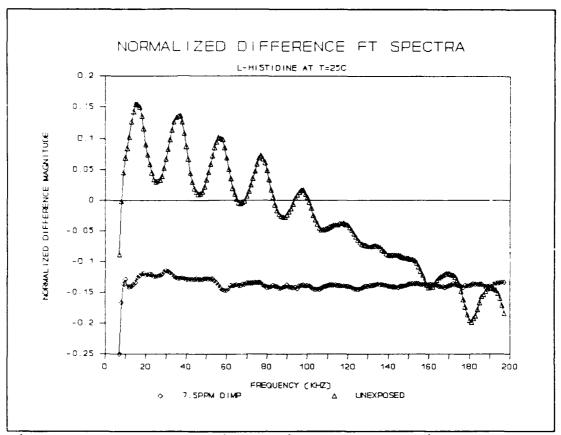


Figure V.38. Normalized Difference Fourier Transform Spectra of the CHEMFET Sensor Coated with the L-Histidine Dihydrochloride Film upon Exposure to the 7.5 ppm DIMP Challenge at 25 °C.

depicted in Figure V.39. The time-domain responses reveal a small change between the exposed and the unexposed response. The impedance data of the film, depicted in Figures F.9 and F.10 (Appendix F), also revealed that an impedance change has occurred. The impedance of the film increased after exposed to the 7.5 ppm DIMP challenge. At frequencies less than 1K HZ, the resistive part of the impedance increased from 10K ohms to nearly 1M ohms. The DC resistance data did not reveal any noticeable change, and thus is not shown.

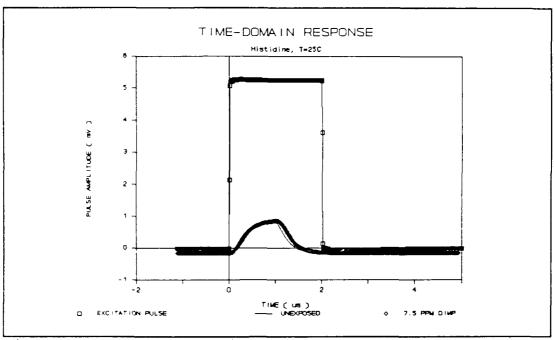


Figure V.39. Time-Domain Response of the CHEMFET Sensor Coated with the L-Histidine Dihydrochloride Film upon Exposure to the 7.5 ppm DIMP Challenge at 25 °C.

### DMMP Challenge Gas at 25 °C.

Figure V.40 depicts the normalized difference Fourier transform spectral data of the CHEMFET sensor coated with L-histidine dihydrochloride at 25 °C upon exposure to the 3 ppm DMMP challenge gas concentration and the response observed prior to the exposure. The response of the interdigitated gate electrode CHEMFET sensor coated with L-histidine dihydrochloride to a pulse excitation changed upon exposure to the 3 ppm DMMP challenge gas compared to the unexposed response. However, contrary to the response observed with the 7.5 ppm DIMP challenge, an increase in the spectral magnitude was observed. An average normalized difference magnitude of -0.11 was observed for the 3 ppm DMMP

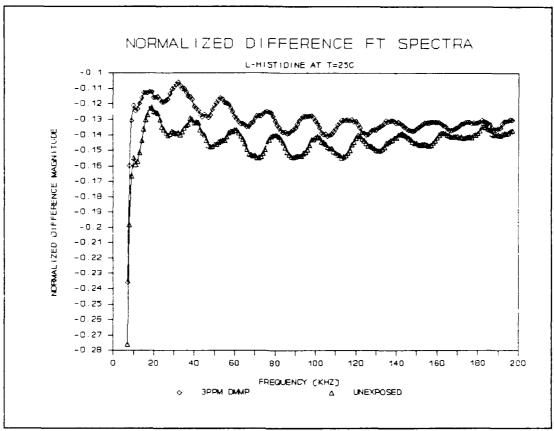


Figure V.40. Normalized Difference Fourier Transform Spectra of the CHEMFET Sensor Coated with the L-Histidine Dihydrochloride Film upon Exposure to the 3 ppm DMMP Challenge at 25 °C.

exposure at those frequencies less than 20 KHZ. For the unexposed trial, an average normalized difference of -0.13 was observed. The 20 KHZ oscillation frequency, which was observed with the responses in the CHEMFET sensor coated with the metal-doped phthalocyanine films, was present in the responses of the CHEMFET sensor.

The increase in the spectral magnitude observed upon exposure to the challenge gas indicated that the impedance of the L-histidine dihydrochloride film decreased after exposure

to the challenge gas. The impedance measurements (Figures F.11 and F.12 in Appendix F) reveal the change. The resistive part of the impedance decreased from 100K ohms to nearly 10K ohms upon exposure. The DC resistance data did not reveal any noticeable change, and it is not shown.

## Summary.

The interdigitated gate electrode CHEMFET sensor coated with L-histidine dihydrochloride showed a change in response upon exposure to both challenge gases (7.5 ppm DIMP and 3 ppm DMMP) at 25 °C. However, the responses were contrary. Exposure to 7.5 ppm DIMP resulted in a increase in the film's impedance, while exposure to 3 ppm DMMP resulted in a decrease. The 20 KHZ oscillation observed with the phthalocyanine films was also present.

# Sensitivity Performance of the CHEMFET Sensor Coated with Succinvlcholine Chloride

## DIMP Challenge Gas Exposure at 25 °C.

Figure V.41 depicts the normalized difference Fourier transform spectra data of the CHEMFET sensor coated with succinylcholine chloride at 25 °C upon exposure to the 7.5 ppm DIMP challenge gas concentration and the response observed prior to the exposure (unexposed).

The response of the interdigitated gate electrode

CHEMFET sensor coated with succinylcholine chloride to a

pulse excitation changed upon exposure to the challenge gas

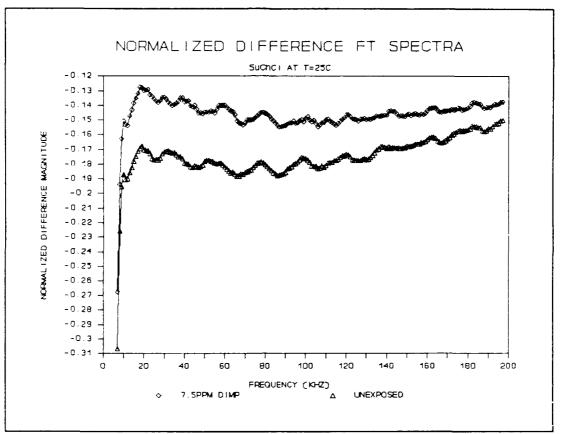


Figure V.41. Normalized Difference Fourier Transform Spectra of the CHEMFET Sensor Coated with the Succinylcholine Chloride Film upon Exposure to the 7.5 ppm DIMP Challenge at 25 °C.

compared to the unexposed response. An average normalized difference magnitude of -0.13 was observed for the 7.5 ppm DIMP exposure at those frequencies less than 20 KHZ. For the unexposed trial, a normalized difference of -0.17 was observed. The 20 KHZ oscillation frequency, which was observed with the CHEMFET sensor coated with metal-doped phthalocyanine films and with L-histidine dihydrochloride film, was also present with the CHEMFET sensor coated with succinylcholine chloride film.

The time-domain responses of the CHEMFET sensor are depicted in Figure V.42. The time-domain responses revealed a small change between the exposed and the unexposed responses. The impedance data of the interdigitated gate electrode coated with the succinylcholine chloride, however, depicted in Figures F.13 and F.14 (Appendix F), did not reveal significant impedance changes.

## DMMP Challenge Gas Exposure at 25 °C.

Figure V.43 depicts the normalized difference Fourier transform spectra data of the CHEMFET sensor coated with succinylcholine chloride at 25 °C upon exposure to the 3 ppm DMMP gas concentration and the response observed prior to the exposure.

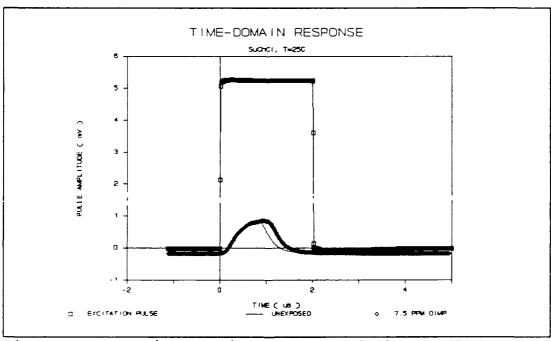


Figure V.42. Time-Domain Response of the CHEMFET Sensor Coated with the Succinylcholine Chloride Film upon Exposure to the 7.5 ppm DIMP Challenge at 25 °C.

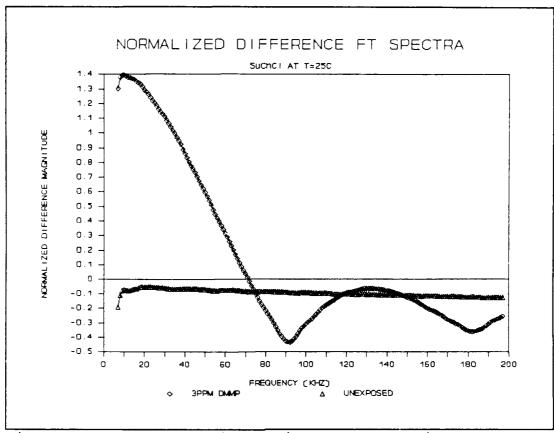


Figure V.43. Normalized Difference Fourier Transform Spectra of the CHEMFET Sensor Coated with the Succinylcholine Chloride Film upon Exposure to the 3 ppm DMMP Challenge at 25 °C.

The response of the interdigitated gate electrode

CHEMFET sensor coated with succinylcholine chloride to a

pulse excitation changed dramatically upon exposure to the

3 ppm DMMP challenge gas compared to the unexposed response.

Again, an increase in the spectral magnitude was observed.

A normalized difference magnitude of 1.4 was observed for the

3 ppm DMMP exposure at those frequencies less than 20 KHZ.

For the unexposed trial, a normalized difference of -0.1 was observed. Instead of the 20 KHZ oscillation frequency, which

was observed with the responses in the CHEMFET sensor coated with metal-doped phthalocyanine films, an oscillation frequency of approximately 80 KHZ was observed in the response of the CHEMFET sensor coated with the succinylcholin chloride film upon exposure to the 3 ppm DMMP challenge.

Figures V.44 and V.45 depict the time-domain responses of the CHEMFET sensor. The time-domain responses also revealed a significant change. The pulse duration changed from 3  $\mu$ s in the unexposed trial to 12  $\mu$ s with the challenge gas exposure.

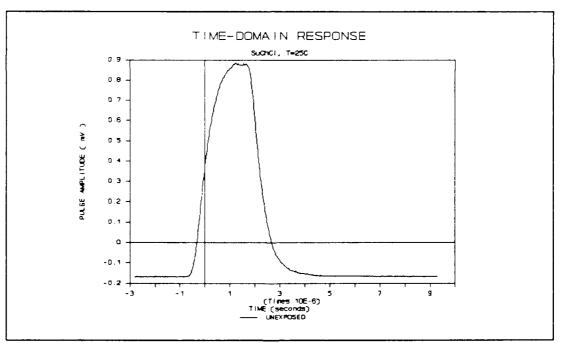


Figure V.44. Time-Domain Response of the CHEMFET Sensor Coated with the Succinylcholine Chloride Film upon Exposure to Air at 25 °C.

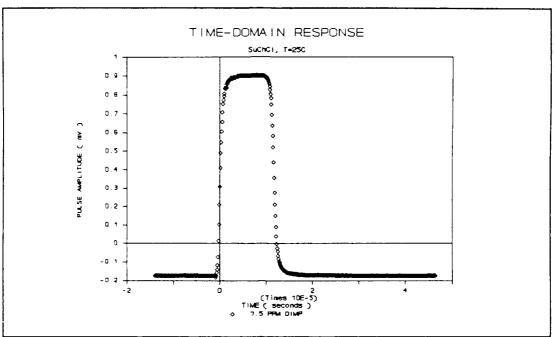


Figure V.45. Time-Domain Response of the CHEMFET Sensor Coated with the Succinylcholine Chloride Film upon Exposure to the 3 ppm DIMP Challenge at 25 °C.

The impedance measurements (Figures F.15 and F.16 in Appendix F), also revealed the impedance change upon exposure to the 3 ppm DMMP gas. The resistive part of the impedance has decreased at frequencies below 2 KHZ and increased at frequencies above 2 KHZ. The reactive part decreased at all frequencies below 100 KHZ.

The DC resistance (Figure V.34) of the interdigitated gate electrode coated with the succinylcholine chloride film decreased during the 3 ppm DMMP gas exposure from 800M ohms to 100M ohms.

## Summary.

The interdigitated gate electrode CHEMFET sensor coated with the succinylcholine chloride filmed manifested a drastic change in its response upon exposure to the 3 ppm DMMP challenge at 25 °C. The impedance of the film decreased during the exposure trial. The magnitudes of the changes observed were by far greater than those observed previously with the CHEMFET sensors coated with the other thin films.

## Summary

The challenge gas exposure sensitivity performance of the interdigitated gate electrode CHEMFET sensors coated with the various metal-doped phthalocyanine films and other organic thin films were evaluated primarily from the normalized difference Fourier transform spectra. With the metal-doped phthalocyanine film coatings, the interdigitated gate electrode CHEMFET sensor with cobalt phthalocyanine provided the most consistent response with respect to both challenge gas (DIMP and DMMP) concentrations, as tabulated in Table V.1. The response of the CHEMFET sensors coated with the metal-doped phthalocyanine films were generally similar in magnitudes and shape. A characteristic 20 KHZ oscillation frequency was observed in responses of all CHEMFET sensors coated with metal-doped phthalocyanine films upon exposure to smaller concentrations of the challenge gases.

With the other organic thin film coatings, with an exception of L-histidine dihydrochloride, the CHEMFET sensor responses were consistent with respect to both challenge gases. The CHEMFET sensors coated with succinylchloride and 2-naphthol( $\beta$ ) showed a decrease in spectral magnitude upon exposure to the challenge gases. For small frequencies, the CHEMFET sensors coated with succinylcholine chloride showed an increase in spectral magnitude upon exposure to the challenge gases. The magnitudes of the responses observed with the other organic thin film coatings were greater than the magnitudes observed with the metal-doped phthalocyanine films, with the exception of the L-histidine dihydrochloride materil.

# VI. Conclusions and Recommendations

## Conclusions

An interdigitated gate electrode CHEMFET was designed and its electrical performance in the frequency-domain was evaluated for detecting DIMP and DMMP challenge gas concentrations with various thin film coatings.

The CHEMFET was designed with ten interdigitated gate electrodes that were connected to an amplifier with a 10 X 1 multiplexer. The amplifier's design performance was verified; it possessed a gain of approximately 30 dB, and it had a 3 dB cut-off frequency at approximately 200 KHZ. The design of the 10 X 1 multiplexer between the gate electrode and the MOS amplifier was, however, found to be electrically incompatible with the thin film coatings used on the interdigitated gate electrode structure. That is, the resistance of the film coatings was significantly larger than the "isolation" resistance of the multiplexer provided to block the signal from passing through the multiplexer (typically 10<sup>10</sup> ohms versus 10<sup>9</sup> ohms).

The vapor exposure sensitivity performance of the CHEMFET sensors toward the organophosphorus challenge gases (DIMP and DMMP) for the various thin film coatings were evaluated primarily from the normalized difference Fourier transform spectra. The CHEMFFT was excited with a 2  $\mu$ s

duration, 5.24 V amplitude pulse which had a 1 KHZ repetition rate. The thin films evaluated were nickel phthalocyanine, cobalt phthalocyanine, lead phthalocyanine, copper phthalocyanine, 2-naphthol( $\beta$ ), L-histidine dihydrochloride, succinylchloride, and succinylcholine chloride. Most of the measurements were accomplished using the metal-doped phthalocyanine films.

Two different phthalocyanine film thicknesses (1500Å and 500Å) were deposited onto the interdigitated gate electrode structure of the CHEMFET by vacuum thermal evaporation. Most of the electrical measurements were made on the 1500Å thick retal-phthalocyanine films at two different temperatures (25 °C and 120 °C) and three different challenge gas concentrations (0.5 ppm, 3 ppm, and 7.5 ppm for DIMP; and 0.1 ppm, 0.5 ppm, and 3 ppm for DMMP). Only one temperature (120 °C) and one challenge gas concentration (7.5 ppm for DIMP and 3 ppm for DMMP) measurement was accomplished for the 500Å thick phthalocyanine films.

The other organic thin films, 2-naphthol( $\beta$ ), L-histidine dihydrochloride, succinylchloride, and succinylcholine chloride, were deposited onto the interdigitated gate electrode of the CHEMFET via a liquid deposition technique (microsyringe and a hypodermic needle). Only one temperature (25 °C) and one challenge gas concentration (7.5 ppm for DIMP and 3 ppm for DMMP) measurement was accomplished for these film coatings.

The challenge gas exposure sensitivity performance evaluation of the phthalocyanine films revealed that the phthalocyanine films were generally more sensitive to the 3 ppm DMMP challenge compared to the 3 ppm DIMP concentration at 120 °C. Among the phthalocyanine film coatings evaluated, the CHEMFET sensor coated with the 1500Å thick cobalt phthalocyanine film responded with the most consistency with respect to both the DIMP and DMMP challenge gases. The sensitivity performance of the 1500Å thick phthalocyanine films were significantly better compared to the 500Å thick phthalocyanine films.

The sensitivity performance evaluation of the other organic thin films, based upon the single DIMP and DMMP challenge gas concentration revealed that, with the exception of L-histidine dihydrochloride, all three films  $(2\text{-naphthol}(\beta), \text{ succinylchloride}, \text{ and succinylcholine}$  chloride) showed promising results. In fact, the shape of the frequency spectra change associated with these films was very different compared to the shape observed for the phthalocyanine films; a further investigation is a must.

## Recommendations

Of course, more data needs to be taken to further investigate and identify the suitable thin films which can be used in the CHEMFET to detect organophosphorus compounds. Of the phthalocyanine films, the cobalt phthalocyanine candidate

is recommended. In addition, a further evaluation of the 2-naphthol( $\beta$ ), succinylchloride, and succinylcholine chloride films appears to be the most urgent. Thus, the following course of actions are recommended for follow-on thesis:

- 1. Overall CHEMFET design do not locate an electronic circuit between the floating gate of the interdigitated electrode and the MOSFET amplifier. The original CHEMFET design consisted of an interdigitated gate electrode structure which was directly connected to the MOSFET's gate contact. This basic design should be preserved; the output of the MOSFET, however, should be suitable for interfacing with a multiplexer.
- 2. Number of Interdigitated Gate Electrode Structures instead of placing ten interdigitated gate electrode structures with a small separation between them, a smaller number of electrodes (for example 4 to 6) with a wider physical separation will facilitate the film deposition process, especially with respect to the liquid solution application procedure.
- 3. MOSFET Amplifier the amplifier design used in this thesis functioned extremely well (30 dP of gain and a 200 KHZ, 3-dB cut-off frequency). If this amplifier design is used again, the voltage offsets for all five stages of the amplifier should be tied together at the integrated circuit level.

- 4. Power Supply Requirements each MOSFET amplifier should have separate voltage supply. Also, input protection features are recommended for the power supply bonding pads to ensure that the amplifier is less susceptible to electrostatic discharge failures.
- 5. Packaged Die always have at least six integrated circuit die packaged. Packaged die are necessary to verify the initial functional performance of the fabricated circuit.
- 6. Film Deposition a more precise and uniform film deposition technique is needed the for 2-naphthol(β), succinylchloride, and succinylcholine chloride films; the liquid deposition technique used in this thesis is not conducive for achieving reproducible results. The current liquid deposition technique can be improved if the interdigitated gate structure's shape is changed from that of a long rectangle, to that of a square, with approximately the same area. Since the liquid droplet on the electrode's surface tends to deposit itself as a circle, a square sized electrode will be more evenly and consistently coated as the solvent evaporates.
- 7. Film Thickness of the Phthalocyanine Films for the continued evaluation of metal-doped phthalocyanine films, a sensitivity performance analysis with respect to film thickness is recommended.

## APPENDIX A

# **Instrumentation and Materials**

### Table A.1. Instrumentation List

Camera Platform, Mask Generation Model 6720P DEKACON III HLC Engineering Co. Oreland, PA

Mask Aligner Karl Suss, Model MJB 3 UV300 Waterbury Center, VT

Photoresist Spinner Headway Research Inc, Model 1-PM101D-R790 Garland, TX

Photoresist Oven
Model Imperial IV
Lab-Line Instruments, Inc.
Melrose Park, IL

Electron Beam Vacuum Deposition System Denton Vacuum, Model DV602 Cherry Hill, NJ

Profilometer Model Dektak 900051 Sloan Technology Corp. Santa Barbara, CA

Micromanipulator Probe Station Micromanipulator Company, Model 6200 Carson City, NV

Digital Multimeter John Fluke Mfg. Co., Model 77/AN Everett, WA

Electrometer Keithley Instruments, Model 617 Cleveland, OH Semiconductor Parameter Analyzer Hewlett-Packard, Model HP 4145B Palo Alto, CA

Impedance/Gain-Phase Analyzer Hewlett-Packard, Model HP 4194A Palo Alto, CA

Pulse Generator Hewlett-Packard, Model HP 8082A Palo Alto, CA

Spectrum Analyzer Hewlett-Packard, Model HP 8556B Palo Alto, CA

Digital Storage Oscilloscope Hewlett-Packard, Model HP 54100A Palo Alto, CA

Active Probe Micromanipulator Company, Model FET-1 Carson City, NV

FET Probe Power Supply Micromanipulator Company, Model FET PS4 Carson City, NV

Microcomputer Zenith Data Systems, Model Z-248 St. Joseph, MI

IEEE-488 interface plug-in card Capitol Equipment Corp., Model 01000-60300 Burlington, MA

DC Power Supply POWERTEC, Model 6C3000

Fower Supply KEPCO, Model CK40-0.8M Flushing, NY

Kapton Strip Heater Watlow, Model K005020C5 St. Louis, MO

Self Adhesive Thermocouple Omega Engineering Inc., Model SA1-K Stamford, CT Sputterer Structure Probe Inc., Model SPI Sputterer West Chester, PA

Digital Hygrometer/Thermometer Thunder Scientific Corp, Model HS-1CHDT-2A Albuquerque, NM

Gas Generation and Delivery System

Test Cell

#### Table A.2. Materials List

Copper Phthalocyanine\*

Lead Phthalocyanine\*\*

Cobalt Phthalocyanine\*

Nickel Phthalocyanine\*

L-histidine dihydrochloride\*

Succinyl chloride\*

Succinylcholine chloride\*

 $2-Naphthol(\beta)*$ 

Kodak High-Resolution Photolithography Plates

Waycoat Negative Photoresist

Photoresist Developer

Copper-Beryllium Foil

Etchant for the Copper-Berylium Foil (Ferric Chloride)

DIMP Permeation Tube

DMMP Permeation Tube

RTV (Room Temperature Vulcanization) Sealant

Syringe and Needle

64-Pin Dual-in-Line Package

- \* These chemicals were provided by Fluka Chemical Corp., Ronkonkoma, NY.
- \*\* This chemical was provided by Pfaltz & Bauer, Inc., Waterbury, CT.

## Appendix B

# **CHEMFET Design Simulations and Fabrication Data**

Table B.1. Initial SPICE Simulation of the Amplifier.

```
DIFFERENTIAL AMPLIFIER WITH FEEDBACK for CHEMFET array
*two micron technology
** establish subcircuit models
*one stage differential feedback amplifier
.subckt fbdamp 1 2 3 4 6
*node 1=vdd
*node 2=vss
*node 3=Vin+
*node 4=offset voltage
*node 6=vout
*node 10=Vin-=feedback
MP1 5 5 1 1 P L=6u W=36u AD=288p AS=288p
MP2 6 5 1 1 P L=6u W=36u AD=288p AS=288p
MN1 5 3 7 7 N L=6u W=24u AD=192p AS=19296p
MN2 6 10 7 7 N L=6u W=24u AD=192p AS=192p
MN3 7 0 2 2 N L=6u W=24u AD=192p AS=192P
R1 6 10 10k
R2 10 4 1k
.ends fbdamp
***********
*analog transmission gate switch model approximation
.subckt tgate 1 2 3 4
*node 1=input
*node 2=N-switch control
*node 3=P-switch control
*node 4=output
*to turn on switch use -5 volts on P-switch and +5 on N-switch
*to turn off wsitch use +5 on P-switch and -5 on N-switch
*bias the switch substrate
vsubn 5 0 dc -5v
vsubp 6 0 dc 5v
*this is the t-gate switch
MN1 1 2 4 5 N 1=4U w=36U as=288P ad=288P
MP1 1 3 4 6 P 1=4U w=72U as=576P ad=576P
.ends tgate
       end of subcircuit models *****
```

```
set-up the simulation model of chemfet
***************
*assuming the input from the floating gate is
*a pulse with 0.1v
*apply the bias voltages
Vdd 1 0 dc 5v
Vss 2 0 dc -5v
Vin+ 3 0 DC 0v AC 0.0010v 0 sin(0 0.1 le6 0 0)
*Vin+ 3 0 DC 0v AC 0.10v 0 pulse(0 0.10 0 1e-6 1e-6 5e-6 10e-6)
*signal must pass through the transmission gate
*turn on gate +5 on N-switch -5 on P-switch
*turn-off is opposite application of voltages
vcN 4 0 dc 5
vcP 5 0 dc -5
x1 3 4 5 5 tgate
*end of the transmission gate
*node 6 is the outpu from the transmission gate
*dummy tgates -- nine of them
x11 3 5 4 6 tgate
x12 3 5 4 6 tgate
x13 3 5 4 6 tgate
x14 3 5 4 6 tgate
x15 3 5 4 6 tgate
x16 3 5 4 6 tgate
x17 3 5 4 6 tgate
x18 3 5 4 6 tqate
x19 3 5 4 6 tgate
*to compensate the cmos offset voltage effect
*offset voltage input provided to the CHEMFET elements
Voff1 7 0 dc 0.0742V
*now pass the signal to first amplifier stage
x2 1 2 6 7 8 fbdamp
* second amplifier stage
Voff2 9 0 dc 0.0742V
x3 1 2 8 9 10 fbdamp
*third amplifier stage
Voff3 11 0 dc 0.0742V
x4 1 2 10 11 12 fbdamp
```

```
*fourth amplifier stage
Voff4 13 0 dc 0.0742V
x5 1 2 12 13 14 fbdamp
Voff5 19 0 dc 3.0842V
*output stage
MP1 15 15 1 1 P L=6u W=36u AD=288p AS=288p
MP2 16 15 1 1 P L=6u W=36u AD=288p AS=288p
MN1 15 14 17 17 N L=6u W=24u AD=192p AS=19296p
MN2 16 18 17 17 N L=6u W=24u AD=192p AS=192p
MN3 17 0 2 2 N L=6u W=24u AD=192p AS=192P
R1 16 18 3k
R2 18 19 10k
R3 16 0 1000k
C1 18 0 10pf
.WIDTH OUT=80
.model P pmos level=4
+ v_i^2b = -.49449 \text{ lvfb} = .0473111 \text{ wvfb} = -.078748
+ phi = .711038 lphi = 0 wphi = 0
+ k1 = .549022 lk1 = -.1098 wk1 = .211133
+ k2 = .0225369 \ lk2 = .0133462 \ wk2 = .0214418
+ eta = -.011378 leta = .0599553 weta = .0109074
+ \text{ muz} = 173.524 \text{ dl} = .502141 \text{ dw} = -.20323
+ u0 = .129663 \ lu0 = .0395758 \ wu0 = -.089559
+ u1 = .0282132 lu1 = .288861 wu1 = -.13103
+ x2mz = 7.49207 1x2mz = -3.3077 wx2mz = 4.43137
+ x2e = -.00081113 \ lx2e = -.0023066 \ wx2e = -.0029608
+ x3e = .000855699  1x3e = -.003979  x3e = -.00061957 
+ x2u0 = .00634967 \ 1x2u0 = -.0021908 \ wx2u0 = .00304801
+ x2u1 = .000525933 lx2u1 = .00057697 wx2u1 = .00896684
+ \text{ mus} = 187.23 \text{ lmus} = 89.9055 \text{ wmus} = -19.539
+ x2ms = 7.00102 lx2ms = -.47434 wx2ms = 8.73424
+ x3ms = -.14304 lx3ms = 11.6728 wx3ms = -7.9883
+ x3u1 = -.016595 lx3u1 = .00351738 wx3u1 = .00384252
+ tox = .028 temp = 27 vdd = 5
+ \text{ cgdo} = 3.09624e-10 \text{ cgso} = 3.09624e-10 \text{ cgbo} = -2.50626e-10
+ xpart = 1
+ n0 = 1 ln0 = 0 wn0 = 0
+ nb = 0 lnb = 0 wnb = 0
+ nd = 0 lnd = 0 wnd = 0
+ rsh = 20.58 cj = .0004015 cjsw = 5.023e-10
+ js = 1.e-08 pb = .8 pbsw = .51
+ mj = .4465 mjsw = .2705 wdf = 0
+ dell = 0
.model N nmos level=4
+ vfb = -.78837 lvfb = -.021873 wvfb = -.12029
+ phi = .801437 lphi = 0 wphi = 0
+ k1 = 1.05382 \ lk1 = .0864105 \ wk1 = .588742
+ k2 = -.0087349 \ 1k2 = .0845206 \ wk2 = .0774966
```

```
+ \text{ muz} = 431.198 \text{ dl} = .7921 \text{ dw} = -.11735
 + u0 = .051871 lu0 = .0428904 wu0 = -.035902
 + u1 = .0252047 lu1 = .608867 wu1 = -.34032
 + x2mz = 11.1852 lx2mz = -22.808 wx2mz = 38.2982
 + x2e = -.00020831 \ lx2e = -.0062271 \ wx2e = -.00071188
 + x3e = .000225369 1x3e = -.000686 wx3e = -.0042937
 + x2u0 = .00301681 lx2u0 = -.014095 wx2u0 = .0297249
 + x2u1 = -.0021476 \ lx2u1 = .00786076 \ wx2u1 = .004818
 + \text{ mus} = 412.323 \text{ lmus} = 259.338 \text{ wmus} = 37.6417
 + x2ms = 4.86473 lx2ms = -19.202 wx2ms = 69.3915
 + x3ms = -2.6586 lx3ms = 47.7003 wx3ms = -13.265
 + x3u1 = -.002006 lx3u1 = .0668089 wx3u1 = -.019504
 + tox = .028 temp = 27 vdd = 5
 + \text{ cgdo} = 4.88415e-10 \text{ cgso} = 4.88415e-10 \text{ cgbo} = -1.44718e-10
 + xpart = 1
 + n0 = 1 ln0 = 0 wn0 = 0
 + nb = 0 lnb = 0 wnb = 0
 + nd = 0 lnd = 0 wnd = 0
 + rsh = 20.58 cj = .0004015 cjsw = 5.023e-10
 + js = 1.e-08 pb = .8 pbsw = .51
 + mj = .4465 mjsw = .2705 wdf = 0
 + dell = 0
 .OPTIONS DEFL=3U DEFW=6U DEFAS=45P DEFAD=45P
 +ITL1=500 ABSTOL=100P VNTOL=100U CHGTOL=1E-14
 +NOPAGE LIMPTS=500 RELTOL=.001 CPTIME=5000 ITL5=0
  . END
  ********************
                            SIMULATION
 *************
 Circuit: DIFFERENTIAL AMPLIFIER WITH FEEDBACK for CHEMFET array
 SPICE3 1 -> ac dec 1 1 1e9
 SPICE3 2 -> asciiplot db(vm(16)/vm(3))
   DIFFERENTIAL AMPLIFIER WITH FEEDBACK for CHEMFET array
          AC analysis curves. Wed Mar 29 23:41:08 EST 1989
 Legend: + = db(vm(16)/vm(3))
                   0.00e+00 1.00e+01 2.00e+01 3.00e+01 4.00e+01
1.000e+05 3.217e+01 .
1.258e+07 3.136e+01 .
2.505e+07 2.751e+01 .
3.753e+07 2.365e+01 .
5.000e+07 1.979e+01 .
6.248e+07 1.593e+01 .
7.495e+07 1.208e+01 .
8.743e+07 8.218e+00 .
9.990e+07 4.361e+00 .
0.00e+00 1.00e+01 2.00e+01 3.00e+01 4.00e+01
FREQ
```

SPICE3 3 -> tran 1e-7 1e-6

Warning: option it15 is currently unsupported.

Warning: option limpts is obsolete.
SPICE3 4 -> asciiplot v(3) v(12) v(16)

## 

TIME v(3) -4.00e-02 -2.00e-02 0.00e+00 2.00e-02 4.00e-02X= 1.000e-09 6.283e-06 . 1.851e-08 1.159e-04 . X =3.602e-08 2.239e-04 . + X 5.353e-08 3.294e-04 . 7.104e-08 4.310e-04 . 8.854e-08 5.275e-04 . 1.061e-07 6.180e-04 . 1.236e-07 7.002e-04 . 1.411e-07 7.737e-04 . 1.586e-07 8.380e-04 . 1.761e-07 8.923e-04 . 1.936e-07 9.361e-04 . 2.111e-07 9.688e-04 . 2.286e-07 9.900e-04 . 2.461e-07 9.995e-04 . 2.636e-07 9.956e-04. 2.811e-07 9.796e-04 . 2.986e-07 9.519e-04 . 3.162e-07 9.130e-0. 3.337e-07 8.633e-04 . 3.512e-07 8.034e-04 . 3.687e-07 7.335e-04 . 3.862e-07 6.555e-04 . 4.037e-07 5.684e-04 . 4.212e-07 4.744e-04 . 4.387e-07 3.749e-04 . 4.562e-07 2.710e-04. 4.737e-07 1.640∈-04 . 4.912e-07 5.492e-05. 5.088e-07 -5.489e-05 . 5.263e-07 -1.642e-04 . 5.438e-07 -2.714e-04 . 5.613e-07 -3.751e-04 . 5.788e-07 -4.743e-04 . 5.963e-07 -5.677e-04 . 6.138e-07 -6.544e-04 . =. 6.313e-07 -7.334e-04 . +. 6.488e-07 -8.038e-04 .

```
6.663e-07 -8.647e-04 . = . *
6.838e-07 -9.143e-04 . = . *
7.014e-07 -9.524e-04 . = . *
7.189e-07 -9.792e-04 . = . *
7.364e-07 -9.944e-04 . = . *
7.539e-07 -9.978e-04 . = . *
7.714e-07 -9.894e-04 . = . *
                                                      +.
                                                      +.
                                                     +.
                                                      +.
                                                      +.
                                                      +.
7.889e-07 -9.692e-04 . = 8.064e-07 -9.376e-04 . = 8.239e-07 -8.935e-04 . = 8.414e-07 -8.384e-04 . =
                                                     +.
                                                     +.
                                                     +.
                                                     +.
 8.589e-07 -7.734e-04 . = .
                                                 * +.
                                       =.
                                                    +.
 8.764e-07 -6.993e-04 .
                                                      +.
 8.939e-07 -6.169e-04 .
 9.115e-07 -5.272e-04 .
 9.290e-07 -4.312e-04 .
9.465e-07 -3.299e-04 .
 9.640e-07 -2.242e-04 .
                                                  = *+.
 9.815e-07 -1.159e-04 .
                                                   = X.
 9.990e-07 -6.275e-06 .
                                                     Χ*
TIME v(3) -4.00e-02 -2.00e-02 0.00e+00 2.00e-02 4.00e-02
SPICE3 5 -> quit
```

Table B.2. SPICE Simulation of the Amplifier with a 30pF Load.

```
R1 16 18 3k
R2 18 19 10k
R3 16 0 1000k
C1 16 0 30pf
asciiplot db(vm(16)/vm(3))
    DIFFERENTIAL AMPLIFIER WITH FEEDBACK for CHEMFET array
       AC analysis curves. Sun Sep 10 11:59:20 EDT 1989
Legend: + = db(vm(16)/vm(3))
FREQ db(vm(16 1.00e+01 2.00e+01 3.00e+01 4.00e+01
_____
1.000e+04 3.217e+01 .
1.436e+06 3.044e+01.
2.861e+06 2.824e+01 .
4.287e+06 2.604e+01 .
5.713e+06 2.385e+01 .
7.139e+0€ 2.165e+01 .
8.564e+06 1.945e+01 .
9.990e+06 1.725e+01 .
FREQ db(vm(16 1.00e+01 2.00e+01
                                   3.00e+01
                                             4.00e+01
SPICE3 11 ->
```

Table B.3. SPICE Simulation of the Amplifier with a 200pF Load.

```
***************
        set-up the simulation model of chemfet
   *************
*apply the bias voltages
Vdd 1 0 dc 5v
Vss 2 0 dc -5v
R1 16 18 3k
R2 18 19 10k
R3 16 0 1000k
C1 16 0 200pf
asciiplot db(vm(16)/vm(3))
     DIFFERENTIAL AMPLIFIER WITH FEEDBACK for CHEMFET array
        AC analysis curves. Sun Sep 10 12:16:46 EDT 1989
Legend: + = db(vm(16)/vm(3))
FREQ
         db(vm(16 2.50e+012.70e+012.90e+013.10e+013.30e+013.50e+01
8.043e+02 3.486e+01.
3.316e+04 3.480e+01.
6.552e+04 3.463e+01 .
9.787e+04 3.437e+01 .
1.302e+05 3.402e+01.
 1.626e+05
           3.362e+01 .
 1.949e+05
           3.317e+01 .
2.273e+05 3.269e+01 .
2.597e+05 3.220e+01 .
2.920e+05 3.170e+01 .
3.244e+05
          3.121e+01 .
3.567e+05 3.072e+01 .
4.214e+05 2.978e+01.
4.538e+05 2.933e+01.
5.185e+05
           2.846e+01 .
5.994e+05 2.746e+01 .
6.641e+05 2.671e+01 .
7.774e+05 2.551e+01 . +
         db(vm(16 2.50e+012.70e+012.90e+013.10e+013.30e+013.50e+01
```

```
**************
       set-up the simulation model of chemfet
*************
*apply the bias voltages
Vdd 1 0 dc 4v
Vss 2 0 dc -4v
R1 16 18 3k
R2 18 19 10k
R3 16 0 1000k
C1 16 0 200pf
asciiplot db(vm(16)/vm(3))
    DIFFERENTIAL AMPLIFIER WITH FEEDBACK for CHEMFET array
       AC analysis curves. Sun Sep 10 12:23:07 EDT 1989
Legend: + = db(vm(16)/vm(3))
FREQ db(vm(16 1.00e+01 2.00e+01
______
8.043e+02 2.915e+01.
1.698e+04 2.913e+01.
3.316e+04 2.906e+01.
8.170e+04 2.864e+01 .
1.141e+05 2.820e+01.
1.464e+05 2.768e+01.
1.788e+05 2.710e+01.
2.111e+05 2.651e+01.
2.435e+05 2.590e+01 .
2.758e+05 2.530e+01 .
3.082e+05 2.470e+01.
3.405e+05 2.414e+01 .
3.729e+05 2.358e+01 .
4.053e+05 2.304e+01.
4.376e+05 2.254e+01.
4.700e+05 2.204e+01.
5.347e+05 2.112e+01.
 .670e+05 2.069e+01 .
_____
FREQ
                               2.00e+01
                                               3.00e+01
      db(vm(16 1.00e+01
```

Table B.4. MOSIS Paprmetric Test Results

FEATURE SIZE: 2 0um VENDOR: ORBIT RUN: M95C / CECIL TECHNOLOGY: SCPE

INTRODUCTION. This report contains the lot average results obtained by obtained from similiar measurements on these wafers are also attached. wafers of this fabrication lot. The SPICE LEVEL 2 and BSIM parameters MOSIS from measurements of the MOSIS test structures on the selected

COMMENTS: This looks like a typical Orbit Semiconductor 2.0um run.

II. TRANSISTOR PARAMETERS:	W/L	N-CHANNEL	P-CHANNEL	
Vth (Vds=.05V)	3/2	1.160	745	Λ
Vth (Vds=.05V) Idss (Vqds=5V)	18/2 18/2	1.055 2279.0	721 -1242.0	V uA
Vpt (Id=1.0uA)	18/2	16.18	-15.45	^
Vth (Vds=.05V)	50/50	1.025	750	^
Vbkd (Ij=1.0uA)	50/50	15.8	-16.5	>
Кр		24.5	10.45	uA/V^2
(Uo*Cox, 2)				
Gamma	50/50	1.109	.441	V^0.5
(2.5v,5.0v)				
Delta Lend		.513	.171	mn
Delta Wid		.046	.032	mn
(Effective awn	n-Delta)			

( .MMENTS: These parameters seem normal.

STINO	<b>N</b> N
SOURCE/DRAIN P + ACTIVE	
SOURCE/DRAIN N + ACTIVE	17.3 17.3 17.4
GATE	Poly Metall Metal2
III. FIELD OXIDE TRANSISTOR PARAMETERS:	<pre>Vth (Vbs=0, I=luA) Poly Vth (Vbs=0, I=luA) Metall Vth (Vbs=0, I=luA) Metal2</pre>

COMMENTS: These parameters seem normal.

UNITS	opw/sd om nm	Ohms	Angst.
	   		`
POLY 2	20.2	8.19	 
_	.029	.035	 
	.089	; ; !	
P DIFF	69.2	39.35	411.
N DIFF	23.7	17.97	! ! !
POLY	<del>-:</del> : 1	8.93	1 8 1
N POLY	te 18.5	7.52	
IV. PROCESS PARAMETERS:	- U 14 ((	Contact Resist. 7.52 (Metall to Layer)	Gate Oxide Thickness:

COMMENTS: These parameters seem normal.

UNITS	fF/um^2	fF/um^2	${ m fF/um^2}2$	fF/um
POLY 2		.474	.045	! ! !
METAL METAL POLY 1 2 2	.024	.022	.036	!
METAL 1	.036	.044	 	}   
P DIFF	.216	!	 	.247
	.072 .412	!!!!!!!!!!!!!!!!!!!!!!!!!!!!!!!!!!!!!!!	1 1 1	.530
POLY	.072	1		( )
V. CAPACITANCE PARAMETERS:	Area Cap	Area Cap	Area Cap	(Layer to metall) Fringe Cap (Layer to subs)

COMMENTS: These parameters seem normal.

VI. CIRCUIT PARAMETERS:

2.32 V 2.52 V	0.00 V 5.01 V 2.66 V -12.29	28.49 MHz (31 stages @ 5.0V)
Vinv, $K = 1$ Vinv, $K = 1.5$	Vlow, K = 2.0 Vhigh, K = 2.0 Vinv, K = 2.0 Gain, K = 2.0	~ ~

COMMENTS: The ring oscillator frequency is typical.

# M95C SPICE LEVEL 2 PARAMETERS

CJ=4.040000E-04 MJ=0.457000 CJSW=5.020000E-10 MJSW=0.369000 PB=0.800000 RSH=23.600000 CGDO=3.073878E-10 CGSO=3.073878E-10 CGBO=6.564240E-10 + UELTA=1.38386 VMAX=71683.1 XJ=0.250000U LAMBDA=1.953712E-02 + NSUB=5.400000E+15 VTO=-0.73 KP=2.007000E-05 GAMMA=0.5039 .MODEL CMOSN NMOS LEVEL=2 LD=0.243906U TOX=411.000000E-10 .MODEL CMOSP PMOS LEVEL=2 LD=0.250000U TOX=411.000000E-10 + NSUB=2.230000E+16 VTO=1.068 KP=5.018000E-05 GAMMA=1.024 NFS=7.327201E+11 NEFF=1 NSS=1.000000E+12 TPG=1.000000 PHI=0.6 U0=597.303 UEXP=0.142861 UCRIT=89159.5 Weff = Wdrawn - Delta\_W The suggested Delta\_W is 0.00 um

DELTA=1.01034 VMAX=41620.5 XJ=0.250000U LAMBDA=5.724220E-02 PHI=0.6 UO=238.902 UEXP=0.215244 UCRIT=21917.9

RSH=70.100000 CGDO=3.150679E-10 CGSO=3.150679E-10 CGBO=6.564240E-10 NFS=1.191843E+12 NEFF=1.001 NSS=1.000000E+12 TPG=-1.000000

CJ=2.080000E-04 MJ=0.466000 CJSW=2.230000E-10 MJSW=0.127000 PB=0.700000

0.00 um

\* Weff = Wdrawn - Delta\_W
\* The suggested Delta\_W is

# M95C SPICE BSIM PARAMETERS

```
*Geometries (W-drawn/L-drawn, units are um/um) of transistors measured were:
* 3.0/2.0, 6.0/2.0, 18.0/2.0, 18.0/5.0, 18.0/5.0
                                                                                                                                                                                                                                                                                                                                                                                                                                                            7.70430093620283e-01, 0.00000000000000e+00, 0.000000000000000e+00
                                                                                                                                                                                                                                                                                                                                                                                                                                                                                          1.58624689948246e+00
                                                                                                                                                                                                                                                                                                                                                                                                                            -6.06924133903353e-01,-2.00753657388490e-02,-7.39219509734510e-01
                                                                                                                                                                                                                                                                                                                                                                                                                                                                                                                        4.98731192385094e-01
                                                                                                                                                                                                                                                                                                                                                                                                                                                                                                                                                          2.32748677517989e-03, 2.27105335887662e-02
                                                                                                                                                                                                                                                                                                                                                                                                                                                                                                                                                                                                                           1.78139126897101e-02, 1.50483950931917e-01,-3.05797177995356e-01
                                                                                                                                                                                                                                                                                                                                                                                                                                                                                                                                                                                                                                                         4.98405575238045e-01
                                                                                                                                                                                                                                                                                                                                                                                                                                                                                                                                                                                                                                                                                       1.11580876629667e+02
                                                                                                                                                                                                                                                                                                                                                                                                                                                                                                                                                                                                                                                                                                                     2.07361417936266e-02
                                                                                                                                                                                                                                                                                                                                                                                                                                                                                                                                                                                                                                                                                                                                                   6.15703103032119e-03
                                                                                                                                                                                                                                                                                                                                                                                                                                                                                                                                                                                                                                                                                                                                                                                       1.69899233879958e-02
                                                                                                                                                                                                                                                                                                                                                                                                                                                                                                                                                                                                                                                                                                                                                                                                                     7.23039962553305e-02
                                                                                                                                                                                                                                                                                                                                                                                                                                                                                                                                                                                                                                                                                                                                                                                                                                                      2.95969591789634e+02
                                                                                                                                                                                                                                                                                                                                                                                                                                                                                                                                                                                                                                                                                                                                                                                                                                                                                      1.32376711544400e+02
                                                                                                                                                                                                                                                                                                                                                                                                                                                                                                                                                                                                                                                                                                                                                                                                                                                                                                                        1.58650083352690e+01
                                                                                                                                                                                                                                                                                                                                                                                                                                                                                                                                                                                                                                                                                                                                                                                                                                                                                                                                                    5.91681643407255e-02
                                                                                                                                                                                                                                                               *Bias range to perform the extraction (Vdd)=5 volts
                                                                                                                                                                                                                                                                                                                                                                                                                                                                                                                                                                                      4.99011937635921e+02,7.46194E-001,-5.52594E-002
                                                                                                                                                                                                                                                                                                                                                                                                                                                                                            9.72185523700295e-02,
                                                                                                                                                                                                                                                                                                                                                                                                                                                                                                                        5.95061988556805e-02,
                                                                                                                                                                                                                                                                                                                                                                                                                                                                                                                                                                                                                                                       3.19396757054450e-01,
                                                                                                                                                                                                                                                                                                                                                                                                                                                                                                                                                                                                                                                                                                                                                                                     1.49207414982358e-03,-4.51425120235782e-03,
                                                                                                                                                                                                                                                                                                                                                                                                                                                                                                                                                                                                                                                                                                                                                                                                                                                                                                                    -6.97307784602596e+00, 7.93937158236720e+01,
                                                                                                                                                                                                                                                                                                                                                                                                                                                                                                                                                                                                                                                                                                                                                                                                                       2.96174757624600e-02,-3.22888269627443e-02,
                                                                                                                                                                                                                                                                                                                                                                                                                                                                                                                                                                                                                                                                                                                                                                                                                                                      4.12414194705069e+02,
                                                                                                                                                                                                                                                                                                                                                                                                                                                                                                                                                                                                                                                                                                                                                                                                                                                                                      4.32124571732670e+00,-2.17988692952133e+01,
                                                                                                                                                                                                                                                                                                                                                                                                                                                                                                                                                                                                                                                                                                                                                                                                                                                                                                                                                    8.17364702083216e-02,
                                                                                                                                                                                                                                                                                                                                                                                                                                                                                                                                                                                                                                                                                         1.37447218152595e+01,-3.45601820689190e+01,
                                                                                                                                                                                                                                                                                                                                                                                                                                                                                                                                                                                                                                                                                                                       -8.58537203292464e-04,-1.19779325441167e-02,
                                                                                                                                                                                                                                                                                                                                                                                                                                                                                                                                                                                                                                                                                                                                                       -2.00969508184277e-03,-2.69070047142389e-03,
                                                                                                                                                              *Gate-oxide thickness= 411.0 angstroms
NM1 PM1 DU1 DU2 ML1 ML2
                                                                                                                                                                                                                                                                                                                                                                                                                                                                                                                      -7.94143604478796e-02,
                                                                                                                                                                                                                                                                                                                                                                                                                                                                                                                                                                                                                                                     1.06741206757391e-01,
                                                                                                                                                                                                                                                                                                                                                                                                                                                                                                                                                                                                                                                                                                                                                                                                                                                    4.67707121717506e+02,
                                                                                                                                                                                                                                                                                                                                                                                                                                                                                          9.15146630862213e-01,
                                                                                                                                                                                                                                                                                                                                                                                                                                                                                                                                                        1.49966373663941e-03,
                                                                                                                                                                                                                                                                                                                                                                                                                                                                                                                                                                                                                                                                                                                                                                                                                                                                                                                                                      -4.60563132878969e-03,
                                                                                                                                                                                                                                                                                                                                                             *NMOS PARAMETERS
                                                                                                                                                                                                                                                                                             *DATE=05-06-89
                                                                  *PROCESS=orbit
                                                                                                  *RUN=m95c
                                                                                                                                    *WAFER=14
```

4.11000E-002, 2.70000000000000e+01, 5.0000000000000000e+00

4.70203E-010,4.70203E-010,6.43058E-010 1.00000E+000,0.00000E+000,0.00000E+000 1.00000E+000,0.00000E+000,0.00000E+000 0.00000E+000,0.00000E+000,0.00000E+000

Gate Oxide Thickness is 410 Angstroms

\*

\*PMOS PARAMETERS

0.0000000000000000e+00, 0.000000000000000e+00 4.76854637197827e-02 5.42635458170274e+00 4.50358458176591e+00 3.90545431363996e-01 5.79689384847231e-02,-6.41128135553033e-03 4.27170395090183e-02 1.08203281075985e-03,-5.92602059644244e-03,-8.91183415220471e-03 2.49427345174033e-04,-4.88369010711971e-03,-4.61885180465470e-03 6.31429635495288e-03 4.00632354728362e-02 2.77831917492407e+01 2.21849471023104e-02 -1.72569434674820e-01,-1.41443883690600e-01,-2.96700437790582e-01 3.45510616946786e+02,-5.06278565405238e+01 4.43911924440849e-02,-1.04315951958508e-01 4.11000E-002, 2.700000000000000e+01, 5.0000000000000000e+00 2.40954546027695e+02,2.77823E-001,-4.19540E-001 1.25829954906707e-01, 9.69747360757807e-02, -9.67538237728308e-03, 1.53852180671895e-02, 5.10019259104388e-01, 3.67228508108751e+01, 1.06341768479827e+01,-4.47387706421899e+00, 1.36584346258480e-02, 1.01108847964610e+01, 8.12999872629999e-03,-6.26088645129279e-03, 6.68559183548914e-01, 3.20688729951411e-01, 1.41576752580660e-01, -4.61691286299804e-02, -2.10608294344991e-02, -3.94434923923152e-03, -2.52681265618659e+00, -1.15286948686628e-04, 2.22743704745999e+02, 6.73486293666905e+00,

1.75066E-010,1.75066E-010,5.54944E-010 1.00000E+000,0.00000E+000,0.00000E+000 1.00000E+000,0.00000E+000,0.00000E+000 0.00000E+000,0.00000E+000,0.00000E+000 0.00000E+000,0.00000E+000,0.00000E+000

<							
*N+ diffusion::	fusion::						
23.6, 0.8.	4.040000e-04,	0e-04,	5.020000e-10,	e-10,		1.000000e-03,	0.8
· *				)			
*P+ diffusion::	fusion::						
*							
70.1,	2.080000e-04,	0e-04,	2.230000e-10,	e-10,		1.000000e-08,	0.7
0.7,	0.466,	0.466, 0.127,	0,	0			
*							
*METAL ]	*METAL LAYER	1					
*							
4.860000e-02,	)e-02,	2.600000e-05,	e-05,	0,	, 0	0	
0,*	0, 0,	0,0					
*METAI,	*METAL LAYER 2	2					
*		1					
2.910000e-02,	0000e-02,	1.300000e-05,	e-05,	٥,	, 0	0	
•	,	•					

# Appendix C

# Film Deposition Procedures

The thin films were deposited onto the interdigitated gate electrode structure of the CHEMFET using two techniques:

i) direct application with a syringe, or ii) vacuum thermal evaporation. The metal-doped phthalocyanines were deposited by vacuum thermal evaporation, while the other organic thin films were deposited as liquid solutions. This section discusses the procedures implemented.

### Vacuum Thermal Evaporation Prodecure

The vacuum thermal evaporation procedure was used to deposit the metal-doped phthalocyanine films onto the interdigitated gate electrode structures of the CHEMFET integrated circuit. This process involved using an appropriately sized mask. The film thickness was monitored with a pre-calibrated piezoelectric quartz crystal microbalance detector, and it was also independently measured with a stylus profilometer. The entire deposition procedure was accomplished with the mask fabrication equipment and vacuum deposition system located in the AFIT Electronic and Materials Cooperative Laboratory (Building 125).

This procedure is described in four parts: i) fabrication of the evaporation masks, ii) vacuum thermal

evaporation of the phthalocyanine films, iii) the film thickness measurement, and iv) the calibration of the piezoelectric quartz crystal microbalance detector.

### Fabrication of the Evaporation Mask.

The masks were fabricated from 6 mil thick berylliumcopper (BeCu) stock. The BeCu stock, provided by the NGK
Metals Corporation (21412 Protecta Drive, Elkhart IN 46516),
had a 25 percent alloy composition and XHM temper (it has a
trade name of Berylco) (1:E-1). The masks were fabricated by
implementing the following procedures:

1. The evaporation mask pattern shown in Figure C.1 was printed on a Kodak High Resolution Plate (HRP) reticle. This procedure involved cutting the enlarged mask pattern on rubylith and then photoreducing it onto the HRP reticle. The dimensions in the mask pattern were identical to the dimensions for one column of the interdigitated gate electrodes.

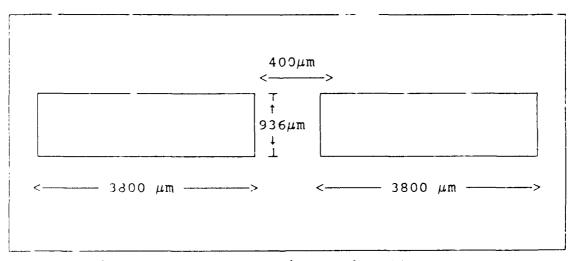


Figure C.1. Evaporation Mask Pattern.

- 2. The BeCu stock was cut into a 3-inch wafer size with a sheet metal shear.
- 3. The BeCu wafer was polished and cleaned before it was coated with photoresist. Both surfaces were polished on a slurry table and then cleaned with a 1:10 mixture of a sodium hydroxide solution and deionized water for 1 minute. The BeCu wafer was then rinsed in deionized water for several minutes and dried with nitrogen gas.
- 4. Two coats of negative photoresist (Waycoat, Stock HR-200) were applied on one side of the BeCu wafer. This photoresist coating protected the unpatterned side of the BeCu wafer from the chemical etching process. The photoresist was spun-on at 2000 rpm for 15 seconds. After each photoresist application, the BeCu wafer was baked at 150°C for 45 minutes.
- 5. The surface of the BeCu wafer to be patterned was then coated with negative photoresist. Prior to the photoresist application, HMDS (Hexamethyldisilazane) was applied to enhance the photoresist's adherence. The HMDS was spun-on at 2000 rpm for 15 seconds. The photoresist was then spun-on at 2000 rpm for 15 seconds (2 coats). The BeCu wafer was pre-baked at 70°C for 30 minutes.
- 6. The mask was then patterned using the mask aligner and the High Resolution Plate reticle. The High Resolution Plate reticle was centered over the photoresist coated BeCu wafer. The emulsion surface of the HRP reticle was contacted

to the BeCu wafer. This sandwiched configuration was then exposed to ultraviolet light for 45 seconds.

- 7. The photoresist pattern printed on the BeCu wafer was developed by spinning the wafer at 2000 rpm and rinsing it for 30 seconds with xylene followed by a 30-second purge with butyl acetate. The BeCu wafer was then spun dry at 4000 rpm for 40 seconds.
- 8. The photoresist pattern was inspected under an optical microscope for edge definition. The photoresist patterned BeCu wafer was then post-baked at 150°C for 45 minutes.
- 9. To insure further protection from the chemical etchant, an additional coat of negative photoresist was applied to the patterned side. The small area over the pattern was covered with a scotch tape. Then, the entire surface was again coated with HMDS and a coat of negative photoresist (both spun at 2000 rpm for 15 seconds). The scotch tape was then removed, and the BeCu wafer was again hard-baked at 150°C for 45 minutes.
- 10. The unwanted BeCu was chemically etched with ferric chloride. A few drops of ferric chloride was applied over the patterned area. The etching process reguired approximately 4 hours to complete.
- 11. The BeCu mask was rinsed with deionized water to remove the ferric chloride after the etching process was completed.

12. As shown in Figure C.2, a dam of RTV (Room Temperature Vulcanization) sealant (Dow Corning, Stock 734 Flowable Sealant, Midland, MI) was applied around the rectangular openings of the BeCu mask with a hypodermic needle and a syringe.

Vacuum Thermal Evaporation of the Phthalocyanine Films.

The following procedures were used to evaporate the metal-doped phthalocyanine films onto the interdigitated gate electrode structures in the CHEMFET integrated circuits:

1. As shown in Figure C.3, the BeCu mask with the RTV dam was placed on the packaged CHEMFET chip. Because, the CHEMFET die was located below the top surface of DIP the cavity, the compliant RTV dam was used to fill the space between the die and the BeCu mask. The mask was affixed to the chip with paper clips. The mask was manually aligned

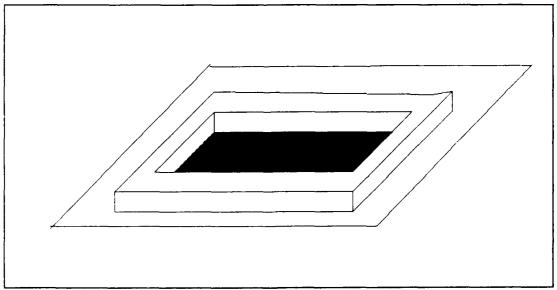


Figure C.2. Structure of the RTV Sealant Dam on the BeCu Mask.

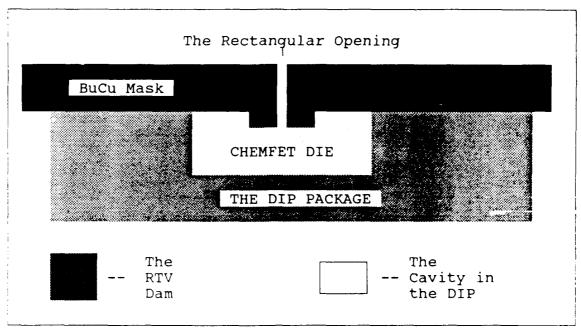


Figure C.3. CHEMFET Mask Arrangement for Thermal Evaporation.

with the CHEMFET's interdigitated gate electrode structures with the aid of a microscope.

- 2. The masked CHEMFET chip and a control silicon wafer with a mask were positioned in the vacuum deposition system's chamber (Denton Vacuum Corporation, model DV-602, Cherry Hill, NJ). Also placed in the chamber at the same height and coplanar as the CHEMFET chip was the piezoelectric quartz crystal microbalance film thickness monitor. The metal-doped phthalocyanine material was placed in an evaporation boat.
- 3. The vacuum chamber was pumped to a pressure of 10° Torr. The following information was programmed into the thickness monitor electronics: the metal-doped phthalocyanine material density, its acoustic impedance, and an

empirical tooling factor. A material density of 1.630 g/cm<sup>3</sup> and an acoustic impedance of 25.04 g/cm<sup>3</sup> sec were used for all the phthalocyanine compounds (1:F-2). The tooling factor for the thickness monitor electronics was established at a calibrated setting that spanned from 100% to 400%.

- 4. An AC current of 150 amperes was supplied to the evaporation boat for a power setting of 2 KVA. These settings were manually adjusted during the evaporation process to obtain an evaporation rate, measured with the piezoelectric thickness monitor, to be on the order of 1-10 4/second. A stable evaporation rate was difficult to achieve, and continuous adjustment of the current supply was required.
- 5. The film thickness was monitored with the calibrated piezoelectric quartz crystal thickness monitor, and the evaporation process was terminated when the desired film thickness was attained.
- 6. After the vacuum chamber was vented, the CHEMFET package and control wafer were removed. The vacuum chamber walls were cleaned with a metal polish and acetone to remove the undesirable phthalocyanine deposits.

### Film Thickness Measurement.

The thickness of a deposited phthalocyanine film was also determined by measuring its thickness on the control silicon wafer with a stylus profilometer (Sloan Technology Corp., Model Dektak 900051, Santa Barbara, CA). The

following procedures were implemented to determine the film's thickness:

- 1. The control silicon wafer was sputter coated with a 700Å thickness of gold (Structure Probe Inc, Model SPI Sputterer, West Chester, PA). This procedure was accomplished because the phthalocyanine films were too soft to be measured directly with the stylus profilometer. The sputtered gold was assumed to have a uniform thickness, and thus, the difference in the surface height between the two materials should remain the same. Figure C.4 illustrates this concept.
- 2. The Dektak profilometer was calibrated with the calibration surface block.
- 3. The thickness of the evaporated phthalocyanine film was measured at several locations (approximately 7) on the

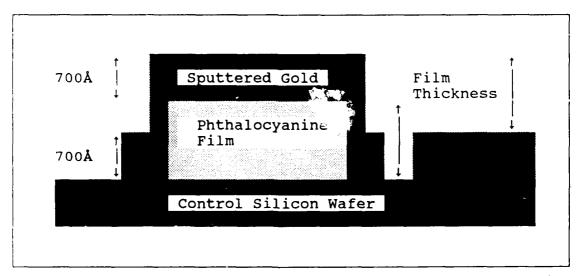


Figure C.4. Thin Gold Film Sputtered onto a Phthalocyanine Film.

control wafer. The average film thickness was then calculated.

Calibration of the Piezoelectric Quartz Crystal Microbalance Film Thickness Monitor.

The calibration of the piezoelectric quartz crystal microbalance film thickness monitor was implemented for each metal-doped phthalocyanine material. The calibration procedure was accomplished by evaporating the phthalocyanine film onto a control silicon wafer with the tooling factor of the thickness monitor electronics set at an initial setting of 100%. The evaporation process was stopped when the thickness monitor indicated the desired film thickness. The evaporated thin film's thickness on the control wafer was subsequently measured with the stylus profilometer as described earlier. The tooling factor on the thickness monitor measurement matched that of the profilometer measurement.

An additional evaporation process was implemented with a control wafer using the adjusted tooling factor. The thin film's thickness was measured again, and the tooling factor was once again adjusted. This process was reiterated until the thickness monitor's measurement matched that of the profilometer to within 50Å. Once the tooling factor of the thickness monitor electronics was established for a particular phthalocyanine film and thickness, the actual film deposition on the CHEMFET IC was implemented.

### Liquid Solution Deposition

The liquid solution deposition procedure was used to deposit the following thin films onto the interdigitated gate electrode structures of the CHEMFET integrated circuit:

i) L-histidine dihydrochloride, ii) succinylcholine chloride, iii) 2-naphthol( $\beta$ ), and iv) succinylchloride.

This process initially involved dissolving the film materials in a non-acidic solution. For L-histidine dihydrochloride and succinylcholine chloride, a 20% isorropyl alcohol solvent was used. The 2-naphthol( $\beta$ ) was dissolved in acetone. Succinylchloride is a liquid at room temperature.

These liquid solutions were then deposited over the gate electrodes using a pipet dispensing technique (a hypodermic needle and a syringe). Prior to the actual film's deposition, the interdigitated gate electrode area of the CHEMFET was isolated with an RTV sealant dam, as shown in Figure C.5, to confine the liquid deposition.

After the liquid solutions were deposited over the gate electrode, the solvents were removed by evaporation to produce a solid thin film. The thicknesses of these thin films were not measured.

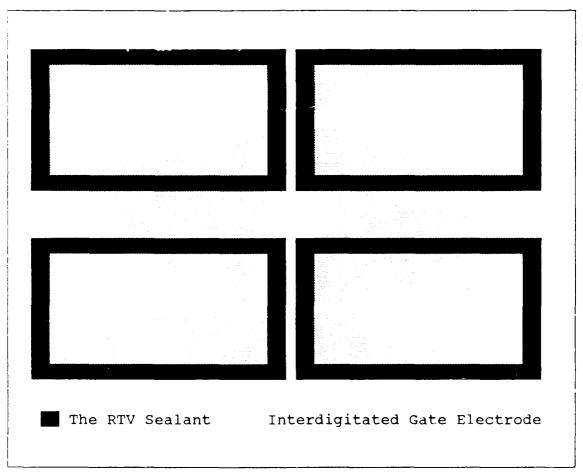


Figure C.5. Interdigitated Gate Electrode with RTV Sealant Dam.

# Appendix D

# Gas Generation and Delivery System

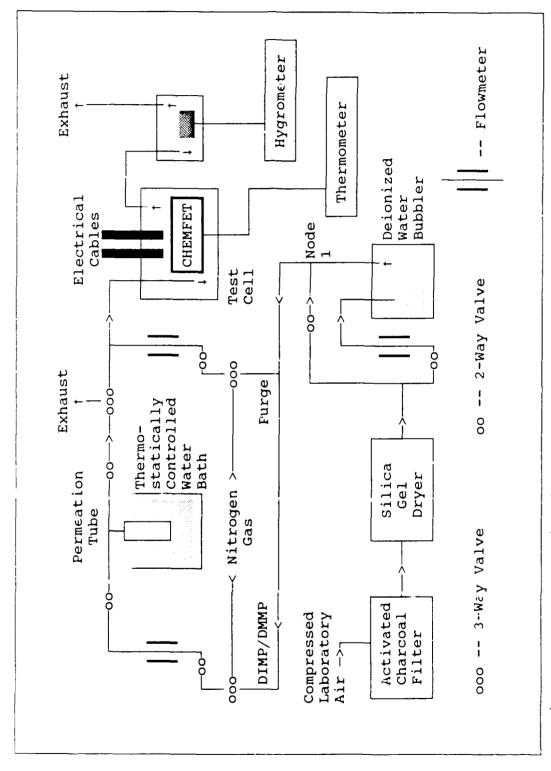
In this thesis, the gas generation and delivery system was used to generate, dilute, control, and transport known concentrations of the two challenge gases (DIMP and DMMP). The gas delivery system also provided humidity control of the carrier gas (filtered room air). As a part of the gas generation and delivery system, a test cell was fabricated. The test cell facilitated the electrical measurements of the CHEMFET circuits when they were exposed to the challenge gases. This section discusses the operation of the gas generation and delivery system and the design of the test cell.

### Gas Generation and Delivery System

The gas generation and delivery system used in this thesis was essentially the system used in the previous AFIT thesis research accomplished by Wiseman (1:4-20). This gas delivery system was slightly modified for this thesis research. A schematic of the gas generation and delivery system is shown in Figure D.1.

### Gas Delivery.

As shown in Figure D.1, compressed laboratory air is filtered with activated charcoal and then a silica gel



Schematic Diagram of the Gas Generation and Delivery System. Figure D.1.

diyer. This process removed organic impurities and dehumidified the air. A portion of the dehumidified air was then passed through a deionized water bubbler and humidified again. The 2-way valves were used to regulate the amount of dry air and humidified air that combined at Node 1. However, because the relative humidity of the air was regulated at 10% in this thesis, the bubbler was not utilized.

The air at Node 1 was either passed to the DIMP/DMMP path or to the purge path, depending on the gas delivery requirements. To either purge the test cell or deliver a zero concentration challenge gas, the filtered air was regulated with the purge flowmeter. To deliver the challenge gas to the test cell, the air was passed to the DIMP/DMMP flowmeter. The exact amount of air passing through each path was controlled by a flowmeter.

Both 3-way valves at the purge path and DIMP/DMMP path also allowed nitrogen gas (instead of the filtered air) to pass into the system. However, in thesis, nitrogen gas was not used.

### Gas Generation.

To generate the challenge gases, commercial gas permeation tubes were used (GC Industries, model 23-7392 for DIMP and model 23-7082 for DMMP, Chatsworth, CA). The permeation tubes were calibrated by the manufacturer to generate a stable gas permeation rate when the temperature is carefully thermostated. The manufacturer's calibration

curves for each permeation tube are shown in Figure D.2, Figur D.3, and Figure D.4.

The following relationship can be used to determine the gas concentration (22):

$$C = \frac{k \times P}{F}$$
 (D.1)

where C is the challenge gas concentration in ppm by volume,

- P is the permeation rate in nanograms/min (ng/min) from the calibration charts (Figures D.2 through D.4),
- k is an empirically determined gas constant provided by the manufacturer, with k=0.136 for the DIMP permeation tube, and k=0.197 for the DMMP permeation tube,

and F is the carrier gas flow rate in ml/min.

The carrier gas for both DIMP and DMMP in this thesis was filtered dry air. The air flow rate for the permeation tube (F) was controlled with the DIMP/DMMP flowmeter (Gilmont Instruments, model F-7660, Great Neck, NY). The manufacturer's calibration curves for the DIMP and DMMP flowmeter and purge flowmeter are given in Figures D.5 and D.6.

To generate the desired challenge gas concentrations, the appropriate DIMP or DMMP permeation tube was placed in the Thermostated Water Bath (Neslab Corp, Model RTE-88D, Newington, NH). The air was then passed through the flowmeter.

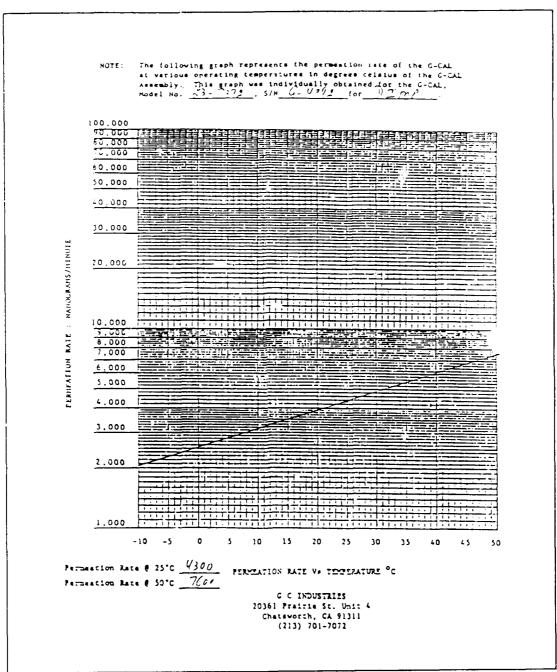


Figure D.2. DIMP Permeation Tube, Model 23-7392, Part Number G-6942 Calibration Chart.

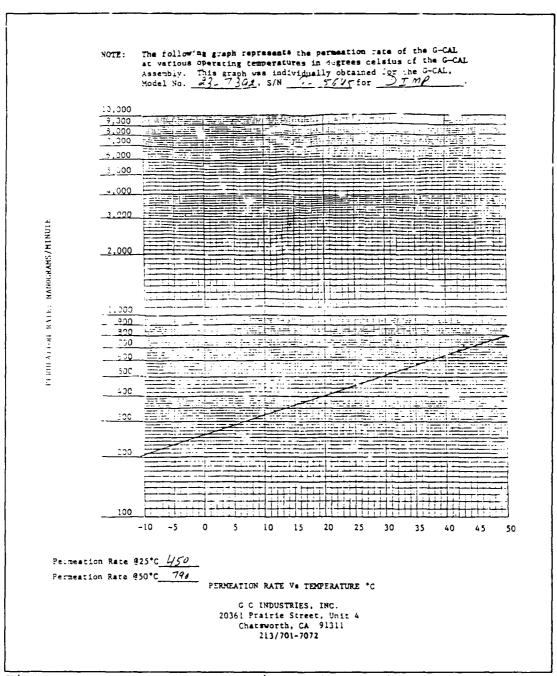


Figure D.3. DIMP Permeation Tube, Model 23-7392, Part Number G-5645, Calibration Chart

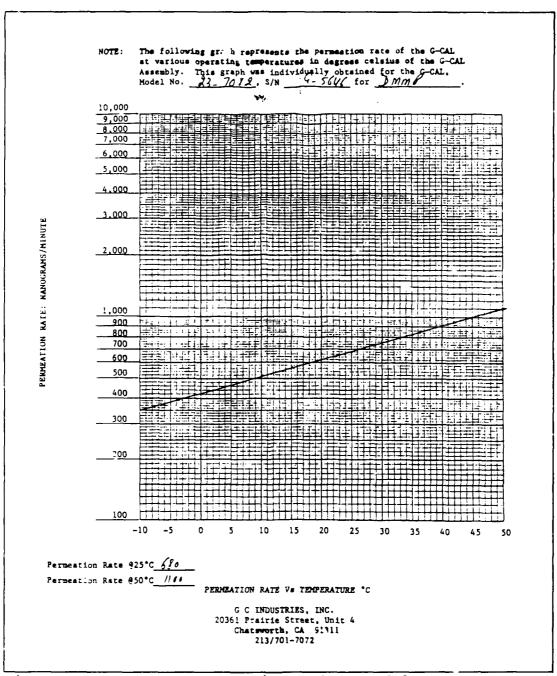


Figure D.4. DMMP Permeation Tube, Model 23-7082, Part Number G-5646, Calibration Chart.

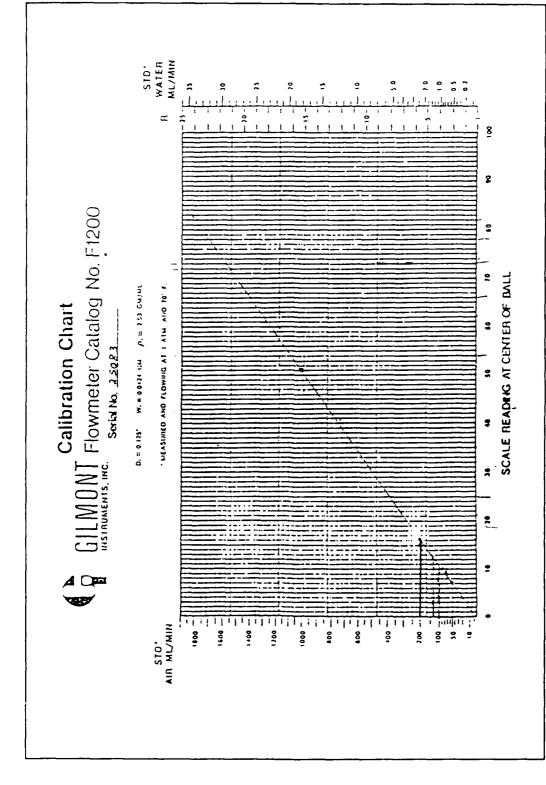
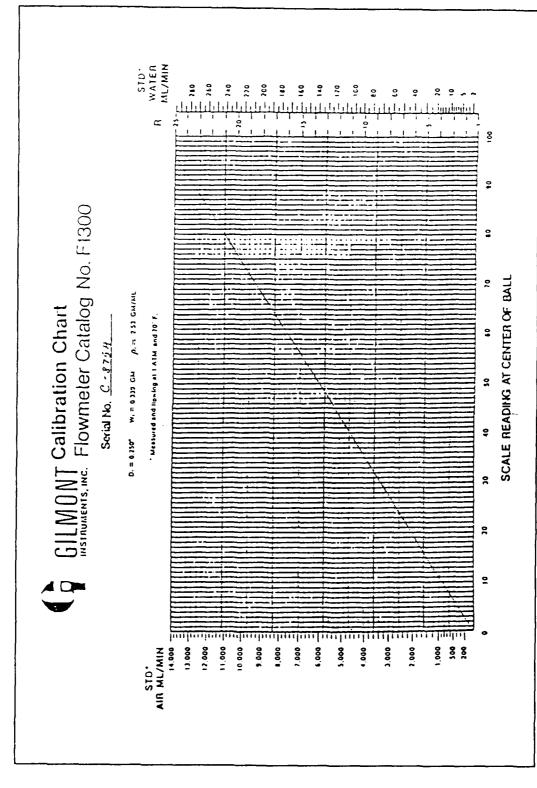


Figure D.5. Gilmont Instruments Flowmeter Model F-1200, Serial Number 25083, Size 2 Calibration Chart for the DIMP and DMMP Flowmeter.



Gilmont Instruments Flowmeter Model F-1300, Serial Number C-8754, Figure D.6. Gilmont Instruments Flowmeter Model Size 3 Calibration Chart for the Purge Flowmeter

The specific challenge gas concentration was initially exhausted into the chemical hood at the 3-way valve. Once assured that an equilibrated gas generation flow was attained, the challenge gas was switched to pass through the test cell.

### Relative Humidity Monitor.

The relative humidity of the environment in the test cell was monitored by sampling the exhaust air. The exhaust from the test cell was passed into a sealed beaker where the humidity sensor was located. The relative humidity of the test cell exhaust air was monitored with an in-line, digital-display hygrometer (Thunder Scientific Corporation, Model HS-1CHDT-2A, Albuquerque, NM).

### Test Cell

A new test cell was designed and fabricated for this thesis. The test cell design requirements remained the same as those considered in Wiseman's thesis (1); that is: i) an optimum chamber volume, ii) ports for adequate external electrical connections, and iii) simple sensor insertion and removal. Figure D.7 shows the overall test cell design and structure.

The description of the test cell is presented in three parts: i) the test cell, ii) the external electrical connections, and iii) the DIP socket for the CHEMFET chip.

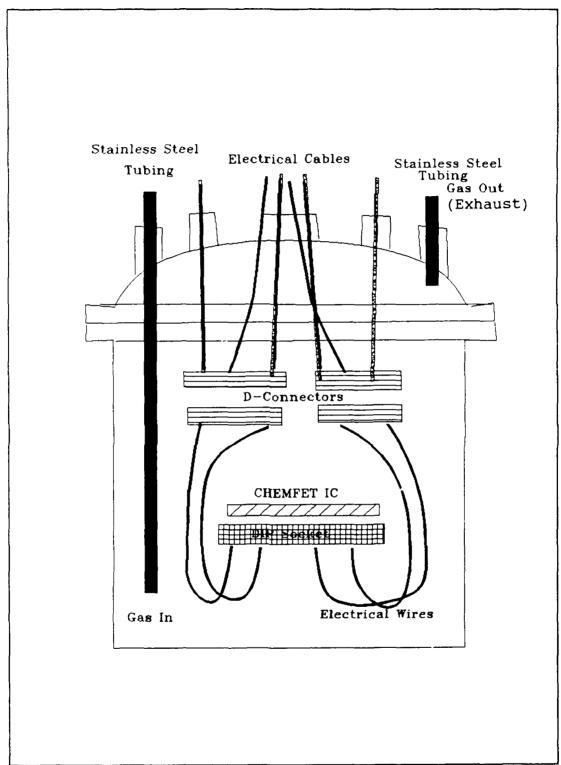


Figure D.7. Schematic Drawing of the Test Cell.

### Test Cell.

As shown in Figure D.7, the test cell was made from a laboratory pyrex container. The pyrex container was approximately 4" in diameter, 5" tall, and its volume was 2000 ml. The chamber volume was sufficiently small to allow rapid equilibration with the challenge gas concentration changes, but large enough to prevent turbulent airflow at large flowrates.

The glass lid for the test cell had a ground-glass joint which provided a good seal. In addition, two large binder clips were used to secure the lid. The top cover of the glass test cell had 14 ports through which the electrical cables and the 1/4" stainless steel tubes were passed.

### Electrical Connections.

For external electrical connections, 12 coax cables, 56, 22-gauge electrical wires, and a thermocouple wire were ported through the glass openings in the lid of the test cell. The 12 coax cables and 52 electrical wires were dedicated for the 64 pins on the CHEMFET's IC package. The 4 remaining electrical wires were used to supply power to the strip heater which was used to thermostat the CHEMFET IC. The coax cables and electrical wires were connected to two 37-pin male D-connectors. Two additional 37-pin female D-connectors were attached to the 64-pin DIP socket as shown in Figure D.7.

### DIP Socket.

As shown in Figure D.8, the 64-pin CHEMFET IC was bonded in the 64-pin DIP socket which was electrically connected to the two 37-pin female D-connectors. The CHEMFET chip was heated to the desired temperature with the Kapton strip heaters (Watlow, Model K005020C5, St. Louis, MO). The strip heaters were placed directly below the CHEMFET IC and held in place with two paper clips. The temperature of the CHEMFET IC was monitored through a self-adhesive thermocouple (Omega Engineering Inc., Model SA1-K, Stamford, CT).

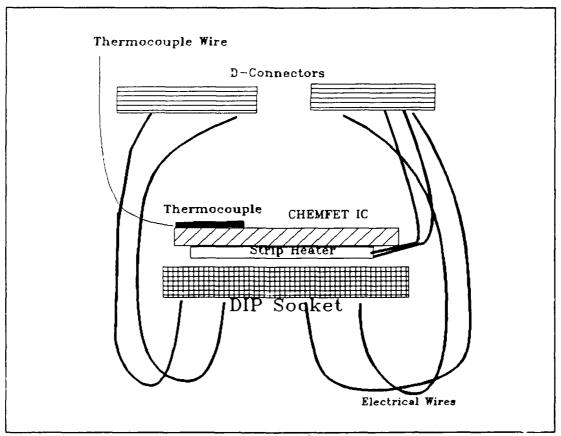


Figure D.8. Schematic Drawing of the DIP Socket.

# Appendix E

# **Computer Programs**

### DC RESISTANCE DATA ACQUISITION: DC.bas

```
100 CLS
200 '
300 '
400 PRINT, " DC (ELECTROMETER) RESISTANCE MEASUREMENT SOFTWARE"
500 PRINT,""
600 '
700 '
1100 DEF SEG=&HC400
                               ' ADDRESS OF GP-IB INTERFACE
                              ' OFFSET OF INITIALIZE ROUTINE
1200 INIT%=0
                               ' OFFSET OF TRANSMIT ROUTINE
1300 TRANSMIT%=3
                               ' OFFSET OF RECIEVE ROUTINE
1400 RECIEVE%=6
                              ' OFFSET OF SEND ROUTINE
1500 SEND%=9
                              ' OFFSET OF SERIAL POLL ROUTINE
1600 SPOLL%=12
                               ' OFFSET OF ENTER ROUTINE
1700 ENTER%=21
1800 '
1900 '
2000 '
2100 ' GP-IB ADDRESSES OF INSTRUMENTS
2300 HP4194%=17: HP4192%=9: PRINTER%=1: MY.ADDR%=21: K617%=27
2400 HP8566%=18: SWITCH%=28
2500 '
2600 SYSCON%=0
                                   'PC488 ACTS AS CONTROLLER
2700 '
2800 CALL INIT% (MY.ADDR%, SYSCON%)
3000 EX$="EX"
3200 ELAPSE.TIME$="00:00:00"
3300 HOURS =0
3400 \text{ MINUTES} = 0
3500 SECONDS = 0
3600 '
3700 INPUT "NAME OF EXPERIMENT: ", EXPERIMENT$
3800 INPUT "NAME OF RESISTANCE DATA FILE: ", IMPFILE$
3900 INPUT "NUMBER OF ELECTRODES TO BE SAMPLED: ", NELECT
4600 OPEN "O", #1, IMPFILE$
4700 PRINT#1, EXPERIMENT$;" ";DATE$;" ";TIME$
4800 PRINT#1, "TIME"; CHR$(9); "ELECTRODE"; CHR$(9); "RESISTANCE"
5000 '
```

```
5005 '
                    SET-UP THE WAVETEK SWITCH
5010 3="SFI" 'SET SINGLE AND MAKE-BEFORE BREAK
5015 CALL SEND% (SWITCH%, S$, STATUS%)
5300 '
5400 '
5500 '
                   SET-UP ELECTROMETER FOR MEASUREMENT
5600 PRINT " "
5650 PRINT "SET-UP THE ELECTROMETER FOR ZERO CORRECT"
5660 INPUT "ENTER RETURN WHEN READY", NULL$
5700 S$="F1"
                               'SET TO MEASURE AMPS
5800 CALL SEND% (K617%, S$, STATUS%)
5900 S$="ROX"
                               'SET TO AUTO RANGE
6000 CALL SEND% (K617%, S$, STATUS%)
6100 S$="Z1X"
                              'PERFORM ZERO CORRECT
6200 CALL SEND% (K617%, S$, STATUS%)
6300 S$="TOX"
6400 CALL SEND% (K617%, S$, STATUS%)
6500 ¹
6600 S$="F5X"
                              'SET TO V/I OHMS MODE
5700 CALL SEND% (K617%, S$, STATUS%)
6800 S$="v0.5X"
                      'SET INTERNAL VOLTAGE SOURCE TO 0.5V
6900 CALL SEND% (K617%, S$, STATUS%)
7000 '
7100 '
7200 '
17300 '
17310 CLS
17320 PRINT "INITIAL ELECTROMETER SET-UP COMPLETE"
17330 PRINT " "
17350 INPUT "CONNECT DUT, HIT RETURN WHEN READY", NULL$
17400 'TURN ON ELAPSE TIMER
17500 CLS
17600 BEGIN.TIMES=TIMES
17700 BEGIN.HRS= VAL(LEFT$(BEGIN.TIME$,2)
17800 BEGIN.MIN= VAL(MID$(BEGIN.TIME$,4,2))
17900 BEGIN.SEC= VAL(RIGHT$(BEGIN.TIME$,2))
18000 ON TIMER (1) GOSUB 47400
18100 TIMER ON
18200 '
18600 '
18650 PRINT "TIME"; CHR$(9); "ELECTRODE"; CHR$(9); "RESISTANCE"
                                 'DATA INPUT LOOP
18800 FOR N=1 TO NELECT 'LOOP THROUGH THE NUMBER OF ELECTRODES
18810 IF N=1 THEN GOTO 18830
18815 IF N=5 THEN GOTO 18835
18820 S$="K"+STR$(N)+"CI" : GOTO 18840
18830 S$="K8OK1CI":GOTO 18840
18835 S$="K4OK5CI":GOTO 18840
18840 CALL SEND%(SWITCH%,S$,STATUS%) 'SELECT ELECTRODE
19100 S$="COX"
                                  'ENABLE READING
19200 CALL SEND% (K617%, S$, STATUS%)
```

```
19250 S$="01X"
                                 'TURN ON VOLTAGE SOURCE
19260 CALL SEND% (K617%, S$, STATUS%)
19300 TEMP$=SPACE$(16)
19400 FOR I=1 TO 20000: NEXT I
                                    'LET ELECTROMETER SETTLE
19500 CALL ENTER% (TEMP$, LENGTH%, K617%, STATUS%)
19600 DC.RESIST= VAL(RIGHT$(TEMP$, 12))
19700 PRINT#1, ELAPSE.TIME$; CHR$(9); N; CHR$(9); DC.RESIST
19800 PRINT ELAPSE.TIME$; CHR$(9); N; CHR$(9); DC.RESIST
                                   'TURN OFF VOLTAGE SOURCE
19900 S$="00X"
20000 CALL SEND% (K617%, S$, STATUS%)
20100 S$="C1X"
                                   'DISABLE READING
20200 CALL SEND% (K617%, S$, STATUS%)
20300 '
21000 NEXT N
                    'LOOP THROUGH THE ELECTRODES
22000 S$="K"+STR$(N)+"OI"
22100 CALL SEND% (SWITCH%, S$, STATUS%)
27400 '
27500 '
27600 '
27700 INPUT "COLLECT MORE DATA, Y OR N:", MOREDATA$
27800 IF MOREDATA$="N" THEN 28100
27900 GOTO 18650
28000 '
28100 CLOSE #1
28800 STOP
28900 '
29000 '
29100 '
29200 '
47400 '
                        TIMER ROUTINE
47500 '
47600 'Y=CSRLIN
47700 'X=POS(0)
47800 TIME.NOW$=TIME$
47900 NOW.HRS= VAL(LEFT$(TIME.NOW$,2))
48000 NOW.MIN= VAL(MID$(TIME.NOW$,4,2))
48100 NOW.SEC= VAL(RIGHT$(TIME.NOW$,2))
48200 SECONDS= NOW.SEC-BEGIN.SEC
48300 IF SECONDS >= 0 THEN 48500
48400 SECONDS=SECONDS+60: NOW.MIN=NOW.MIN-1
48500 MINUTES=NOW.MIN-BEGIN.MIN
48600 IF MINUTES >= 0 THEN 48800
48700 MINUTES=MINUTES+60: NOW.HRS=NOW.HRS-1
48800 IF NOW.HRS<BEGIN.HRS THEN NOW.HRS=NOW.HRS+24
48900 HOURS=NOW.HRS-BEGIN.HRS
49000 IF SECONDS<10 THEN SECONDS$="0" + RIGHT$(STR$(SECONDS),1)
49100 IF SECONDS >= 10 THEN SECONDS$=RIGHT$(STR$(SECONDS),2)
49200 IF MINUTES<10 THEN MINUTES$="0" + RIGHT$(STR$(MINUTES),1)
49300 IF MINUTES >= 10 THEN MINUTES$=RIGHT$(STR$(MINUTES),2)
49400 ELAPSE.TIME$= STR$(HOURS) + ":" + MINUTES$ +":" + SECONDS$
49500 'LOCATE 20,45: PRINT "ELAPSED TIME: "; ELAPSE.TIME$
49600 'LOCATE Y, X
49700 RETURN
```

### IMPEDANCE DATA ACQUISITION: IMP.bas

```
100 CLS
200 '
300 '
400 '
                          IMPEDANCE DATA TRANSFER SOFTWARE
500 '
600 '
700 '
900 DIM MAG(400), PHS(400), REAL(400), IMAG(400)
1000 DIM GFREQ(400)
1100 DEF SEG=&HC400
                            ' ADDRESS OF GP-IB INTERFACE
                            ' OFFSET OF INITIALIZE ROUTINE
1200 INIT%=0
                            ' OFFSET OF TRANSMIT ROUTINE
1300 TRANSMIT%=3
                            ' OFFSET OF RECIEVE ROUTINE
1400 RECIEVE%=6
                            ' OFFSET OF SEND ROUTINE
1500 SEND%=9
                            ' OFFSET OF SERIAL POLL ROUTINE
1600 SPOLL%=12
                          ' OFFSET OF ENTER ROUTINE
1700 ENTER%=21
1800 '
1900 '
2000 '
2100 ' GP-IB ADDRESSES OF INSTRUMENTS
2300 HP4194%=17: HP4192%=9: PRINTER%=1: MY.ADDR%=21: K617%-27
2400 SWITCH%=28
2500 '
2600 SYSCON%=0 'PC488 ACTS AS CONTROLLER
2700 '
2800 CALL INIT% (MY.ADDR%, SYSCON%)
2900 '
3000 EX$="EX"
3200 ELAPSE.TIME$="00:00:00"
3300 HOURS =0
3400 \text{ MINUTES} = 0
3500 \text{ SECONDS} = 0
3600
8600 '
              SET-UP 4194 FOR IMPEDANCE MEASUREMENTS
8700 '
8800 '
8900 S$="RST" 'INITIALIZE 4194 TO POWER ON SETTING
9000 CALL SEND% (HP4194%, S$, STATUS%)
9100 S$="RQS2"
                           'UNMASK AND ENABLE BIT1 FOR SRQ
9200 CALL SEND% (HP4194%, S$, STATUS%)
                               'SET TO R AND X MODE
9300 S$="IMP2"
9400 CALL SEND% (HP4194%, S$, STATUS%)
                               'MONITOR THE VOLTAGE
9500 S$="IVM1"
9600 CALL SEND% (HP4194%, S$, STATUS%)
9700 S$="SWM2"
                               'SET SWEEP MODE TO SINGLE
```

```
9800 CALL SEND% (HP4194%, S$, STATUS%)
9900 S$="SWT2"
                                'SET TO LOG SWEEP
10000 CALL SEND% (HP4194%, S$, STATUS%)
10100 S$="OSC=1V"
                                'SET OSC LEVEL TO 1V
10200 CALL SEND% (HP4194%, S$, STATUS%)
10300 S$="MCF0"
                                'TURN MARKERS OFF
10400 CALL SEND% (HP4194%, S$, STATUS%)
                           'SET INTEGRATION TIME TO 1mSEC
10900 S$="ITM1"
11000 CALL SEND% (HP4194%, S$, STATUS%)
11100 S$="STOP=1000000HZ"
                                        'SWEEP TO 1MHz
11200 CALL SEND% (HP4194%, S$, STATUS%)
11400 INPUT "PERFORM OFFSET REF STORE, RETURN WHEN READY", NULL$
11500 '
12700 '
12800 S$="X?"
                               'READ IN FREQUENCY POINTS
12900 CALL SEND% (HP4194%, S$, STATUS%)
13000 S$="MLA FALK 17"
                                         '4194 TO OUTPUT
13100 CALL TRANSMIT%(S$,STATUS%)
13200 TEMP$=SPACE$(15)
13300 FOR I=0 TO 400
13400 CALL RECIEVE% (TEMP$, LENGTH%, STATUS%)
13500 GFREQ(I)=VAL(LEFT$(TEMP$,12))
13600 NEXT I
13700 '
13820 '
17400 'TURN ON ELAPSE TIMER
1/500 CLS
17600 BEGIN.TIME$=TIME$
17700 BEGIN.HRS= VAL(LEFT$(BEGIN.TIME$,2))
17800 BEGIN.MIN= VAL(MID$(BEGIN.TIME$,4,2))
17900 BEGIN.SEC= VAL(RIGHT$(BEGIN.TIME$,2))
18000 ON TIMER (1) GOSUB 47400
18100 TIMER ON
18200 '
18300 INPUT "NAME OF EXPERIMENT: ", EXPERIMENT$
18400 INPUT "NAME OF IMPEDANCE DATA FILE:", GATEGP.FILE$
18510 INPUT "NUMBER OF ELECTRODES TO BE SAMPLED: ", NELECT
18520 OPEN "O", #2, GATEGP.FILE$
18521 S$="BIAS=0.5V"
                                'SET DC BIAS TO 0.5V
18522 CALL SEND% (SWITCH%, S$, STATUS%)
18530 '
18540 CLS
18550 INPUT "CONNECT 4194 ACROSS GATE, RETURN WHEN READY", NULL$
18600 WRITE #2, EXPERIMENT$, DATE$, TIME$
18610 ' SET UP THE WAVETEK SWITCH
18611 S$="SF1"
                   'SET SINGLE AND MAKE-BEFORE BREAK
18612 CALL SEND% (SWITCH%, S$, STATUS%)
                                 'DATA INPUT LOOP
18700 '
18800 FOR N=1 TO NELECT 'LOOP THROUGH THE NUMBER OF ELECTRODES
18810 IF N=1 THEN GOTO 18830
18815 IF N=5 THEN GOTO 18835
```

```
18820 S$="K"+STR$(N)+"CI" : GOTO 18840
18830 S$="K80K1CI":GOTO 18840
19835 S$="K4OK5CI":GOTO 18840
18840 CALL SEND% (SWITCH%, S$, STATUS%) 'SELECT ELECTRODE
19000 '
                    ' GO GET DATA
21700 GOSUB 32100
21800 WRITE #2, "ELECTRODE", N, TIME$, ELAPSE.TIME$
21850 WRITE #2, "FREQ", "MAG", "PHASE", "REAL", "IMAG"
21890 FOR I= 0 TO 400
21900 WRITE #2, GFREQ(I), MAG(I), PHS(I), REAL(I), IMAG(I)
22000 NEXT I
22100 NEXT N ' LOOP THROUGH THE ELECTRODE
27400 S$="K"+STR$(N)+"OI"
27440 CALL SEND% (SWITCH%, S$, STATUS%)
27480 CLOSE #2
27500 '
27600 '
27700 INPUT "COLLECT MORE DATA, Y OR N:", MOREDATA$
27800 IF MOREDATA$="N" THEN 28200
27900 GOTO 18300
28000 '
28200 '
28800 STOP
32100 '
32200 '
32300 '
                                HP4194 DATA INPUT ROUTINE
32400 '
32500 '
32600 CALL SPOLL% (HP4194%, POLL%, STATUS%)
32610 S$="IMP1"
                               'SET TO Z AND PHASE MODE
32620 CALL SEND% (HP4194%, S$, STATUS%)
                                      'PERFORM SINGLE SWEEP
32700 S$="SWTRG"
32800 CALL SEND% (HP4194%, S$, STATUS%)
32900 CALL SPOLL%(HP4194%, POLL%, STATUS%) 'IS SWEEP COMPLETE?
33000 IF ((POLL% AND 64) <> 64) THEN 42900
33100 '
                                       'AUTOSCALE DISPLAY A
33200 S$="AUTOA"
33300 CALL SEND% (HP4194%, S$, STATUS%)
33400 S$="AUTOB"
                                       'AUTOSCALE DISPLAY B
33500 CALL SEND% (HP4194%, S$, STATUS%)
33600 S$="A?"
                                       'READ IN MAG VALUE
33700 CALL SEND%(HP4194%,S$,STATUS%) 'FROM THE ARRAY REG A
35300 '
35400 S$= "MLA TALK 17"
35500 CALL TRANSMIT% (S$, STATUS%)
35600 TEMP$= SPACE$(13)
35700 \text{ FOR I} = 0 \text{ TO } 400
35800 CALL RECIEVE% (TEMP$, LENGTH%, STATUS%)
35900 MAG(I)=VAL(LEFT$(TEMP$,12)) 'EXTRACT MAG VALUE
36000 NEXT I
36100 '
36200 S$="B?"
                       'READ IN PHASE FROM ARRAY REGISTER B
```

```
36300 CALL SEND% (HP4194%, S$, STATUS%)
36400 S$= "MLA TALK 17"
36500 CALL TRANSMIT% (S$, STATUS%)
36600 FOR I= 0 TO 400
36700 CALL RECIEVE% (TEMP$, LENGTH%, STATUS%)
36800 PHS(I) = VAL(LEFT$(TEMP$, 12)) 'EXTRACT PHASE VALUE
36900 NEXT I
37000 '
37100 '
37200 CALL SPOLL% (HP4194%, POLL%, STATUS%)
42100 'MAKE SURE SRQ NOT SET
42200 '
42400 '
42500 S$="IMP2" 'SET THE IMPEDANCE MEASUREMENT IN R AND X
42600 CALL SEND% (HP4194%, S$, STATUS%)
42700 S$="SWTRG"
                                   'PERFORM SINGLE SWEEP
42800 CALL SEND% (HP4194%, S$, STATUS%)
42900 CALL SPOLL% (HP4194%, POLL%, STATUS%) 'IS SWEEP COMPLETE?
43000 IF ((POLL% AND 64) <> 64) THEN 42900
43100 '
43200 S$="AUTOA"
                                     'AUTOSCALE DISPLAY A
43300 CALL SEND% (HP4194%, S$, STATUS%)
43400 S$="AUTOB"
                                     'AUTOSCALE DISPLAY B
43500 CALL SEND% (HP4194%, S$, STATUS%)
43600 S$="A?"
                                     'READ IN REAL VALUE
43700 CALL SEND% (HP4194%, S$, STATUS%) 'FROM THE ARRAY REG A
45300 '
45400 S$= "MLA TALK 17"
45500 CALL TRANSMIT% (S$, STATUS%)
45600 TEMP$= SPACE$(13)
45700 \text{ FOR I} = 0 \text{ TO } 400
45800 CALL RECIEVE% (TEMP$, LENGTH%, STATUS%)
45900 REAL(I)=VAL(LEFT$(TEMP$,12)) 'EXTRACT MAG VALUE
46000 NEXT I
46100 '
46200 S$="B?" 'READ IN IMAGINARY FROM ARRAY REGISTER B
46300 CALL SEND% (HP4194%, S$, STATUS%)
46400 S$= "MLA TALK 17"
46500 CALL TRANSMIT% (S$, STATUS%)
46600 FOR I= 0 TO 400
46700 CALL RECIEVE% (TEMP$, LENGTH%, STATUS%)
46800 IMAG(I) = VAL(LEFT$(TEMP$, 12)) 'EXTRACT PHASE VALUE
46900 NEXT I
47000 '
47100 '
47200 CALL SPOLL% (HP4194%, POLL%, STAT. 7%) 'MAKE SURE SRQ
47300 RETURN
                                           'IS NOT SET
47400 '
                        TIMER ROUTINE
47500 '
47600 Y=CSRLIN
47700 X = POS(0)
47800 TIME.NOW$=TIME$
```

```
47900 NOW.HRS= VAL(LEFT$(TIME.NOW$,2))
48000 NOW.MIN= VAL(MID$(TIME.NOW$,4,2))
48100 NOW.SEC= VAL(RIGHT$(TIME.NOW$,2))
48200 SECONDS= NOW.SEC-BEGIN.SEC
48300 IF SECONDS >= 0 THEN 48500
48400 SECONDS=SECONDS+60: NOW.MIN=NOW.MIN-1
43500 MINUTES=NOW.MIN-BEGIN.MIN
48500 IF MINUTES >= 0 THEN 48800
48700 MINUTES=MINUTES+60: NOW.HRS=NOW.HRS-1
48800 IF NOW.HRS<BEGIN.HRS THEN NOW.HRS=NOW.HRS+24
48900 HOURS=NOW.HRS-BEGIN.HRS
49000 IF SECONDS<10 THEN SECONDS$="0" + RIGHT$(STR$(SECONDS),1)
49100 IF SECONDS >= 10 THEN SECONDS$=RIGHT$(STR$(SECONDS),2)
49200 IF MINUTES<10 THEN MINUTES$="0" + RIGHT$(STR$(MINUTES),1)
49300 IF MINUTES >= 10 THEN MINUTES$=RIGHT$(STR$(MINUTES),2)
49400 ELAPSE.TIME$= STR$(HOURS) + ":" + MINUTES$ +":" + SECONDS$
49500 LOCATE 20,45: PRINT "ELAPSED TIME: "; ELAPSE.TIME$
49600 LOCATE Y,X
49700 RETURN
```

#### GAIN-PHASE DATA ACQUISITION: GP.bas

```
100 CLS
200 '
300 '
400 '
                                GAIN/PHASE DATA TRANSFER SOFTWARE
500 '
600 '
700 '
900 DIM GAIN(400), PHS(400)
1000 DIM GFREQ(400)
                              ' ADDRESS OF GP-IB INTERFACE
1100 DEF SEG=&HC400
1200 INIT%=0
                               ' OFFSET OF INITIALIZE ROUTINE
                            OFFSET OF TRANSMIT ROUTINE
OFFSET OF RECIEVE ROUTINE
OFFSET OF SEND ROUTINE
OFFSET OF SERIAL POLL ROUTINE
OFFSET OF ENTER ROUTINE
1300 TRANSMIT%=3
1400 RECIEVE%=6
1500 SEND%=9
1600 SPOLL%=12
1700 ENTER%=21
1800 '
1900 '
2000 '
2100 ' GP-IB ADDRESSES OF INSTRUMENTS
2200 '
```

```
2300 HP4194%=17: HP4192%=9: PRINTER%=1: MY.ADDR%=21: K617%=27
2400 '
2500 '
2600 SYSCON%=0
                              'PC488 ACTS AS CONTROLLER
2800 CALL INIT% (MY.ADDR%, SYSCON%)
2900 '
3000 EX$="EX"
3200 ELAPSE.TIME$="00:00:00"
3300 HOURS ≈0
3400 \text{ MINUTES} = 0
3500 SECONDS = 0
3600 '
8600 '
                    SET-UP 4194 FOR G/P MEASUREMENTS
8700 '
8800 '
8900 S$="RST"
                'INITIALIZE 4194 TO POWER ON SETTING
9000 CALL SEND% (HP4194%, S$, STATUS%)
9100 S$="ROS2"
                         'UNMASK AND ENABLE BIT1 FOR SRQ
9200 CALL SEND% (HP4194%, S$, STATUS%)
9300 S$="FNC2"
                         'SET 4194 TO GAIN PHASE MODE
9400 CALL SEND% (HP4194%, S$, STATUS%)
9500 S$="PHS2"
                          'SET PHASE SCALE TO EXPANSION MODE
9600 CALL SEND% (HP4194%, S$, STATUS%)
9700 S$="SWM2"
                          'SET SWEEP MODE TO SINGLE
9800 CALL SEND% (HP4194%, S$, STATUS%)
9900 S$="SWT2"
                          'SET TO LOG SWEEP
10000 CALL SEND% (HP4194%, S$, STATUS%)
10100 S$="OSC=-10DBM"
                          'SET SWEEP OSCILLATOR TO -10DBM
10200 CALL SEND% (HP4194%, S$, STATUS%)
10300 S$="MCF0"
                          'TURN MARKERS OFF
10400 CALL SEND% (HP4194%, S$, STATUS%)
10500 S$="ZIR1"
                          'SET REF CHANNEL INPUT IMP.=1Mohm
10600 CALL SEND% (HP4194%, S$, STATUS%)
10700 S$="ZIT1"
                          'SET TEST CHANNEL INPUT IMP=1Mohm
10800 CALL SEND% (HP4194%, S$, STATUS%)
10900 S$="ITM1"
                         'SET INTEGRATION TIME TO 1mSEC
11000 CALL SEND% (HP4194%, S$, STATUS%)
11100 S$="STOP=1000000HZ"
                              'SWEEP TO 1MHz
11200 CALL SEND% (HP4194%, S$, STATUS%)
11400 INPUT "CONNECT 4194 FOR OFFSET REF STORE,
              RETURN WHEN READY", NULL$
11500 '
11600 '
                                    'PERFORM SINGLE SWEEP
11700 S$="SWTRG"
11800 CALL SEND% (HP4194%, S$, STATUS%)
11900 CALL SPOLL% (HP4194%, POLL%, STATUS%)
12000 IF ((POLL% AND 64) <> 64) THEN 11900
12100 S$="OFSTR"
                                    'STORE OFFSET DATA
12200 CALL SEND% (HP4194%, S$, STATUS%)
```

```
12300 S$="AOF1"
                                         'OFFSET A ON
12400 CALL SEND% (HP4194%, S$, STATUS%)
12500 S$="BOF1"
                                         'OFFSET B ON
12600 CALL SEND% (HP4194%, S$, STATUS%)
12700 '
12800 S$="X?"
                            'READ IN FREQUENCY POINTS
12900 CALL SEND% (HP4194%, S$, STATUS%)
13000 S$="MLA TALK 17"
                                      '4194 TO OUTPUT
13100 CALL TRANSMIT% (S$, STATUS%)
13200 TEMP$=SPACE$(15)
13300 FOR I=0 TO 400
13400 CALL RECIEVE% (TEMP$, LENGTH%, STATUS%)
13500 GFREQ(I)=VAL(LEFT$(TEMP$,12))
13600 NEXT I
13700 '
13820 '
17400 'TURN ON ELAPSE TIMER
17500 CLS
17600 BEGIN.TIME$=TIME$
17700 BEGIN.HRS= VAL(LEFT$(BEGIN.TIME$,2))
17800 BEGIN.MIN= VAL(MID$(BEGIN.TIME$,4,2))
17900 BEGIN.SEC= VAL(RIGHT$(BEGIN.TIME$,2))
18000 ON TIMER (1) GOSUB 47400
18100 TIMER ON
18200 '
18300 INPUT "NAME OF EXPERIMENT:", EXPERIMENT$
18800 INPUT "NAME OF GATE GAIN/PHASE DATA FILE:", GATEGP.FILE$
18810 INPUT "NUMBER OF ELECTRODES TO BE SAMPLED:", NELECT
18820 OPEN "O", #2, GATEGP.FILE$
21200 '
21300 CLS
21400 INPUT "CONNECT 4194 ACROSS THE FIRST ELECT,
             RETURN WHEN READY", NULL$
21500 WRITE #2, EXPERIMENT$, DATE$, TIME$
21600 FOR N= 1 TO NELECT
21610 WRITE #2, "ELECTRODE#", N, ELAPSE.TIME$
21620 PRINT "ELECTRODE ";N
21700 GOSUB 42100
21800 FOR I= 0 TO 400
21900 WRITE #2, GFREQ(I), GAIN(I), PHS(I)
22000 NEXT I
22050 IF N=NELECT THEN GOTO 22200
22100 INPUT "CONNECT 4194 ACROSS THE NEXT ELECT,
             RETURN WHEN READY", NULL$
22200 NEXT N
27400 CLOSE #2
27500 '
27600 '
27700 INPUT "COLLECT MORE DATA, Y OR N:", MOREDATAS
27800 IF MOREDATA$="N" THEN 28200
27900 GOTO 18300
```

```
28000 '
28200 '
28800 STOP
42100 '
42200 '
                           HP4194 DATA INPUT ROUTINE
42300 '
42400 '
42500 '
42600 CALL SPOLL% (HP4194%, POLL%, STATUS%)
42700 S$="SWTRG"
                                      'PERFORM SINGLE SWEEP
42800 CALL SEND% (HP4194%, S$, STATUS%)
42900 CALL SPOLL% (HP4194%, POLL%, STATUS%) 'IS SWEEP COMPLETE?
43000 IF ((POLL% AND 64) <> 64) THEN 42900
43100 '
43200 S$="AUTOA"
                                    'AUTOSCALE DISPLAY A
43300 CALL SEND% (HP4194%, S$, STATUS%)
43400 S$="AUTOB"
                                    'AUTOSCALE DISPLAY B
43500 CALL SEND% (HP4194%, S$, STATUS%)
44600 '
44700 S$="A?"
                      'READ IN GAIN FROM ARRAY REGISTER A
44800 CALL SEND% (HP4194%, S$, STATUS%)
44900 '
45300 '
45400 S$= "MLA TALK 17"
45500 CALL TRANSMIT% (S$, STATUS%)
45600 TEMP$= SPACE$(13)
45700 \text{ FOR I} = 0 \text{ TO } 400
45800 CALL RECIEVE% (TEMP$, LENGTH%, STATUS%)
45900 GAIN(I)=VAL(LEFT$(TEMP$,12)) 'EXTRACT GAIN VALUE
46000 NEXT I
46100 '
46200 S$="B?"
                         'READ IN PHASE FROM ARRAY REGISTER B
46300 CALL SEND% (HP4194%, S$, STATUS%)
46400 S$= "MLA TALK 17"
46500 CALL TRANSMIT% (S$, STATUS%)
46600 FOR I= 0 TO 400
46700 CALL RECIEVE% (TEMP$, LENGTH%, STATUS%)
46800 PHE (I) = VAL(LEFT$(TEMP$, 12)) 'EXTRACT PHASE VALUE
46900 NEXT I
47000 '
47100 '
47200 CALL SPOLL% (HP4194%, POLL%, STATUS%) 'MAKE SURE SRQ NOT SET
47300 RETURN
47400 '
                         TIMER ROUTINE
47500 '
47600 Y=CSRLIN
47700 X=POS(0)
47800 TIME.NOW$=TIME$
47900 NOW.HRS= VAL(LEFT$(TIME.NOW$,2))
48000 NOW.MIN= VAL(MID$(TIME.NOW$, 4, 2))
48100 NOW.SEC= VAL(RIGHT$(TIME.NOW$,2))
```

```
48200 SECONDS= NOW.SEC-BEGIN.SEC
48300 IF SECONDS >= 0 THEN 48500
48400 SECONDS=SECONDS+60: NOW.MIN=NOW.MIN-1
48500 MINUTES=NOW.MIN-BEGIN.MIN
48600 IF MINUTES >= 0 THEN 48800
48700 MINUTES=MINUTES+60: NOW.HRS=NOW.HRS-1
48800 IF NOW.HRS<BEGIN.HRS THEN NOW.HRS=NOW.HRS+24
48900 HOURS=NOW.HRS-BEGIN.HRS
49000 IF SECONDS<10 THEN SECONDS$="0" + RIGHT$(STR$(SECONDS),1)
49100 IF SECONDS >= 10 THEN SECONDS$=RIGHT$(STR$(SECONDS),2)
49200 IF MINUTES<10 THEN MINUTES$="0" + RIGHT$(STR$(MINUTES),1)
49300 IF MINUTES >= 10 THEN MINUTES$=RIGHT$(STR$(MINUTES),2)
49400 ELAPSE.TIME$= STR$(HOURS) + ":" + MINUTES$ +":" + SECONDS$
49500 LOCATE 20,45: PRINT "ELAPSED TIME: "; ELAPSE.TIME$
49600 LOCATE Y,X
49700 RETURN
```

### SPECTRUM ANALYZER AND DIGITAL OSCILLOSCOPE DATA ACQUISITION:

#### FFT.bas

```
10 REM PROGRAM TO DUMP SPECTRUM FROM HP8566 TO PC FILE
20 REM ----- Initialization & Setup -----
30 DEF SEG=&HC400
                                  PC-488 memory address
40 INIT=0 : XMIT=3 : RECV=6 : SEND=9 : SPOLL=12
50 PPOLL=15 : ENTER=21 : TARRAY=200 : RARRAY=203 : DMA2=206
60 DIM D%(2048), VPOINT(1300)
70 MY.ADDR%=0 : SYS.CONTROL%=0
                               ' initialize as system ctrlr
80 CALL INIT (MY.ADDR%, SYS.CONTROL%)
90 REM ----- Transmit -----
100 S$="UNL UNT"
110 CALL XMIT (S$,STATUS%)
120 IF STATUS%<>0 THEN GOTO 1200
130 CLS : PRINT " "
140 PRINT "
                 HP8566 (SPECTRUM ANALYZER) Control Software"
150 PRINT " "
160 PRINT "
                           SET-UP OPERATION"
                       (1)
170 PRINT "
                           X-FER DATA TO PC FILE"
                       (2)
180 PRINT "
                           EXIT TO DOS"
                       (3)
181 PRINT "
                           GET DIGITAL OSCOPE DATA"
                       (4)
190 PRINT "" :INPUT "ENTER CHOICE: ", MENU
200 IF MENU=1 THEN GOSUB 240
210 IF MENU=2 THEN GOSUB 710
220 IF MENU=3 THEN GOTO 1150
221 IF MENU=4 THEN GOSUB 4000
```

```
230 GOTO 130
240 REM SET UP HP8566 TO INITIAL STATE
241 CLS: INPUT "CALIBRATE THE SPECTRUM ANALYZER? [Y/N] ", ANS$
242 IF ANS$="n" OR ANS$="N" THEN GOTO 250
243 IF ANS$="Y" OR ANS$="y" THEN GOTO 245
244 GOTO 241
245 GOSUB 1300
250 CLS: INPUT "RECALL A SAVED INSTRUMENT STATE? [Y/N] ", ANS$
260 IF ANS$="n" OR ANS$="N" THEN GOTO 350
270 IF ANS$="Y" OR ANS$="y" THEN GOTO 290
280 GOTO 250
290 INPUT "ENTER THE REGISTER NUMBER: ",S$
300 S$="RC "+S$
310 REM ----- Send ------
                                           ' device address
320 ADDR%=18
330 CALL SEND (ADDR%,S$,STATUS%)
340 IF STATUS%<>0 THEN GOTO 1200
341 REM determine if calibrated data will be used
342 CLS: INPUT "USE CALIBRATED DATA? [Y/N] ", ANS$
343 IF ANS$="n" OR ANS$="N" THEN GOTO 350
344 IF ANS$="Y" OR ANS$="y" THEN GOTO 346
345 GOTO 342
346 GOSUB 1400
350 REM ESTABLISH FREQUENCY DATA POINTS TO STORE IN FILE
360 S$="FA OA"
                                            ' device address
370 ADDR%=18
380 CALL SEND (ADDR%, S$, STATUS%)
390 IF STATUS%<>0 THEN GOTO 1200
400 R$=SPACE$(80)
                              'allocate receive buffer
410 CALL ENTER (R$, LENGTH%, ADDR%, STATUS%)
420 IF STATUS%<>0 THEN GOTO 1200
430 ST=VAL(LEFT$(R$, LENGTH%))
440 S$="FB OA"
450 CALL SEND (ADDR%, S$, STATUS%)
460 IF STATUS%<>0 THEN GOTO 1200
470 R$=SPACE$(80)
                              'allocate receive buffer
480 CALL ENTER (R$, LENGTH%, ADDR%, STATUS%)
490 IF STATUS%<>0 THEN GOTO 1200
500 FINAL=VAL(LEFT$(R$, LENGTH%))
510 REM
520 REM DETERMINE FREQ STEP SIZES
530 STP=(FINAL - ST)/1000
540 REM SET END OF TEXT AND WRITE TITLE
550 S$="DT@ KSE TJCHEMFET " + DATE$ +"@ HD"
560 CALL SEND (ADDR%,S$,STATUS%)
570 IF STATUS%<>0 THEN GOTO 1200
580 REM CHECK SWEEP TIME SINCE LONG SWEEPS WILL CAUSE TIME-OUT
590 REM CONDITION WHEN CAPTURING DATA
600 S$="ST OA"
610 CALL SEND (ADDR%,S$,STATUS%)
```

620 IF STATUS%<>0 THEN GOTO 1200

```
630 R$=SPACE$(80)
                            'allocate receive buffer
640 CALL ENTER (R$, LENGTH%, ADDR%, STATUS%)
650 IF STATUS%<>0 THEN GOTO 1200
660 SWEEP=VAL(LEFT$(R$, LENGTH%))
670 S$="HD"
680 CALL SEND (ADDR%, S$, STATUS%)
690 IF STATUS%<>0 THEN GOTO 1200
700 RETURN
710 REM CAPTURE DATA AND X-FER TO PC
720 REM TAKE A SWEEP AND FORMAT DATA FOR TRANSFER
730 CLS:PRINT "CAPTURING DATA..."
740 S$="S2 TS O3 TA"
750 ADDR%=18
760 CALL SEND (ADDR%,S$,STATUS%)
770 IF STATUS%=0 THEN GOTO 820
780 REM COULD BE A LONG SWEEP TIME IS HOLDING UP SYSTEM
790 IF STATUS%<>8 OR (STATUS%=8 AND SWEEP < 10) THEN GOTO 1200
800 CALL SPOLL (ADDR%, POLL%, STATUS%)
810 GOTO 770
820 CLS:PRINT "DATA CAPTURED ON HP8566"
830 INPUT "ENTER FILE NAME TO STORE DATA: ", N$
840 OPEN "O", #1, N$
850 PRINT#1, "FFT DATA "; DATE$;" ";TIME$
860 PRINT#1, "FREQ";CHR$(9);"AMPLITUDE"
870 REM ----- Transmit -----
880 S$="MLA TALK 18"
890 CALL XMIT (S$,STATUS%)
900 IF STATUS%<>0 THEN GOTO 1200
910 REM ----- Receive -----
920 REM DRESS-UP THE PC SCREEN OUTPUT
                                     VALUE"
930 CLS:PRINT "POINT# FREQ
940 R$=SPACE$(32)
                            ' allocate receive buffer
950 FOR I=0 TO 1000
          CALL RECV (R$, LENGTH%, STATUS%)
970
           IF STATUS%<>0 THEN GOTO 1200
980
           A=VAL(R$)
990
          FREQ=ST + (I*STP)
          PRINT#1, FREQ; CHR$(9); A
1010
            IF (I MOD 100)=0 THEN PRINT I, FREQ, A
1020 NEXT I
1030 CLOSE #1:PRINT "":PRINT "X-FER COMPLETED TO ";N$
1040 INPUT "RETURN TO CONTINUE", DUMMY
1050 REM ------ Transmit -----
1060 S$="UNL UNT"
1070 CALL XMIT (S$,STATUS%)
1080 IF STATUS%<>0 THEN GOTO 1200
1090 REM PUT HP8566 BACK INTO CONTINUOUS SWEEP
1100 S$="S1"
1110 ADDR%=18
1120 CALL SEND (ADDR%,S$,STATUS%)
11'0 IF STATUS%<>0 THEN GOTO 1200
1140 RETURN
```

```
1150 REM MAKE SURE HP8566 IS LISTENING- Serial Poll
1160 ADDR%=18
                                            ' device address
1170 CALL SPOLL (ADDR%, POLL%, STATUS%)
1180 IF STATUS%<>0 THEN PRINT "SPOLL": GOTO 1200
1190 CLS: SYSTEM
1200 PRINT "COMM PROBLEM -- CHECK SET-UP AND RESTART PROGRAM"
1210 STOP
1300 REM THIS IS THE CALIBRATION ROUTINE
1310 CLS:PRINT "CONNECT THE CAL OUTPUT TO THE INPUT CONNECTOR"
1305 PRINT "":
1320 INPUT "ENTER RETURN WHEN CONNECTED", DUMMY
1330 S$="KSW"
1340 ADDR%=18
1345 CALL SEND (ADDR%, S$, STATUS%)
1350 IF STATUS%=0 THEN GOTO 1375
1355 REM CAL TAKES A LONG TIME WHICH CAUSES TIME OUT ON STATUS
1357 PRINT "CALIBRATION IN PROGRESS..."
1360 IF STATUS%<>8 THEN GOTO 1200
1365 CALL SPOLL (ADDR%, POLL%, STATUS%)
1370 GOTO 1350
1375 CLS:PRINT "CALIBRATION IS COMPLETE"
1380 PRINT "CONNECT DUT":PRINT "":PRINT ""
1385 INPUT "ENTER RETURN WHEN CONNECTED", DUMMY
1390 RETURN
1400 REM TURN ON THE CALIBRATION
1405 S$="KSX"
1410 ADDR%=18
1420 CALL SEND (ADDR%, S$, STATUS%)
1430 IF STATUS%<>0 THEN GOTO 1200
1440 RETURN
1500 END
4000 '
4010 REM PROGRAM TO CAPTURE SCOPE CHANNEL 1 DISPLAY IN PC FILE
4180 K=1 : 'CHANNEL 1
4200 REM ----- Initialization & Setup ------
4210 DEF SEG=&HC400
                                   ' PC-488 memory address
1220 INIT=0 : XMIT=3 : RECV=6 : SEND=9 : SPOLL=12
4230 PPOLL=15 : ENTER=21 : TARRAY=200 : RARRAY=203 : DMA2=206
4250 MY.ADDR%=21: SYS.CONTROL%=0 'initialize as system ctrlr
4260 CALL INIT (MY.ADDR%, SYS.CONTROL%)
4270 '
4280 '
4290 '
4300 REM ----- Send ------
4310 CLS:LOCATE 1,1
4320 PRINT"SCOPE GRABBER NOW GRABBING CHANNEL ";K
4330 S$="CLEAR; HEADER OFF"
                                          ' device address
4340 ADDR%=15
4350 CALL SEND (ADDR%, S$, STATUS%)
4360 IF STATUS%<>0 THEN 5500
```

```
4370 REM ------ Send ------
4380 N$=RIGHT$(STR$(K),1)
4390 S$="CHANNEL "+N$;";DISPLAY FORMAT 2"
                                      ' device address
4400 ADDR%=15
4410 CALL SEND (ADDR%,S$,STATUS%)
4420 IF STATUS%<>0 THEN 5500
4430 REM ------ Send ------
4440 S$="ACQUIRE TYPE AVERAGE COUNT 32 COMPLETE 90 POINTS 1000;"
4450 CALL SEND (ADDR%, S$, STATUS%)
4455 FOR SCOPEW=1 TO 10000: NEXT SCOPEW
4460 IF STATUS%<>0 THEN 5500
4470 REM ------ Send ------ Send -----
4480 S$="DIGITIZE CHANNEL"+N$+";
4490 ADDR%=15
                                      ' device address
4500 CALL SEND (ADDR%, S$, STATUS%)
4510 IF STATUS%<>0 THEN 5500
4520 REM ----- Send ------
4530 ADDR%=15
                                      ' device address
4540 S$="WAVEFORM POINTS?"
4550 CALL SEND (ADDR%, S$, STATUS%)
4560 IF STATUS%<>0 THEN 5500
4570 REM ----- Enter -----
4580 R$=SPACE$(13)
                          'allocate receive buffer
4590 ADDR%=15
                                     ' device address
4600 CALL ENTER (R$, LENGTH%, ADDR%, STATUS%)
4610 IF STATUS%<>0 THEN 5500
4620 POINTS=VAL(R$):PRINT "THE NUMBER OF WAVE POINTS=";POINTS,
4630 IF POINTS>1300 THEN PRINT "WARNING:
                           EXCESS POINTS (MAX 1300)"
4640 REM ----- Send -----
                                  ' device address
4650 ADDR%=15
4660 S$="WAVEFORM XINC?"
4670 CALL SEND (ADDR%,S$,STATUS%)
4680 IF STATUS%<>0 THEN 5500
                          'allocate receive buffer
4690 R$=SPACE$(30)
4700 ADDR%=15
                                       ' device address
4710 CALL ENTER (R$, LENGTH%, ADDR%, STATUS%)
4720 IF STATUS%<>0 THEN 5500
4730 XINC=VAL(R$):'----- Send ------
4740 ADDR%=15
                                      ' device address
4750 S$="WAVEFORM XOR?"
4760 CALL SEND (ADDR%, S$, STATUS%)
4770 IF STATUS%<>0 THEN 5500
                          'allocate receive buffer
4780 R$=SPACE$(30)
4790 ADDR%=15
                                       ' device address
4800 CALL ENTER (R$, LENGTH%, ADDR%, STATUS%)
4810 IF STATUS%<>0 THEN 5500
4820 XORG=VAL(R$):'----- Send ------
                                      ' device address
4830 ADDR%=15
4840 S$="WAVEFORM YREF?"
4850 CALL SEND (ADDR%, S$, STATUS%)
4860 IF STATUS%<>0 THEN 5500
```

```
4870 R$=SPACE$(13) 'allocate receive buffer
4880 ADDR%=15
                                        ' device address
4890 CALL ENTER (R$, LENGTH%, ADDR%, STATUS%)
4900 IF STATUS%<>0 THEN 5500
4910 YREF=VAL(R$):'----- Send -------
4920 ADDR%=15
                                        ' device address
4930 S$="WAVEFORM YINC?"
4940 CALL SEND (ADDR%, S$, STATUS%)
4950 IF STATUS%<>0 THEN 5500
4960 R$=SPACE$(13)
                            'allocate receive buffer
4970 ADDR%=15
                                        ' device address
4980 CALL ENGER (R$, LENGTH%, ADDR%, STATUS%)
4990 IF STATUS%<>0 THEN 5500
5000 YINC=VAL(R$):'----- Send ------
                                       ' device address
5010 ADDR%=15
5020 S$="WAVEFORM YOR?"
5030 CALL SEND (ADDR%, S$, STATUS%)
5040 IF STATUS%<>0 THEN 5500
5050 REM ----- Enter ------
5060 R$=SPACE$(13) 'allocate receive buffer
5070 ADDR%=15
5080 CALL ENTER (R$, LENGTH%, ADDR%, STATUS%)
5090 IF STATUS%<>0 THEN 5500
5100 YOR=VAL(R$)
5120 S$="WAVEFORM FORMAT ASCII; WAVEFORM DATA? "
                                        ' device address
5130 ADDR%=15
5140 CALL SEND (ADDR%, S$, STATUS%)
5150 IF STATUS%<>0 THEN 5500
5160 REM ----- Transmit -----
5170 S$="MLA TALK 15"
5180 CALL XMIT (S$,STATUS%)
5190 IF STATUS%<>0 THEN 5500
5200 INPUT "SCOPE FILE NAME: ", TRACE$
5205 INPUT "EXPERIMENT INFORMATION: ", EXPERIMENT$
5214 OPEN "O", #1, TRACE$
5215 PRINT#1, EXPERIMENT$;" "; DATE$;" "; TIME$
5227 PRINT#1, "TIME"; CHR$(9); "VOLTAGE"
5230 PRINT " "
5240 PRINT "(INDEX) TIME VOLTAGE"
5250 PRINT "-----"
5260 FOR I=1 TO POINTS
5270 REM ----- Receive -----
5280 R1$=SPACE$(32) 'allocate receive buffer
5290 IF STATUS%<>0 THEN 5500
5300 TPOINT=XINC*I+XORG
5310 CALL RECV (R1$, LENGTH%, STATUS%)
5320 IF STATUS%<>0 THEN 5500
5330 VPOINT(I) = ((VAL(R1\$) - YREF) * YINC) + YOR
5350 IF (I MOD 100)=0 THEN PRINT "(";I;")", TPOINT;", ", VPOINT(I)
5360 PRINT#1, TPOINT; CHR$(9); VPOINT(I)
5370 NEXT I
5430 CLOSE #1
```

```
5471 '
5472 ' RETURN CONTROL OF SCOPE TO OPERATOR
5480 S$="LOCAL"
5490 CALL SEND (ADDR*,S$,STATUS*)
5491 S$="UNL UNT"
5492 CALL XMIT (S$,STATUS*)
5493 IF STATUS*<>0 THEN 5500
5494 PRINT:PRINT"FINISHED":RETURN
5500 PRINT "CHECK EQUIPMENT SET-UP AND RE-EXECUTE":RETURN
```

# BASIC PROGRAM FOR FILTERING FOR FOURIER TRANSFORM SPECTRA:

#### HARM.bas

```
100 '
                     HARMONIC FREQUENCY FINDER
200 '
300 '
400 ' ASK FOR INPUT AND OUTPUT FILENAMES
600 INPUT "INPUT DATA FILE NAME: ",
                                         IFILE$
700 INPUT "OUTPUT DATA FILE NAME: ", OFILE$
900 '
1000 DIM FREQ(1000), AMP(1000)
1100 '
1200 '
1300 OPEN "I", #1, IFILE$
1400 OPEN "O", #2, OFILE$
1500 '
1600 '
1700 INPUT #1, FXP$
                        'TRANSFER EXPERIMENT
1800 INPUT #1, FREQ$
                         'INFORMATION
1900 PRINT #2, FXP$
2000 PRINT #2, FREQ$
2100 '
2200 '
2300 K=0
2400 FOR I= 0 TO 7
2500 INPUT #1, FREQ(I), AMP(I)
2550 K=K+1
2600 NEXT I
2650 \text{ AMP}(0) = SQR(0.05 *10^(AMP(0)/10)) *1000
2660 \text{ AMP}(5) = SQR(0.05 *10`(AMP(5)/10)) *1000
2700 PRINT #2, FREQ(U), AMP(O) 'WRITE IN OHZ DATA 2800 PRINT #2, FREQ(5), AMP(5) 'WRITE IN 1K HZ DATA
2900 '
```

```
3000 '
4000 \text{ FOR } J = 1 \text{ TO } 198
4100 GOSUB 13000
4200 NEXT J
4300 '
4400 '
4450 MAMP= AMP(K-1)
4460 '
4500 FOR I= K TO 1000
4600 INPUT #1, FREQ(I), AMP(I)
4620 IF AMP(I) > MAMP THEN MAMP=AMP(I)
4700 NEXT I
4800 '
5000 PRINT #2, FREQ(1000), MAMP
5100 '
5200 '
5300 CLOSE #1
5400 CLOSE #2
5500 STOP
5600 END
13000 '
13010 '
13050 MAMP=AMP(K-1)
13100 FOR I= K TO K+4
13200 INPUT #1, FREQ(I), AMP(I)
13300 IF AMP(I) > MAMP THEN MAMP=AMP(I)
13400 NEXT I
13450 \text{ MAMP} = SQR(0.05 * 10^(MAMP/10)) *1000
13500 PRINT #2, FREQ(K+2), MAMP
13600 '
15700 '
15800 K=K+5
15900 RETURN
```

# Appendix F

## Impedance Data

This appendix contains some of the impedance data associated with the interdigitated gate electrode coated with the thin films. These impedance data were taken during the challenge gas exposures. The impedance data are displayed in the plots of resistance (R) and reactance (X) versus frequency.

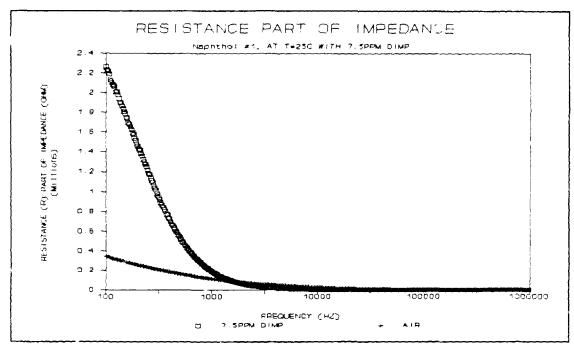


Figure F.1. Resistive Part of the Impedance for the 2-Naphthol( $\beta$ ) Film upon Exposure to the 7.5 ppm DIMP Challenge at 25°C.

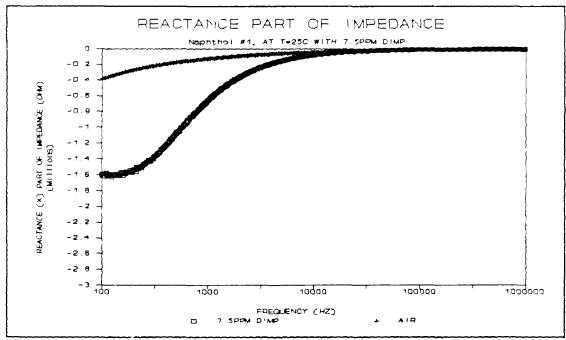


Figure F.2. Reactive Part of the Impedance for the 2-Naphthol( $\beta$ ) Film upon Exposure to the 7.5 ppm DIMP Challenge at 25°C.

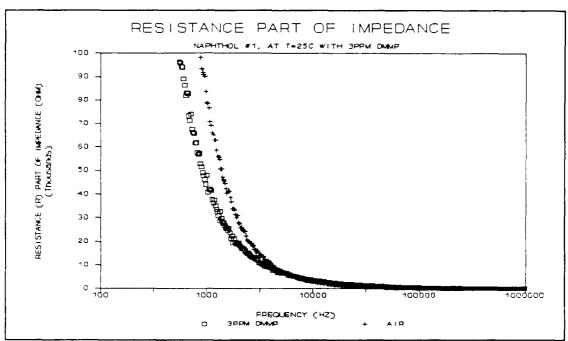


Figure F.3. Resistive Part of the Impedance for the 2-Naphthol( $\beta$ ) Film upon Exposure to the 3 ppm DMMP Challenge at 25°C.

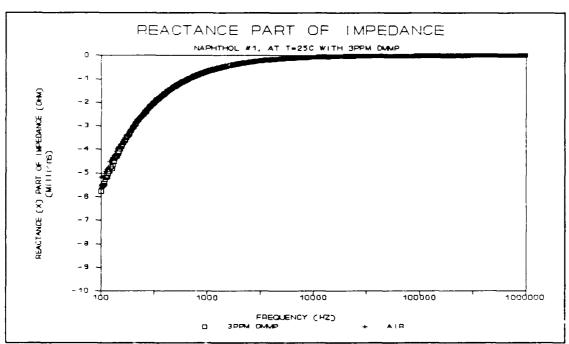
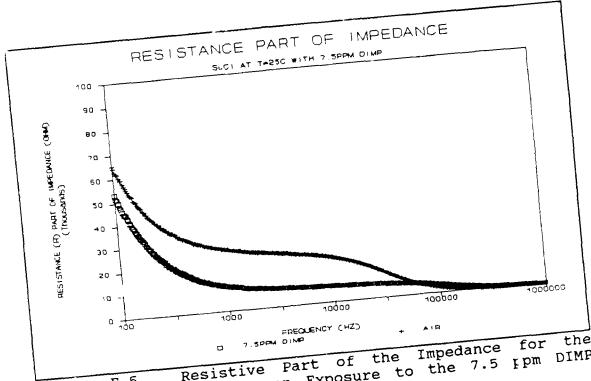
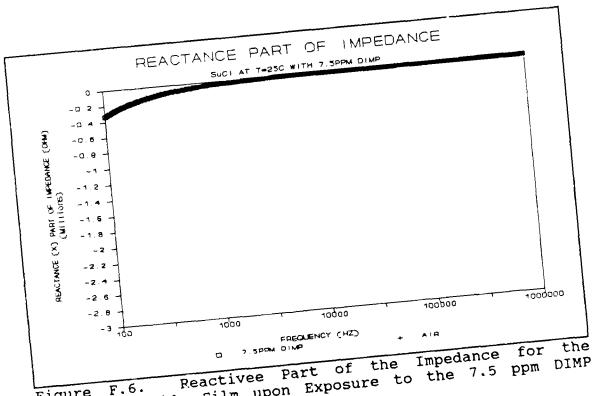


Figure F.4. Reactive Part of the Impedance for the 2-Naphthol( $\beta$ ) Film upon Exposure to the 3 ppm DMMP Challenge at 25°C.



Resistive Part of the Impedance for Succinylchloride Film upon Exposure to the 7.5 pm DIMP Challenge at 25°C.



Succinylchloride Film upon Exposure to the 7.5 ppm DIMP Challenge at 25°C.

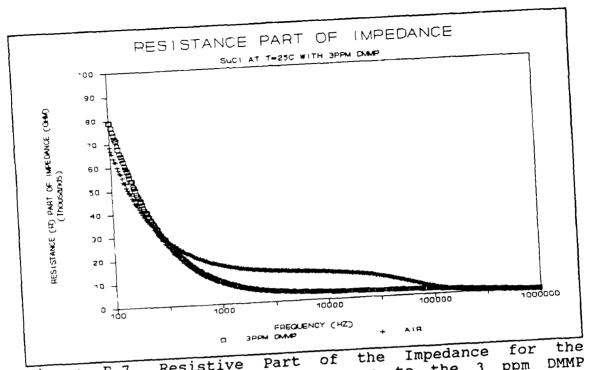


Figure F.7. Resistive Part of the Impedance for the Succinylchloride Film upon Exposure to the 3 ppm DMMP Challenge at 25°C.

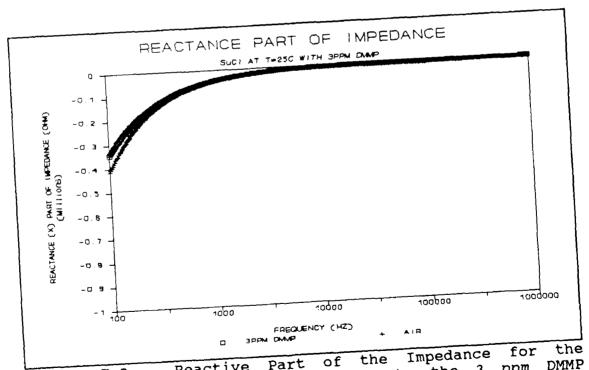


Figure F.8. Reactive Part of the Impedance for the Succinylchloride Film upon Exposure to the 3 ppm DMMP Challenge at 25°C.

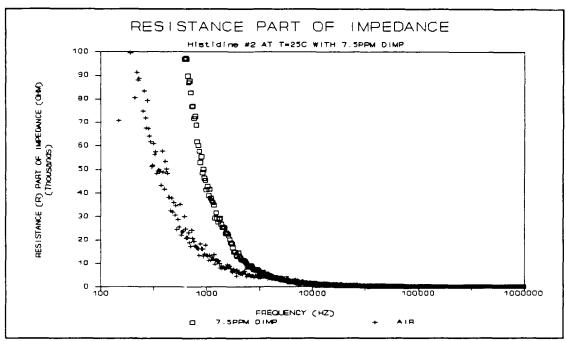


Figure F.9. Resistive Part of the Impedance for the L-Histidine Dihydrochloride Film upon Exposure to the 7.5 ppm DIMP Challenge at 25 °C.

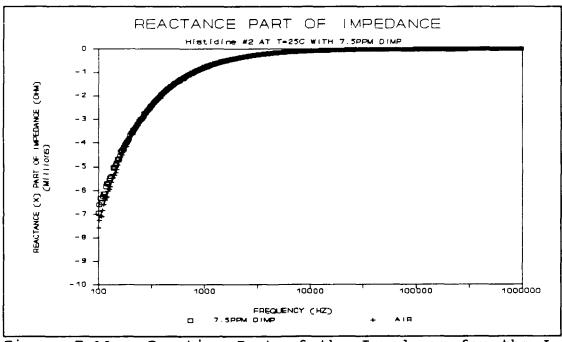


Figure F.10. Reactive Part of the Impedance for the L-Histidine Dihydrochloride Film upon Exposure to the 7.5 ppm DIMP Challenge at 25 °C.

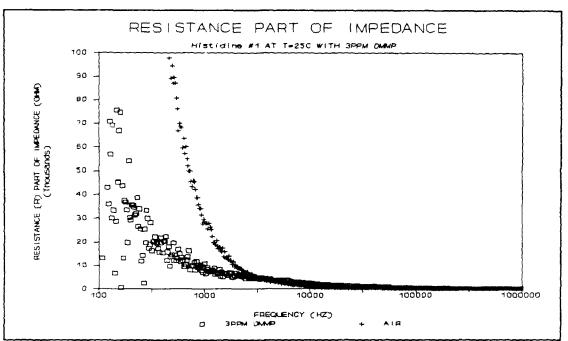


Figure F.11. Resistive Part of the Impedance for the L-Histidine Dihydrochloride Film upon Exposure to the 3 ppm DMMP Challenge at 25 °C.

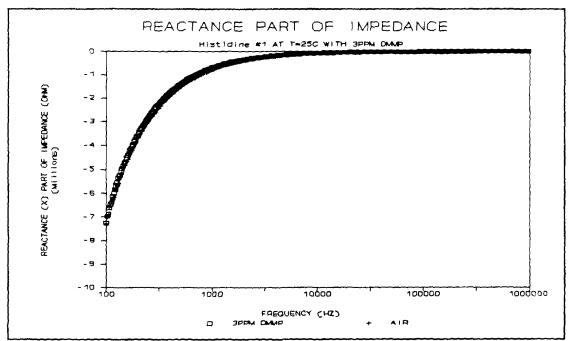


Figure F.12. Reactive Part of the Impedance for the L-Histidine Dihydrochloride Film upon Exposure to the 3 ppm DMMP Challenge at 25 °C.

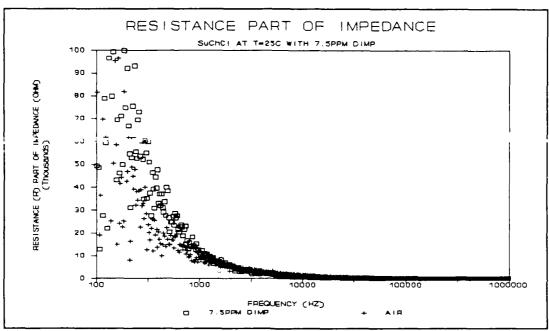


Figure F.13. Resistive Part of the Impedance for the Succinylcholine Chloride Film upon Exposure to the 7.5 ppm DIMP Challenge at 25 °C.

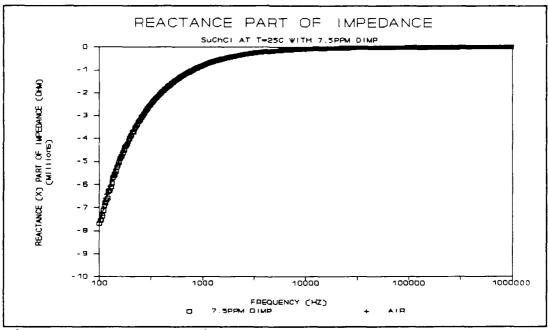


Figure F.14. Reactive Part of the Impedance for the Succinylcholine Chloride Film upon Exposure to the 7.5 ppm DIMP Challenge at 25 °C.

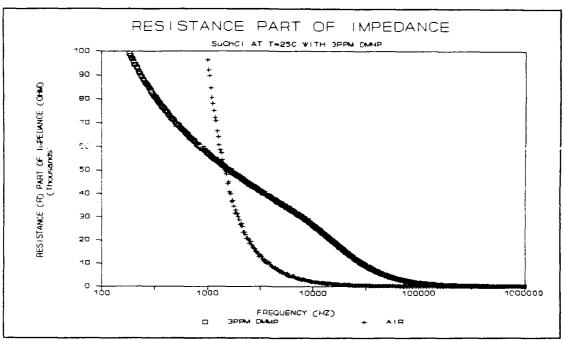


Figure F.15. Resistive Part of the Impedance for the Succinylcholine Chloride Film upon Exposure to the 3 ppm DMMP Challenge at 25 °C.

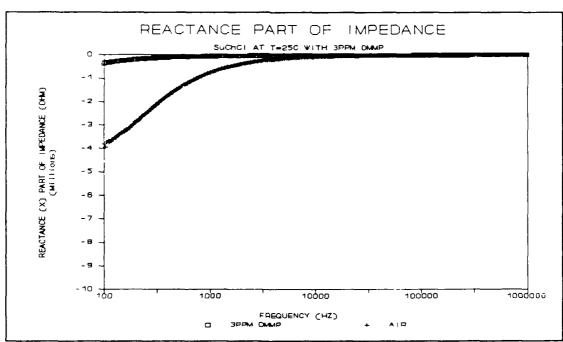


Figure F.16. Reactive Part of the Impedance for the Succinylcholine Chloride Film upon Exposure to the 3 ppm DMMP Challenge at 25 °C.

## **Bibliography**

- 1. Wiseman, J. <u>Investigation of the Impedance</u>

  <u>Modulation of Thin Films with a Chemically-Sensitive</u>

  <u>Field-Effect Transistor</u>. MS Thesis, AFIT/GE/ENG/88D-6.61.

  Department of Electrical and Computer Engineering, Air

  Force Institute of Technology, 1988.
- Kolesar, E. and J. Wiseman. "Interdigitated Gate Electrode Field Effect Transistor for the Selective Detection of Nitrogen Dioxide and Diisopropyl Methylphosphonate," <u>Analytical Chemistry</u>, 61: 2355-2361, Nov 1989.
- 3. Worthington Biochemical Corporation. <u>Worthington Enzyme</u>
  <u>Manual: Enzymes and Related Biochemicals</u>. Freehold, New Jersey, 1988.
- 4. Snow, A. et al. Review of Organofluorophosphonate Ester Chemistry and Proposed Adaptation for Chemical Detection.
  Naval Research Laboratory, Washington, D.C., April 7,
  1983, NRL Memorandum Report 5050.
- 5. Guilbault, G. et al. "A Coated Piezoelectric Crystal to Detect Organophosphorus Compounds and Pesticides," <u>Sensors and Actuators</u>, 2: 43-57, 1981.
- 6. Schiede E. and G. Guilbault. "Piezoelectric Detectors for Organophosphorus Compounds and Pesticides," <u>Analytical Chemistry</u>, 44: 1764-1768, Sep 1972.
- 7. Wohltjen, H. et al. "A Vapor-Sensitive Chemiresistor Fabricated with Planar Microelectrodes and a Langmuir-Blodgett Organic Semiconductor Film," I.E.E.E Transactions on Electron Devices, ED-32: 1170-1174, July 1985.
- 8. Barger, W. et al. "Chemiresistor Transducers Coated with Phthalocyanine Derivatives by the Langmuir-Blodgett Technique," <u>I.E.E.E International Conference on Solid State Sensors and Actuators</u>, 410-413, 1985.
- Janata, J. and R. Huber. "Chemically Sensitive Field-Effect Transistors," <u>Ion-Selective Electrodes in</u> <u>Analytical Chemistry 2:</u> 107-174, Modern Analytical Chemistry Series. New York: Plenum Press, 1980.

- 10. Janata, J. et al. "Chemically Sensitive Field-Effect Transistor to Detect Organophosphorus Compounds and Pesticides," <u>Aviation, Space, and Environmental Medicine</u>, 666-671, Nov 1981.
- 11. Kolesar, E. <u>Electronic Detection of Low Concentrations of Organophosphorus Compounds with a Solid State Device Utilizing Supported Copper and Cuprous Oxide Island Films.</u> PhD Dissertation. University of Texas, Austin, TX, May 1985 (AD-A158181).
- 12. Kolesar, E. and R. Walser. "Organophosphorus Compound Detection with a Supported Copper + Cuprous Oxide Island Film. 1. Gas-Sensitive Film Physical Characteristics and Direct Current Studies", Analytical Chemistry, 60: 1731-1736, 1988.
- 13. Janata, J. and E. Kolesar. <u>Chemically Sensitive Field-Effect Transistor Chemical Warfare Agent Detector</u>, USAFSAM-TR-82-10. Salt Lake City, UT: University of Utah, Apr 1982 (AD-B065108).
- 14. Fluka Chemical Corp., <u>Catalog 1988/89.</u> Ronkonkoma NY, 1988.
- 15. Van Woerkom, P., <u>The Effect of Gases on the Conductive Properties of Organic Semiconductors.</u> VI. Results for films of Phthalocynine and  $\beta$ -Naphthol in a Flow System, Chemisch Laboratorium TNO Report 1975-16.
- 16. Stremler, F., <u>Introduction to Communication Systems</u> (2nd Edition). Reading, Massachusetts: Addison-Wesley, 1982.
- 17. Sklar, B., <u>Digital Communications: Fundamentals and Applications</u>. Englewood Cliffs, New Jersey: Prentice Hall, 1988.
- 18. Weste, N. and K. Eshraghian. <u>Principles of CMOS VLSI</u>
  <u>Design: A Systems Perspective</u>. Reading, Massachusetts:
  Addison-Wesley, 1985.
- 19. Sze, S. M., <u>Semiconductor Devices: Physics and Technology.</u> New York: John Wiley & Sons, 1985.
- 20. Allen, Phillip E. and Douglas R. Holberg. <u>CMOS Analog Circuit Design</u>. New York: Holt, Rinehart and Winston, 1987.

- 21. Boylestad, R. and L. Nashelsky. <u>Electronic Devices and Circuit Theory.</u> Englewood Cliffs, NJ: Prentice-Hall, 1982.
- 22. GC Industries, <u>G-Cal Permeation Device Instruction Sheet.</u>
  Chatsworth CA, 1989.

### VITA

Captain Jenny E. Shin

Her family came to United States in 1973. attended Lowell High School in San Francisco, California and graduated from the high school in 1978. She attended the University of California at Berkeley, from which she received the degree of Bachelor of Science in Chemical Engineering in June 1982. She joined the United States Air Force in 1983. She attended Officer Training School from April 1983 through July 1983. Under the undergraduate degree conversion program, she received the degree of Bachelor of Science in Electrical Engineering from Air Force Institute of Technology in March She served in the Electronic Combat Division, 4950th Test Wing, Wright-Patterson AFB, OH as a test director and project manager from Mar 1985 through May 1988. At the end of May 1988, she entered the School of Engineering, Air Force Institute of Technology.

